Investigations of Conformational and Functional Relationship of Selected Serine Proteases at Molecular Level

Thesis Submitted to **AcSIR**
For the Award of the Degree of
DOCTOR OF PHILOSOPHY
In
BIOLOGICAL SCIENCES

By
Sayli Anil Dalal

10BB11J26115

Under the guidance of

Dr. Narendra Kadoo (Research Supervisor)

Dr. (Mrs.) Sushama Gaikwad (Research Co-Supervisor)

DIVISION OF BIOCHEMICAL SCIENCES
CSIR-NATIONAL CHEMICAL LABORATORY
PUNE – 411008, INDIA

DECEMBER 2015

Dedicated to

Dearest Aai, Baba and Manas…

सीएसआयआर–राष्ट्रीय रासायनिक प्रयोगशाला
(वैज्ञानिक तथा औद्योगिक अनुसंधान परिषद)
डॉ. होमी भाभा मार्ग, पुणे – 411 008. भारत
CSIR-NATIONAL CHEMICAL LABORATORY
(Council of Scientific & Industrial Research)
Dr. Homi Bhabha Road, Pune - 411008. India

CERTIFICATE

This is to certify that the work incorporated in this Ph.D. thesis entitled **"Investigations of conformational and functional relationship of selected serine proteases at molecular level"** submitted by **Ms. Sayli Anil Dalal** to Academy of Scientific and Innovative Research (AcSIR) in fulfillment of the requirements for the award of the Degree of **Doctor of Philosophy**, embodies original research work under our guidance.

We further certify that this work has not been submitted to any other University or Institution in part or full for the award of any degree or diploma. Research material obtained from other sources has been duly acknowledged in the thesis. Any text, illustration, table etc., used in the thesis from other sources, have been duly cited and acknowledged.

SADalal

Date: 22nd December 2015
Place: Pune

Sayli Anil Dalal
(Student)

Dr. Narendra Kadoo
(Research Supervisor)

Dr. Sushama Gaikwad
(Research Co-supervisor)

☎ FAX WEBSITE
Communications Channels
NCL Level DID : 2590
NCL Board No. : +91-20-25902000
Four PRI Lines : +91-20-25902000
Director's Office : +91-20-25902601
COA's Office : +91-20-25902660
SPO's Office : +91 20 25902664
www.ncl-india.org

DECLARATION OF THE CANDIDATE

I declare that the thesis entitled "**Investigations of conformational and functional relationship of selected serine proteases at molecular level**" submitted by me for the degree of Doctor of Philosophy is the record of work carried out by me during the period from 3rd January 2011 to 4th September 2015 under the guidance of **Dr. Narendra Kadoo** and **Dr. Sushama Gaikwad** and has not formed the basis for the award of any degree, diploma, associateship, fellowship, titles in this or any other University or other institute of higher learning. I further declare that the material obtained from other sources has been duly acknowledged in the thesis.

SADalal

Date: 22nd December 2015

Signature of the candidate

Sayli Anil Dalal

Acknowledgement

PhD is not just another degree, but it marks the culmination of very long years of academic education. I would like to take this opportunity to thank one and all who has contributed to my learning process in this journey.

First and foremost I would like to thank my mentor Dr. Sushama Gaikwad for being the driving force behind my success as a PhD student. Since the day I joined NCL, she has introduced me to the ways of the scientific world. She has given me the freedom to think and work on varied aspects of the research undertaken. I am very grateful for her patience, motivation and enthusiasm during the course of the study. I would always be indebted for her support and guidance.

I am thankful to Dr. Narendra Kadoo, my research supervisor, for his unconditional support during the course of study and thesis writing.

I thank my Doctoral assessment committee (DAC) members, Dr. C. G. Suresh, Prof. Sushma Sabharwal (Dept. of Chemistry, S. P. Pune University) and Dr. H. V. Thulasiram for their timely suggestions and for monitoring my progress throughout my PhD Tenure. Further I would like to acknowledge Dr. Suresh Kumar Ramaswamy for his kind help in the crystallization studies and Dr. Sudip Roy for the valuable discussion during MD simulation studies. I must thank Dr. Moneesha Fernandes for the CD facility and Dr. Siddharth Bhosale for technical help in time-resolved fluorescence studies. I am also grateful to Dr. R. Seeta Laxman for her kind gift of *Beauveria* culture to initiate the studies. I am grateful to Dr. Sumedha Deshmukh, Dr. Vaishali Javdekar (A.G. College, Pune) and Mrs. Snehal More for their support.

Completion of this work would not have been possible without the support of friends and lab mates who made this period memorable. So to begin with I would like to express gratitude towards my seniors Dr. Ansary, Dr. Avinash, Dr. Madhurima and Dr. Sonali, I have learnt so much from all of them and will always cherish unforgettable times spent with everyone. I would also like to thank my present labmates Priya, Ekta and Sanskruthi for their help and support.

I take this opportunity to show my gratitude towards my friends who have helped me in this work. I thank Deepak Chand and Shiva for teaching me basic techniques of protein crystallization. I must acknowledge Anil Mhashal for his remarkable help in molecular dynamics simulation studies. I appreciate the help and inputs from Ashish Deshpande and Dr. Hemangi Chidley in cloning trials.

I would like to express my special appreciation for my friends, without their love and encouragement; my life here in Pune and NCL would be so incomplete. I will always treasure the memories of time spent with Dr. Hemangi Bhonsale, Dr. Hemangi Chidley, Dr. Urvashi, Dr. Nishant Varshney, Dr. Tulika Jaokar, Dr. Priyabrata Panigrahi, Dr. Parth Patel, Dr. Prashant Sonawane, Dr. Ravi, Dr. Shadab, Dr. Pallavi Shankar, Dr. Ganesh Barhate, Dr. Suprit Kumar, Sana Moeez and Vidya Ghantani. I am grateful to my batch-mates Ruchira Mukharjee, Ashish Deshpande, Sheon Mary, Deepak Chand, Ruby Singh, Arati Deshmukh, Rubina Kazi and Shweta Bhat for being wonderful company. I must mention Hrishikesh Mungi, Deepanjan Ghosh, Ameya Bendre, Aditi Bhand, Shridhar Chougule and Pranjali Oak for fun times enjoyed with them in the division. All the moral support from my college buddies Ambreen, Nikita, Rutuja and Manasi is extremely treasured.

No words can express my gratitude towards my parents who made me capable of taking on this expedition and have been a continuous source of motivation to overcome every challenge encountered. I am obliged by the support extended by my in-laws, Juili and the family members during the course of the study. I take this opportunity to thank Manas, who has been my best friend, a helpful senior and most importantly a companion in every situation in this journey. I cannot imagine completing this task without his support.

I thank the Director, CSIR-National Chemical Laboratory and Head, Division of Biochemical Sciences, for permitting me to carry out my research work in the Division of Biochemical Sciences, CSIR- National Chemical Laboratory. I am also thankful to the scientists, staff of Biochemical Sciences Division, library staff, student academic office, administrative and technical staff for their help during the course of my study. The financial assistance from the Council of Scientific and Industrial Research, India is duly acknowledged.

Finally, I would like to thank all those who have helped me directly or indirectly during my journey to date.

Sayli Dalal

LIST OF ABBREVIATIONS USED

ANS	1-anilino-8-naphthalenesulfonate
Asp	Aspartate
Bprot	Protease from *Beauveria sp.* MTCC 5184
CD	Circular dichroism
F_a	Accessible fraction
GdnHCl	Guanidine hydrochloride
His	Histidine
kDa	Kilo Dalton
KLK	Kallikrein
KLKp	Porcine pancreatic kallikrein
K_{sv}	Stern-Volmer (dynamic) quenching constant
MD	Molecular dynamics
MG	Molten globule
MRE	Mean Residual Ellipticity
NBS	N-Bromosuccinimide
NRMSD	Normalized root mean square deviation
PAGE	Polyacrylamide gel electrophoresis
PDB	Protein Data Bank
PMSF	Phenylmethylsulfonyl fluoride
Rg	Radius of gyration
RMSD	Root mean square deviation
RMSF	Root mean square fluctuation
rpm	Revolutions per minute
SASA	Solvent accessible surface area
SDS	Sodium dodecyl sulphate
Ser	Serine
Trp	Tryptophan

ABSTRACT

Chapter 1: Introduction

The significance and updates in protein folding/ unfolding research have been described. A brief introduction to serine proteases in terms of their classification, structure and function is given. The available information on fungal proteases and tissue kallikreins has been summarized as the basis of studies undertaken in the thesis.

Chapter 2: Biophysical characterization of Serine Protease from *Beauveria sp.* MTCC 5184

Biophysical characterization of the subtilisin-like serine protease from *Beauveria* sp. MTCC 5184 (Bprot) was performed using steady state and time resolved fluorescence, circular dichroism, FT-IR spectroscopy and x-ray crystallography. Also, the enzyme was examined for its kinetic stability. The microenvironment of a single tryptophan residue in Bprot was studied using steady state and time resolved fluorescence. The emission maximum of intrinsic fluorescence was observed at 339 nm indicating Trp to be buried in the hydrophobic core. Solute quenching studies were performed with neutral (acrylamide) and ionic (I^- and Cs^+) quenchers to probe the exposure and accessibility of Trp residue of the protein. Maximum quenching was observed with acrylamide. In native state, quenching was observed with I^- and not with Cs^+ indicating presence of positively charged environment surrounding Trp residue. However, in denatured protein, quenching was observed with $Cs^{+,}$ indicating charge reorientation after denaturation. Time resolved fluorescence measurements established presence of two conformers of Trp. Bprot was proposed to have α/β hydrolase fold based on the far UV CD spectrum and known structural elements reported for subtilases. Preliminary crystallization and X-ray diffraction data for Brot was reported. Structural resistance of Bprot towards SDS and proteolytic environment suggested that it could be kinetically stable protein.

Chapter 3: Functional and Conformational transitions of Serine Protease from *Beauveria sp.* MTCC 5184

Beauveria protease (Bprot) was studied for its functional and conformational stability under denaturing conditions using spectroscopic approach. Retention of total activity of the protease in the vicinity of (1) 3 M GdnHCl for 12 h, (2) 50 % methanol and dimethyl sulfoxide each for 24 h indicated its unusual stability. Also, the structure of the protein was stable at pH 2.0 upto 4 hours. The secondary structure of Bprot was stable in 3 M GdnHCl as seen in far-UV CD spectra. The active fraction of Bprot obtained from size-exclusion chromatography in the presence of GdnHCl (1.0–3.0 M) eluted at reduced retention time. The peak area of inactive or denatured protein with the same retention time as that of native protein increased with increasing concentration of denaturant (1.0–4.0 M GdnHCl). However, the kinetics of GdnHCl-induced unfolding as studied from intrinsic fluorescence revealed k_{unf} of native protein to be 5.407×10^{-5} s^{-1} and a half-life of 3.56 hours. The enzyme is thermodynamically stable in spite of being resistant to the denaturant, which could be due to the effect of GdnHCl imparting rigidity to the active fraction and simultaneously unfolding the partially unfolded protein that exists in equilibrium with the folded active protein. Functional stability of Bprot in 50% methanol correlated well with the maintenance of secondary structure after 24 hours. Thermal denaturation of Bprot indicated the T_m to be 56℃ by both fluorescence and CD studies. Acid denatured Bprot exhibited interesting structural transitions in presence of organic solvents. In presence of fluoroalcohols, Bprot was less stable in HFIP as compared to TFE. HFIP served as better helix inducer for acid denatured Bprot.

Chapter 4: Functional and conformational transitions of Kallikrein

Porcine pancreatic kallikrein (KLKp) was taken up as a model for functional and conformational dynamics studies under denaturing conditions like presence of GdnHCl, thermal denaturation and pH induced denaturation by spectroscopic approach (fluorescence and CD spectroscopy). Fluorescence and solute quenching studies revealed the positively charged and partial hydrophilic environment of Trp residues. β-sheet dominant secondary structure of KLKp was studied by far UV CD studies that correlated well with existing crystal structure information available. Although kallikrein was

structurally stable up to 90°C as indicated by secondary structure monitoring, it was functionally stable only up to 45°C, implicating thermolabile active site geometry. In GdnHCl [1.0 M], 75% of the activity of KLKp was retained after incubation for 4h, indicating its denaturant tolerance. A molten globule like structure of KLKp formed at pH 1.0 was more thermostable and exhibited interesting structural transitions in organic solvents.

Chapter 5: Stability of Kallikrein in organic solvents

Porcine pancreatic kallikrein (KLKp) was investigated for its functional and conformational transitions in presence of organic solvents using biochemical and biophysical techniques and molecular dynamics (MD) simulations approach. The enzyme was exceptionally stable in isopropanol and ethanol showing 110% and 75% activity, respectively after 96h, showed moderate tolerance in acetonitrile (45% activity after 72 h) and much lower stability in methanol (40% activity after 24h) (all the solvents [90% *v/v*]). Far UV CD and fluorescence spectra indicated apparent reduction in compactness of KLKp structure in isopropanol system. MD simulation studies of the enzyme in isopropanol revealed 1) minimal deviation of the structure from native state 2) marginal increase in radius of gyration (Rg) and solvent accessible surface area (SASA) of the protein and the active site and 3) loss of density barrier at the active site possibly leading to increased accessibility of substrate to catalytic triad as compared to methanol and acetonitrile.

Chapter 6: Summary and conclusion

CONTENTS

Chapter 1

Introduction

1. Introduction

1.1 Protein folding

Proteins are the molecular instruments through which biological functions are executed. The transformation of a linearly translated strand of amino acid into a fully functional three dimensional protein i.e. folding of protein proved to be one of the most complex stages of protein chemistry. The protein folding problem was born fifty years ago as a challenge of basic science and continues to motivate much theoretical and experimental work.

1.1.1 Protein folding theories:

Protein folding can be defined as the self-organization of proteins into three-dimensional units, frequently under the eventual coordinated action of chaperones (Carvalho et al 2013**)**. It was known from seminal experiments by Christian Anfinsen that small proteins could spontaneously refold from their denatured states, and so the primary structure (sequence) of a protein dictates its tertiary structure (Fersht 2008). Protein folding is an extremely fast process that cannot possibly depend on a purely random-search mechanism, as stated by the Levinthal's paradox (Fersht 2008). A few suggestions have been put forward to explain possible mechanisms of protein folding. Two alternative models prevailed, the first of which was the framework model and the related diffusion–diffusion model, in which secondary structure is proposed to fold first, followed by docking of the pre-formed secondary structural units to yield the native, folded protein. The second was the hydrophobic collapse model, in which hydrophobic collapse drives compaction of the protein so that folding can take place in a confined volume, thereby narrowing the conformational search to the native state (Daggett and Fersht 2003). Further experimental work on chymotrypsin inhibitor 2 (CI2) (Otzen et al 1994) led to nucleation condensation mechanism which unites features of both the hydrophobic collapse and framework mechanisms. Nucleation-condensation triggers the formation of long range and other native hydrophobic interactions in the transition state to form stable folds.

As per current understanding of protein folding, the mechanism can be illustrated in energetic terms as a folding funnel, such as the represented in Fig. 1. In short, the funnel concept states that as the protein folding reaction proceeds, the entropy of the polypeptide chain (and the surrounding solvent) decreases as more intricate and compact structures are formed that are richer in intra- molecular interactions and thus have lower entropy. The transiently stable conformations accumulate, with the deeper energy minima promoting the formation of more stable intermediate conformations (Gomes 2012). However, in spite of this wealth of information, a detailed understanding of the protein folding process demands additional experimental data.

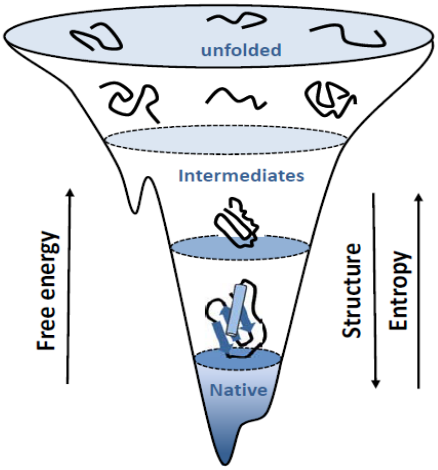

Figure 1: A folding funnel diagram depicting the folding process of a typical small globular protein. Unfolded polypeptides in random conformations are represented at the top of the funnel, where entropy is maximal; as structure is gradually acquired, free energy decreases and the number of conformers narrows via intermediate states down to the native state which is represented by the basin at the bottom of the funnel. (Figure adapted from Gomes 2012).

1.1.2 Protein misfolding in disease: destabilized folds and aggregates

The cellular machinery has evolved a stringent quality control system as part of the proteostasis network that ensures proper protein folding, trafficking and degradation (Lindquist and Kelly 2011). However, a number of proteins still fail to reach or maintain their native conformation subsequently leading to protein misfolding. When unfolded or misfolded proteins cannot be refolded by protein chaperones, they are

targeted to the proteasome or the lysosome for degradation (Denny et al 2013). The factors contributing to misfolding include somatic or genetic mutations, aging, changes in the intracellular environment such as pH, temperature, oxidative stress and metal ions, etc., which are summarized in Fig. (2).

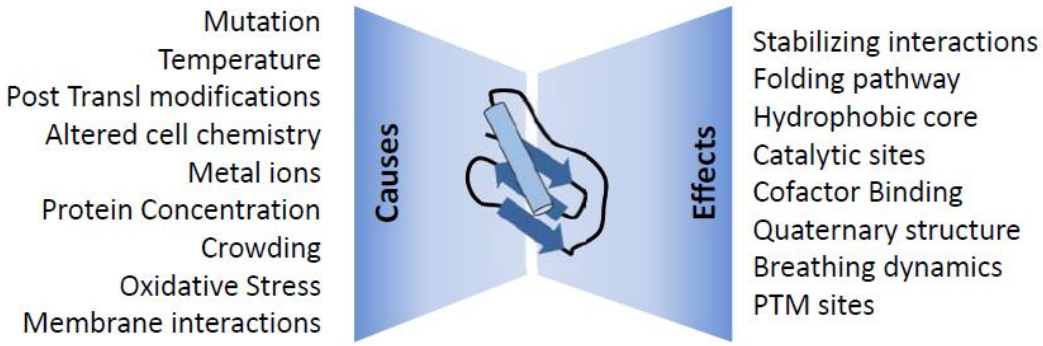

Figure 2: Outline of factors that cause protein misfolding or defects in protein folding and consequent effects. Cell homeostatic processes attempt to minimize both causes and effects but disease arises upon significant perturbation of the system. (Figure adapted from Gomes 2012).

These factors lead to accumulation of misfolded proteins resulting in toxic gain of function due to protein aggregation, or loss of function due to protein instability, inefficient folding or defective trafficking (Gomes 2012). The disorders arising from the cumulative effect of these errors are collectively referred to protein misfolding diseases. Some pathologies within this group also result from defects on molecular chaperones. Representative examples of the protein misfolding diseases are given below in table 1:

Table1: Examples of protein folding diseases and corresponding affected proteins

Disease	**Protein** (Gomes 2012)	**Chemical Chaperone/ Pharmacological Chaperone** (Leandro and Gomes 2008)
Diseases resulting from protein misfolding and destabilization with no aggregation		
Phenylketonuria (PKU)	Phenylalanine hydroxylase (PAH)	Glycerol, BH_4

Gaucher's Disease	Glucosylceramidase	Deoxynojirimycin derivatives
Cystic fibrosis	Cystic fibrosis transmembrane conductance regulator (CFTR)	Glycerol, DMSO,TMAO, 4-PB, TS3 (limonoid compound), VRT325, corr-2b; corr-4a
Pompe Disease	Acid alpha-glucosidase	Deoxynojirimycin derivatives
Fabry Disease	Alpha-galactosidase (GLA)	Galactose, 1-deoxy-galactonojirimycin
Homocystinuria	Cystathionine beta-synthase (CBS)	TMAO, glycerol, sorbitol, proline; DMSO
Multiple acyl-CoA Dehydrogenase deficiency (or Glutaric aciduria type II)	Electron transfer flavoprotein (ETF) ETF ubiquinone oxidoreductase (ETF: QO)	
Diseases resulting from protein misfolding with aggregation (amyloid)		
Alzheimer's disease (AD)	Amyloid β peptide	TMAO, glycerol
Spongiform encephalopathies (TSE)	Prion protein	
Parkinson's disease (PD)	α-Synuclein	TMAO
Amyotrophic lateral sclerosis (ALS)	Superoxide dismutase 1	
Huntington's disease (HD)	Huntingtin (polyQ)	Trehalose
Lysozyme amyloidosis	Lysozyme	
Type II diabetes	Amylin	Glycerol; TMAO; DMSO
Familial amyloidotic polyneuropathy (FAP)	Transthyretin	Thyroxin, TTR ligands
Light chain amyloidosis	Immunoglobulin light chains	
Hemodialysis-related	β2-microglobulin	

amyloidosis		
Diseases resulting from defects in molecular chaperones (chaperonopathies)		
Hereditary Spastic Paraplegia	Hsp60	
Spastic ataxia Charlevoix-Saguenay	Sacsin (DnaJC29)	
Cataracts Myofibrillar Myopathy	α crystalline B	

1.1.3 Chemical chaperones as possible therapeutic strategies:

The protein misfolding disorders present exciting drug discovery opportunities in a wide range of therapeutic areas. In recent years the use of small molecules to rescue folding defects in proteins involved in conformational disorders has been explored and overviewed in several reviews (Gomes 2012, Lindquist and Kelly 2011, Leandro and Gomes 2008, Perlmutter 2002, Chaudhuri and Subhankar Paul 2006, Cohen & Kelly 2003, Valastyan and Lindquist 2014). These compounds, known as "chemical chaperones", include mainly of osmolytes and protein stabilizers. One group of these chemical chaperones includes polyols (e.g. glycerol, sorbitol), sugars (e.g. trehalose), methylamines (e.g. trimethylamine-N-oxide, glycine, betaine and glycerophosphorylcholine) or even free amino acids (e.g. glycine, taurin) or its derivatives (e.g. ectoine and gama-aminobutyric acid). Other low molecular weight compounds such as deuterium oxide (D_2O), dimethyl sulfoxide (DMSO) and 4-phenylbutyrate (4- PB) have also been associated to a chaperone-like function (Leandro and Gomes 2008). The mechanisms by which chemical chaperones function are not fully understood but are thought to include stabilization of improperly folded proteins, reduction of aggregation, prevention of nonproductive interactions with other resident proteins and alteration of the activity of endogenous chaperones in such a way that the affected proteins are more efficiently transported to the appropriate intracellular or extracellular destination (Perlmutter 2002). The other group of these molecules comprises of competitive inhibitors, ligands, agonists/antagonists, and

protein cofactors, including metal ions which affect only the specific proteins with which they interact as compared to the non-specific effect exerted by small molecules described earlier. Thus, the understanding of the mechanisms of protein folding, unfolding, refolding, and misfolding is of great interest from the point of view of the medical, pharmaceutical and industrial uses of proteins (Righetti and Verzola 2001). Molecular understanding of the effect of cosolvents on conformational dynamics of the protein will likely pave the way to the development of novel therapeutics to treat many devastating diseases.

1.1.4 Studying folding/ unfolding transitions of proteins:

A protein exists in equilibrium with unfolded conformational states in solution with the folded ensemble being favored at ambient conditions. This equilibrium between the folded and the unfolded states can be perturbed by changing the thermodynamic state of the system (temperature, pressure, pH) or by changing the composition by the addition of cosolvents to the solution. The shift in the conformational equilibrium from folded to unfolded states is known as denaturation (Canchi and García 2013). Also, the effect of cosolvents on the protein folding ensemble can be favored in any direction. Cosolvents such as urea and guanidinium chloride induce disorder and favor the unfolded states are thus known as denaturants/ chaotrpoes. On the other hand, protecting osmolytes/ kosmotropes like Trimethylamine N-oxide (TMAO), glycine, betaine, glycerol, and sugars induce stabilization of the folded proteins. The Structural and conformational transitions of proteins depending on solvent conditions are a significant way to elucidate their stability, folding pathways, and intermolecular aggregation behavior (Varshney et al 2014).

Protein stability encompasses several aspects in which the environment affects protein structure and function. It is majorly dictated by forces that help in maintaining the native structure of a protein which include disulfide bonds and the weak (noncovalent) interactions like hydrogen bonds, and hydrophobic and ionic interactions. **The biochemical stability** of a protein is related to its resistance to experience changes in its activity/structure when subjected to stress conditions. Low biochemical stability results in progressive decline in population of active molecules

in irreversible manner that compromises function of the protein (Sancho 2013). Thus, increasing the chemical stability of protein molecules is of interest in order to increase their applicability in biotechnological processes that require extreme conditions such as high temperature, low pH, presence of cosolvents, etc. (Eijsink et al 2004). Moreover, increasing application of biologics as therapeutic agents (Gecse et al 2013) makes the optimization of biological stability an important goal.

The **conformational/ thermodynamic stability** relates to maintenance of equilibrium between the folded native state of the protein with the unfolded fraction of molecules. The term **kinetic stability** is used to describe proteins that are trapped in a specific conformation because of an unusually high-unfolding barrier that results in very slow unfolding rates (Manning and colon 2004). Resistance towards SDS, proteolytic environment and guanidine hydrochloride are common tests for establishing the kinetic stability of a protein. A particular type of kinetic stability is **mechanical stability** that refers to the resistance of native proteins to be unfolded by external forces, and it is studied with atomic force microscopes or optical tweezers. It plays important roles in essential cellular processes such as cell division, cell adhesion, protein translocation, locomotion, etc. (Crampton and Brockwell 2010). Experiments on protein stability as a function of the various control parameters like pressure, temperature, cosolvent, pH, etc., are numerous. However, experiments in which the complete stability phase diagram was determined in correlation to function of the enzyme are still quite scarce (Scharnagl et al 2005).

1.1.5 Tools for probing protein stability and folding/ unfolding dynamics:

Over last 25 years, detailed experimental and theoretical studies of a number of proteins have advanced our understanding of protein folding and dynamics. Table 2 gives the summary of techniques used to probe the protein unfolding and structural intermediates formed during the process.

Table 2: Experimental techniques used to measure folding/ unfolding (Table adapted from Radford 2000)

Sr.No.	Technique	Structural parameter probed	Reference
1	Fluorescence		(Eaton et al 2000)
a	Intrinsic	Environment of Trp and Tyr	
b	ANS binding	Exposure of hydrophobic surface area	
c	Substrate binding	Formation of the active site	
d	FRET	Inter-residue distances	
e	Anisotropy	Correlation time	
f	Fluorescence Correlation Spectrocopy	Autocorrelation analysis of fluctuations in fluorescence emission due to internal dynamics	(Haustein, E., & Schwille 2007)
g	2-D fluorescence lifetime correlation spectroscopy	Correlation of the fluorescence photon pairs with respect to the excitation−emission delay times	(Ishii and Tahara 2013)
h	Single molecule spectroscopy (Sm-FRET and sm-PET)	Distance between fluorophores dynamics	(Schuler et al 2013)
i	Red Edge Excitation Shift	Rate of solvent relaxation around an excited state fluorophore in a protein	(Chattopadhyay, and Haldar 2013)
2	Circular dichroism		(Kelly et al 2005)
a	Far UV	Secondary-structure formation	
b	Near UV	Tertiary-structure formation	

3	Protein engineering	Role of individual residues in stabilizing intermediates and transition states	(Eijsink et al 2004)
4	Small-angle X-ray scattering	Dimension and shape of polypeptide	(Pollack et al 1999)
5	Absorbance (near UV)	Environment of aromatic residues or co-factors	(Eaton et al 2000)
6	FTIR	Secondary-structure formation	(Troullier et al 2000)
7	NMR		(Neira et al 2013)
a	Real time	Environment of individual residues	
b	Dynamic NMR	Lineshape analysis provides folding–unfolding rates close to equilibrium	
8	Hydrogen exchange (HX)		(Miranker et al 1996)
a	Native state	Global stability and metastable states	
b	Pulsed HX NMR	Hydrogen-bond formation in specific residues	
9	Pulsed HX ESI MS	Folding populations	
10	Force spectroscopy (AFM or ‘optical tweezers’)	Unfolding forces and unfolding-rate constants of single molecules	(Carvalho et al 2013)
11	Differential scanning calorimetry (DSC) or micocalorimetry	Energetics	(Johnson 2013)
12	Differential scanning	Environment of fluorescent	(Senisterra and

	fluorimetry (DSF)	dye	Finerty 2009)
13	Differential static light scattering(DSLS)	Temperature of aggregation of a protein	

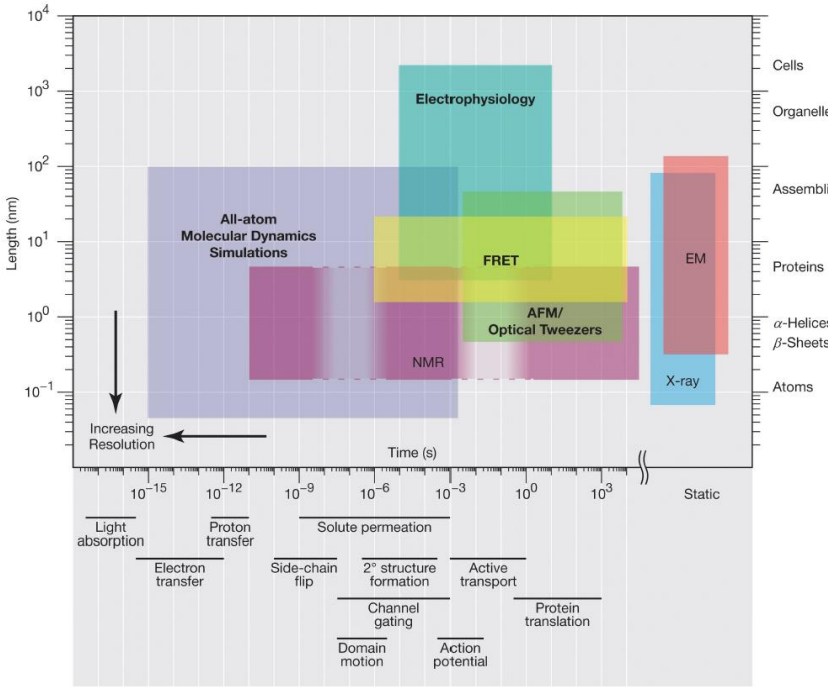

Figure 3: Spatiotemporal resolution of various biophysical techniques: The temporal (abcissa) and spatial (ordinate) resolutions of each technique are indicated by colored boxes. Techniques capable of yielding data on single molecules (as opposed to only on ensembles) are shown in bold. Nuclear magnetic resonance methods can probe a wide range of timescales, but they provide limited information on motion at certain intermediate timescales, as indicated by the lighter shading and dashed lines. The timescales of some fundamental molecular processes, as well as composite physiological processes, are indicated below the abcissa. The (spatial) resolution needed to resolve certain objects is shown at right. AFM, atomic force microscopy; EM, electron microscopy; FRET, Förster resonance energy transfer; NMR, nuclear magnetic resonance (Figure adapted from Dror et al 2010).

1.1.6 Theoretical studies of protein unfolding:

A number of theoretical techniques are employed to complement experiment to provide an overall picture of the process. Among other simulation techniques,

molecular dynamics (MD) plays a distinctive role in the area of protein folding owing to its simplicity and accuracy for sampling the energy landscape of a macromolecule in an unbiased way (Rizzuti and Daggett 2013). Simulation studies of protein unfolding during thermal denaturation or in presence of co-solvents supplement the experimental data providing both a framework for data interpretation and a guide for further investigations.

Present studies concentrate on selected serine proteases for their functional and conformational transitions under denaturing conditions. Following is a brief account of information available about this important group of enzymes:

1.2 Proteases

A protease is defined as an enzyme that hydrolyses peptide bonds and is also referred to as peptidase or proteinase (Hooper 2002). The physiological function of proteases is necessary for all living organisms, from viruses to humans, and proteolytic enzymes can be classified based on their origin: microbial (bacterial, fungal and viral), plant, animal and human enzymes (Mótyán et al 2013).

Proteases belong to the class of hydrolase enzymes (EC 3) and subclass of the peptidases (EC 3.4). Proteases are subdivided into exopeptidases and endopeptidases depending on the site of enzyme action. Exopeptidases catalyze the hydrolysis of the peptide bonds near the N- or C-terminal ends of the substrate and can be classified into aminopeptidases and carboxypeptidaes. Endopeptidases cleave peptide bonds within and distant from the ends of a polypeptide chain (Rao et al 1998).

Based on the catalytic mechanism and the presence of amino acid residue(s) at the active site the proteases can be grouped as aspartic-, cysteine-, glutamic-, metallo-, asparagine-, serine-, threonine- proteases, and proteases with mixed or unknown catalytic mechanism (Rawlings et al 2012). The catalytic mechanisms differ most evidently in the presence or absence of a covalent acyl-enzyme intermediate on the reaction pathway. The catalyses of serine and cysteine peptidases involve the covalent intermediate (ester and thiolester, respectively), whereas the aspartic and the metallopeptidase catalyses do not. During hydrolysis carried out by the latter two

groups, the substrate is attacked directly by a water molecule rather than by a serine or cysteine residue (Polgar 2005). At present, 3% of the proteases in the human genome have been identified as aspartic proteases, 23% as cysteine proteases, 36% as metalloproteases and 32% as serine proteases (Southan 2001).

Rawlings and Barett devised a classification scheme based on statistically significant similarities in sequence and structure of all known proteolytic enzymes and compiled the information in MEROPS database in 1996. The database has been expanding since then to track the advances in knowledge pool of proteases. Storage and retrieval of this information is facilitated by the use of a hierarchical classification system, in which homologous peptidases are divided into clans and families (Polgar 2005). The classification system divides peptidases into clans based on catalytic mechanism and families on the basis of common ancestry (Page and Di Cera 2008).

1.2.1 Serine proteases

Over one third of all known proteolytic enzymes are serine peptidases. According to MEROPS database version 9.9 (https://merops.sanger.ac.uk) over 183000 serine proteases are known with >250 structure depositions in PDB. The serine peptidases have been classified into 15 clans comprising of numerous families. A summary of catalytic units in all serine peptidase families and their characteristic folds is provided in Table 3. Characteristic folds and representative structures from each clan have been presented in figure 3.

Table 3. Known diversity of serine peptidase structure and catalytic mechanism. (Table adapted from Page and Di Cera 2008).

Clan	Families	Representative members	Fold	Catalytic residues	PDB
PA	12	Trypsin	Greek-key β-barrels	His, Asp, Ser	1DPO
PB	1	Protease from *Thermoplasma*	α/β/β/α	His, Glu, Ser	1PMA

		acidophilum			
PC	1	Aspartyl dipeptidase	α/β/α	Ser, His	1FYE
SB	2	Subtilisin, sedolisin	3-layer sandwich	Asp, His, Ser	1SCN
SC	2	Prolyl oligopeptidase	α/β hydrolase	Ser, Asp, His	1QFS
SE	6	D-Ala–D-Ala carboxypeptidase	α-helical bundle	Ser, Lys	3PTE
SF	3	LexA peptidase	all β	Ser, Lys/His	1JHH
SH	2	Cytomegalovirus assemblin	α/β Barrel	His, Ser, His	1LAY
SJ	1	Lon peptidase	α+β	Ser, Lys	1RR9
SK	2	Clp peptidase	αβ	Ser, His, Asp	1TYF
SP	3	Nucleoporin	all β	His, Ser	1KO6
SQ	1	Aminopeptidase DmpA	4-layer sandwich	Ser	1B65
SR	1	Lactoferrin	3-layer sandwich	Lys, Ser	1LCT
SS	14	L,D-Carboxypeptidase	β-sheet+ β-barrel	Lys, Ser	1ZRS
ST	5	Rhomboid	α-barrel	His, Ser	2IC8

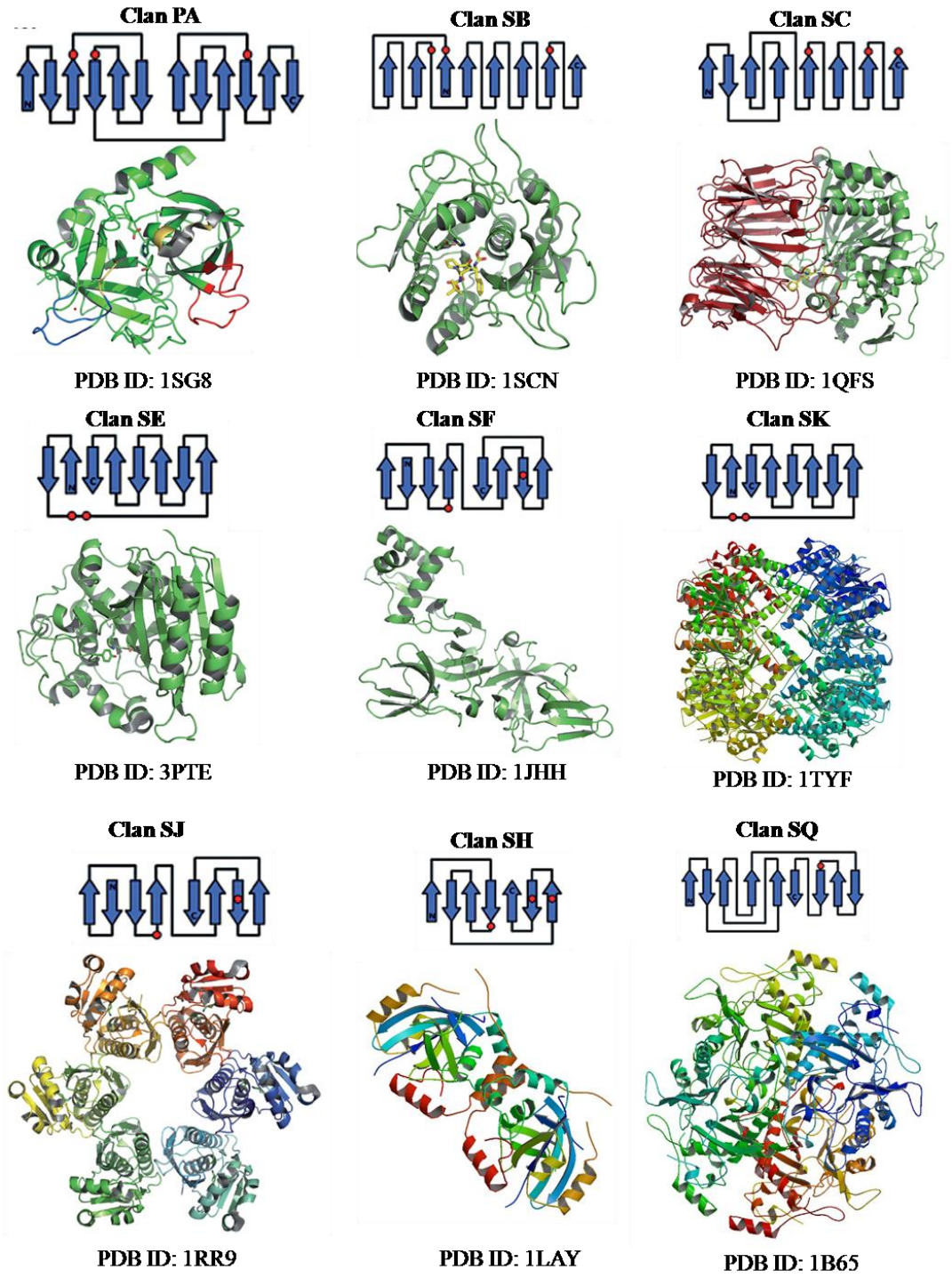

Figure 3: β-Strand topology and representative structures of different clans of serine peptidases: Positions of the catalytic residues are indicated with red dots. β-Strand topologies adapted from Page and Di Cera [2008]. Representative structures from each clan are shown with respective PDB ID mentioned below.

1.2.2 Catalytic mechanism of serine proteases

Nearly all clan PA peptidases utilize the canonical catalytic triad of Ser195, Asp-102 and His-57 (chymotrypsin numbering). Catalysis proceeds through formation of H-bond between Asp-102 and His-57, which facilitates the abstraction of the proton from Ser195 and generates a potent nucleophile (Page and Di Cera 2008). The catalytic triad is stabilized through a network of additional H-bonds formed by conserved amino acid residues surrounding the triad, which are Thr54, Ala56 and Ser214. The reaction pathway involves two tetrahedral intermediates. Initially, the hydroxyl O atom of Ser195 attacks the carbonyl of the peptide substrate as a result of His57 in the catalytic triad acting as a base. The backbone N atoms of Gly193 and Ser195 stabilize the tetrahedral intermediate and generate a positively charged pocket within the active site known as the oxyanion hole. Collapse of the tetrahedral intermediate results in acyl-enzyme intermediate. In the second half of the mechanism, a water molecule displaces the free polypeptide fragment and attacks the acyl-enzyme intermediate. Again, the oxyanion hole stabilizes the second tetrahedral intermediate of the pathway and collapse of this intermediate liberates a new C terminus in the substrate.

Activation of many chymotrypsin-like serine peptidases requires proteolytic processing of an inactive zymogen precursor protein. Zymogen activation provides a powerful regulatory mechanism that provides temporal control over peptidase activity, prevents premature enzyme inhibition, and places these enzymes within the context of chains of proteolytic events. The chymotrypsin fold assists all these properties and creates a proteolytic network responsible for key biological processes responsible for human health.

Clan SB and SC peptidases have similar geometry of catalytic triad to that of clan PA peptidases but the surrounding protein fold bears no similarity. The difference in structural fold from clan PA peptidases provides a versatile catalytic platform to clan SB and SC peptidases. This is the primary reason for subtilisin being a model for protease engineering in order to enhance its catalytic efficiency.

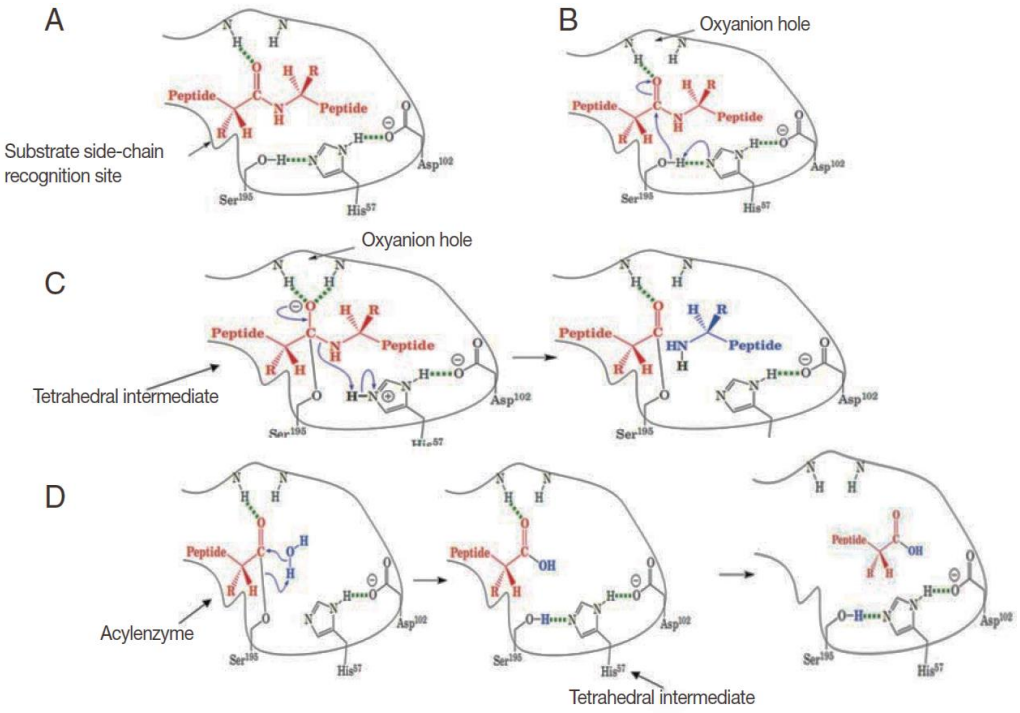

Figure 4: A schematic illustration of general catalytic mechanism for serine proteases (A) Substrate binding: substrate binds to the recognition site of the serine protease and exposes the carbonyl of the scissile amide bond. (B) Nucleophilic attack: His 57 attracts the proton from the hydroxyl group of Ser 195 and the Sser 195 attacks the carbonyl of the peptide substrate. (C) Protonation: The amide of peptide subtract accepts a proton from His 57 and dissociates. (D) Deacylation: water molecule attacks the acyl-enzyme complex and catalytic triad is restored. (Figure adapted from Yang et al 2015)

1.2.3 Distribution and biological functions of clans of serine peptidases:

The serine proteases are widely distributed in nature and found in all kingdoms of cellular life as well as many viral genomes. The distribution of each clan across species differs significantly.

- Clan PA proteases comprise of two subfamilies: S1A peptidases which are more abundant in vertebrates to mediate extracellular processes as compared to plants, prokaryotes and the archaea and S1B peptidasaes that are responsible for intracellular protein turnover and are found in all cellular life. Many chymotrypsin-like serine peptidases in clan PA require proteolytic processing of an inactive zymogen precursor protein for activation.

- Clan SB peptidases are prevalent in plant and bacterial genomes with few representatives in animal genome. However, these proprotein convertases are vital for protein processing in all metazoa (Rockwell and Thorner 2004).

- Clan SC peptidases are the second largest family of serine peptidases in the human genome. They contain α/β hydrolase fold that provides a versatile catalytic platform for these peptidases which can also act as esterase, lipase, dehalogenase, haloperoxidase, lyase or epoxide hydrolase under specific conditions. They are particularly important in cell signaling mechanisms.

- Clan SE peptidases are important in bacterial cell wall metabolism and have low distribution in higher animals. Biological roles of peptidases belonging to other clans has been summarized by Page and Di Cera (2008).

1.2.4 Applications of proteases:

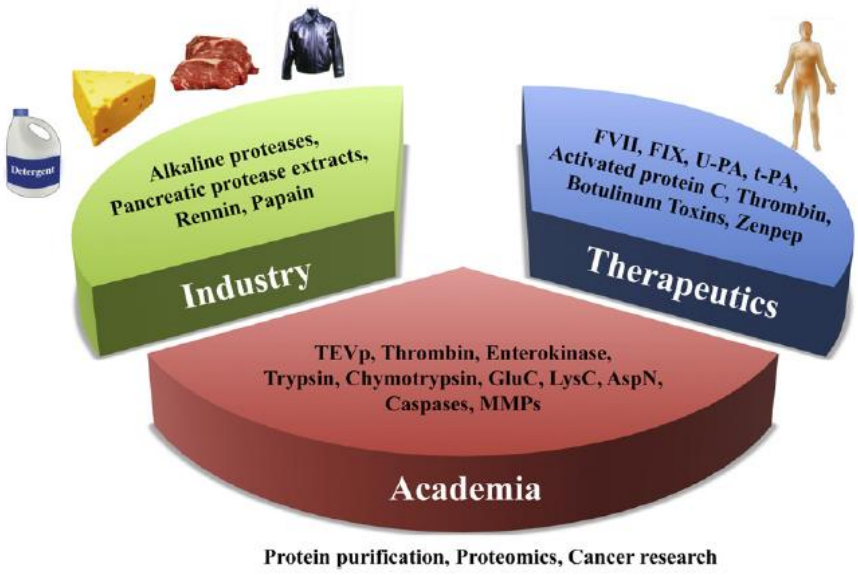

Figure 5: An overview of protease applications (Figure adapted from Li et al 2013)

Proteases have been applied in the detergent, leather and food industries for several hundred years. For example, alkaline proteases have been used to remove hair from hides, pancreatic protease extracts for use in detergents, leather processing and peptide synthesis. Using proteases in detergents for improved stain removal

contributes to almost 60% of total enzyme market (Niyonzima and More 2015). Other uses of proteases include silver recovery from photographic films by gelatin hydrolysis, in membrane and equipment cleaning processes and in biopolishing of wool fabrics (Sumantha et al 2006). Food industry applies several proteases, for example, acidic protease rennet from unweaned calves to coagulate milk for cheese production, papain and bromelein to tenderize meat as well as to improve the nutritional value of feeds, neutral proteases in extraction of rice starch,etc. (Sumantha et al 2006).

Apart from being commercially important, proteases find crucial role in research applications that involve production of Klenow fragments, peptide synthesis, digestion of unwanted proteins during nucleic acid purification, cell culturing and tissue dissociation, preparation of recombinant antibody fragments for research, diagnostics and therapy, exploration of the structure-function relationships by structural studies, removal of affinity tags from fusion proteins in recombinant protein techniques, peptide sequencing and proteolytic digestion of proteins in proteomics (Mótyán et al 2013). Craik et al (2011) have reviewed the emerging importance of proteases in recent times. Table 4 gives an account of FDA approved serine protease drugs. Numerous other proteases are under pre-clinical and clinical stages of development.

Table 4: FDA-approved serine protease drugs. Table adapted from (Craik et al 2011)

Usage	Protease	Indications	Source of protein	Target protein or pathway
Thrombolysis	Urokinase (u-PA)	Thrombus, catheter clearing	Extracted from urine or from primary kidney cell culture	Converts plasminogen into plasmin
	t-PA (alteplase, Activase®)	AMI, stroke, catheter clearing	Recombinant in CHO cells	Plasminogen activator

	Reteplase (Retevase)	AMI	Recombinant in *E. coli*	Plasminogen activator
	TNK-tPA (tenecteplase, Metalyse®)	Myocardial infarction	Recombinant in CHO cells	Plasminogen activator
Procoagulant	FIX	Haemophilia B	Human plasma	FX activator
	FIX (BeneFIX®)	Haemophilia B	Recombinant in CHO cells	FX activator
	FVIIa (NovoSeven®)	Haemophilia A and B	Recombinant in BHK cells	FX and FIX activator
	Topical thrombin in bandages	Bleeding	Bovine	Fibrinogen activator
	Thrombin (Recothrom®)	Bleeding	Recombinant in CHO cells	Fibrinogen activator
Sepsis	Activated protein C, (drotrecogin alfa, Xigris®)	Sepsis, septic shock	Recombinant in human cell line	Plasminogen activator
Digestion	Zenpep® (pancrelipase)	Exocrine Pancreatic Insufficiency	Porcine pancreatic extract	Aids digestion of protein

Several aspects of proteases have stimulated research on the study of biochemical, regulatory and molecular aspects of proteolytic enzyme systems (Rao et al.1998). However, the commercial application of proteases often requires maintainance of activity and specificity under extreme conditions such as high temperatures and pH, intensive calcium chelating agents, detergents, solvents and oxidizing agents (Li et al 2013). A lot of research has been aiming at discovery and engineering of novel enzymes that are more robust with respect to their environment and reaction conditions. Protease engineering by site-directed mutagenesis or directed-evolution can generate proteases with improved functions to meet the requirements of commercial applications. This involves increased half-life, altered specificity and increased tolerance towards stress conditions. These alterations require molecular understanding of principles that govern protease function and stability.

Present thesis uptakes investigation of following two serine proteases from different clans as model proteins for their functional and conformational dynamics under denaturing conditions:

1. Subtilisin-like protease from *Beauveria sp.* MTCC 5184 (Bprot)
2. Porcine pancreatic kallikrein (KLKp)

1.3 Fungal proteases:

Owing to their physiological and industrial applications, protease production and characterization from microbial sources has been an area of interest for many years. Microorganisms are preferred as a protease source because of their great biochemical diversity, susceptibility to genetic manipulation and high production rate. Bacterial proteases are the most commercialized enzymes. The most studied microorganisms belong to Bacillus genera (Borgi and Gargouri 2013). Nevertheless, several studies report biochemical and molecular characterization of fungal proteases (Rao et al., 1998), which are more advantageous owing to the ease of preparation of cell-free enzymes. In recent years, various reviews have summarized the commercial production and application of fungal proteases (Souza et al 2015, Srilakshmi et al 2015, Nirmal et al 2011) from psychrophilic, mesophilic and thermophilic fungi that encompasses over 60 species. The major share of these fungal proteases market is contributed by *Aspergillus* species. Subtilisins are particularly attractive as they display broad substrate specificity and high stability at neutral and alkaline pH (Ruan et al., 2008). They are widely used in biotechnology, mainly in detergent, food and leather industries, in ecological bioremediation processes and in the therapeutic peptides.

Fungal proteases also play an important role in fungal physiology, nutrition as well as are known to have physiological implications in higher animals including humans. Both saprophytic and pathogenic species rely on external digestion of protein substrates by secreted proteases for survival and growth. Proteolytic enzymes from fungi contribute to inflammation through interactions with the kinin system as well as the coagulation and fibrinolytic cascades. Their effect on the host protease–

antiprotease balance results from activation of endogenous proteases and degradation of protease inhibitors. Recent studies of the role of fungi in human health point to the growing importance of proteases not only as pathogenic agents in fungal infections but also in asthma, allergy, and damp building related illnesses (Yike 2011). Figure 6 summerizes functions of fungal proteases in physiology, disease, and biotechnology.

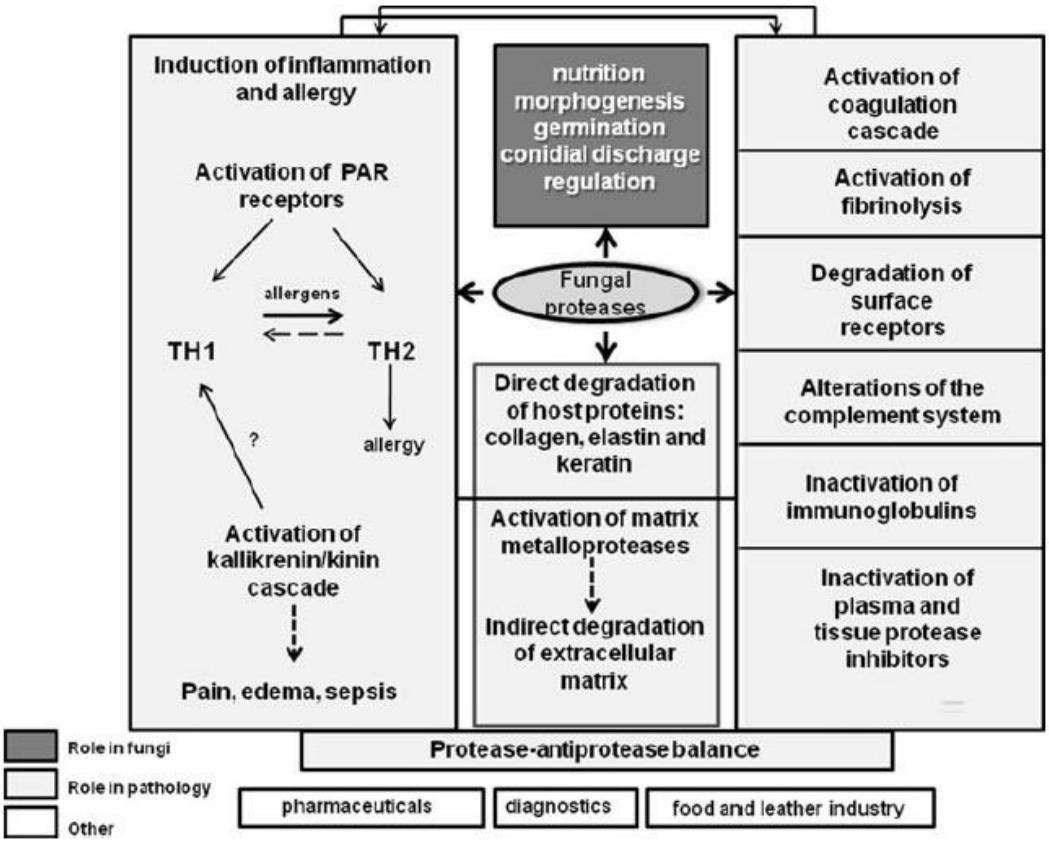

Figure 6: Schematic model summarizing multiple functions of fungal proteases in physiology, disease, and biotechnology. Proteolytic enzymes that are indispensible in fungal physiology play a crucial role in the establishment of infection and inflammation and interact with host defense systems. Secreted fungal proteases can be produced in large quantities and used in industry and medicine (PAR: Protease activated receptors; Th1/2: T helper cells 1/2) (Figure adapted from Yike 2011).

Entomopathogenic fungi produce a variety of degrading enzymes like proteases, chitinases and lipases, that facilitate their entry through the massive barriers of insect cuticle. Common examples of these entomopathogenic fungi involve *Metarhizium*

anisopliae, Beauveria bassiana and *Lecanicillium muscarium* (formerly known as *Verticillium lecanii), Beauveria* species being the most effective and commercially applied. Isolates of these fungi vary considerably in their proteolytic activity and virulence. The insect infection proceeds by piercing the insect cuticle, composed mainly of proteins and chitin, and involves the combination of mechanical forces and hydrolytic enzymes which include proteases and chitinases. Zare et al (2014) have established that the proteolytic potency of secreted proteases is directly proportional to the virulence of *Beauveria* species. There is growing evidence that subtilisins are major proteases as determinants of pathogenicity (Huang et al 2004; Campos et al., 2005).

Beauveria sp. MTCC 5184 was isolated from rabbit dung and was found to produce hydrolytic enzymes such as protease, amylase, lipase, etc., singly or in combination. Optimization of protease production and scale-up, as well as various applications of the protease in dehairing of animal skins, removal of silver from photographic films, separation of cells in animal cell culture, and synthesis of silver and gold nanoparticles have been patented (Laxman et al 2013). Purification and preliminary characterization of this subtilisin-like alkaline protease (Bprot), which is active at pH 9.0, 50°C, and stable over a wide range of pH and temperature with half-life of 2 h at 50 °C, is published (Shankar et al 2011). In the present studies, biophysical characterization of Bprot has been carried out to understand the structural elements of the protease. Bprot is also subjected to denaturing conditions in order to establish its stability towards stress conditions. Functional and conformational dynamics of Bprot were monitored using biochemical assay (Caseinolytic activity), Fluorescence spectroscopy and CD spectropolarimetry.

1.4 Tissue Kallikreins (KLK):

Kallikreins comprise of family of 15 closely related proteases encoded by genes located on chromosome 19q13.4. In 1930, KLK1 was originally identified to be involved in the regulation of blood pressure through its kininogenase activity. Now, in the 21st century, other members of this family are well known to be involved in a wide range of physiological processes depending on their tissue distribution.

Additionally, dysregulation of KLK expression, activity or localization is frequently associated with pathological disorders. Last decade has seen kallikreins as emerging area of research in order to explore its physiological importance and therapeutic applications. All kallikreins are single polypeptides composed of 244-253 residues and share 40% identity with each other. The first described tissue kallikrein was named KLK1; the remaining 14 are called kallikrein-related proteases (KLK2-KLK15). Interestingly, plasma kallikrein, the first enzyme discovered to release kinins was found to be an unrelated protease, encoded by the KLKB1 gene, located on chromosome 4q34-35. Although the traditional name plasma kallikrein is still in use, the enzyme is not regarded as a member of the kallikrein family of peptidases (Kalinska et al 2015).

1.4.1 Kallikreins as proteases:

Tissue kallikreins S1 family of serine peptidases which is a subgroup of PA clan as described by MEROPS classification and show trypsin-like, chymotrypsin-like or dual specificity. The catalytic triad of three amino acids His57, Asp102, Ser195 (chymotrypsin numbering) is highly conserved amongst them and acts as a charge relay system for proteolytic activity. 10 highly conserved cysteine residues that form five disulfide bridges stabilize the overall protein fold of kallikreins. KLK-2 and -3 are distinguished in containing a "kallikrein loop" that is longer than the corresponding loop of chymotrypsin (99-loop). The other six surface loops of kallikreins that surround the active site display high variability and thus contribute to differences in substrate specificities among kallikreins. Also, the amino acids immediately contacting a substrate at S1 site determine the observed selectivity for the residues. In kallikreins, either Asp189 or Ser189 (chymotrypsin numbering) at the S1 pocket determine substrate cleavage specificity, with preference for basic or hydrophobic amino acids, respectively. Figure 7 shows the comparison of active sites of human kallikreins.

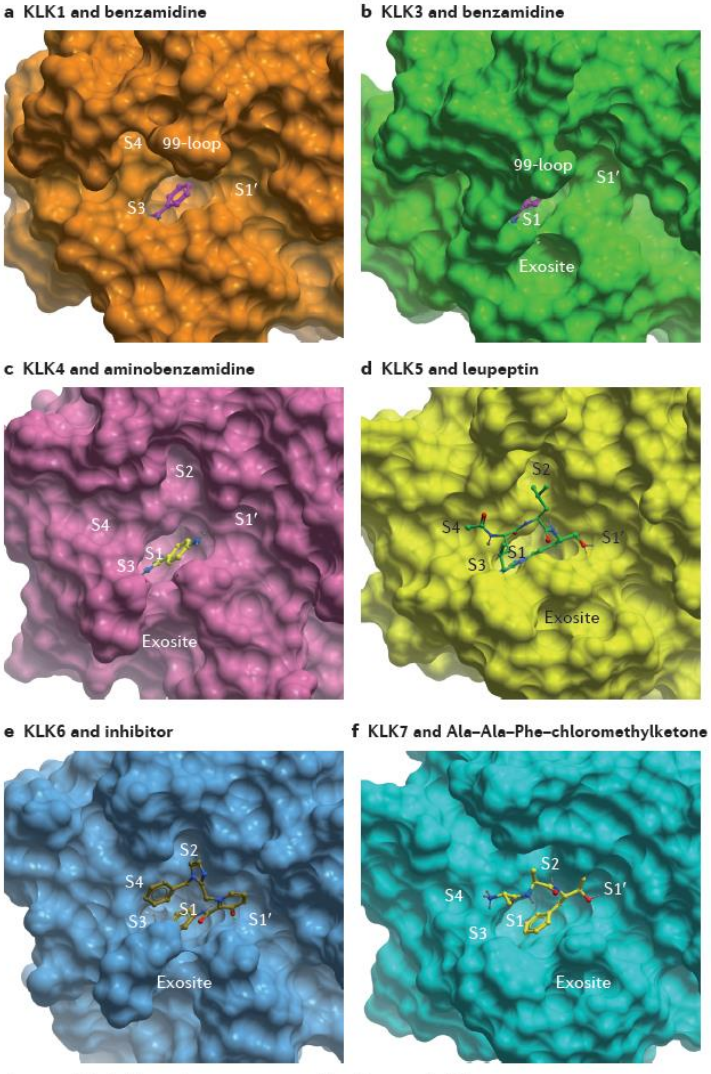

Figure 7: Side-by-side comparison of six human kallikrein structures. The surfaces of the active sites of six kallikreins are depicted. Sub-pockets that are common to all serine proteases are labelled S1–S4 and S1′. The exosite is labelled where present. (a) Human KLK1 (PDB ID: 1SPJ) is shown with benzamidine (b) KLK3 (PDB ID: 2ZCH) is shown with benzamidine. The longer (up to 11 residues long) 99-loop is more obvious in the KLK1 and KLK3 than in the other KLKs. (c) KLK4 (PDB ID: 2BDH) with aminobenzamidine (d) KLK5 bound to leupeptin. KLK5 has a markedly smaller S3 pocket, owing to the bulky Tyr218 (e) KLK6 (PDB: 4D8N) is shown with a drug-like small-molecule inhibitor (PubChem ID: 57404341) (f) The structure of KLK7 (PDB ID: 2QXG) with Ala–Ala–Phe–chloromethylketone. The S4 pocket of KLK7 is notably different, owing to the presence of its polar Thr217 residue. (Figure adapted from Prassas et al 2015).

Regulation of endogenous KLK activity is achieved by different mechanisms and factors. The kallikreins are synthesized as inactive pre-pro-proteins that are secreted to the extracellular space. The zymogen form of pro-KLKs are activated extracellularly by the trypsin-like cleavage of their pro-peptide after either an arginine or lysine. This serves as the key mechanism in regulating KLK activity in tissues (Yousef and Diamandis 2002). The autocatalytic activity of kallikreins and glycosylation adds to the control over tissue specific activity of kallikreins.

Circulatory molecules such as serpins, macroglobulins and tissue serine protease inhibitors from the lympho-epithelial Kazal-type-related inhibitor family (LEKTIs) act as endogenous KLK inhibitors. Microenvironmental conditions like pH and single-metal-ion inhibitors of KLKs such as Zn^{2+} also contribute towards this regulation. Failure of these regulatory mechanisms gives rise to pathophysiological conditions. Thus, apart from endogenous inhibitory compounds mentioned above, screening of small synthetic inhibitors and natural polypeptidic exogenous inhibitors is important for developing targeted drugs. Various small molecule inhibitors (Sulfonyfluorides, Benzamidines, leupeptin, antipain, chymostatin, chloromethyl ketones) and polypeptide inhibitors (BPTI, hirustatin) have been well characterized biochemically (Goettig et al 2010). Implimentation of these inhibitors for therapeutic purposes requires further studies.

1.4.2 Distribution and physiological role of kallikreins:

Over a century of basic research has contributed to the elucidation of the putative functions of each kallikrein and their protein interaction networks within the human proteome (Emami and Diamandis 2007). Novel functions for each kallikrein continue to be revealed with ongoing research. The KLK proteases are now known to be involved in mechanistic pathways that regulate skin desquamation, tooth enamel formation, kidney function, seminal liquefaction, synaptic neural plasticity, and brain function (Kalinska et al 2015).

KLKs within the skin

Reports suggest that a range of kallikreins are involved in maintaining healthy skin [Lundwall and Brattsand 2008]. KLK5 and KLK7 are the major enzymes involved in keratinocyte detachment (desquamation) and inflammatory processes of the skin. Also KLK8 has been described to have potential function in skin barrier proteolytic function.

KLKs within tooth enamel

Formation of tooth enamel is a multistep process involving a cascade of proteins and proteases. KLK4 (known as enamel-matrix protease) is involved in the

final stages of this process, degradation of enamel-matrix proteins (enamelin and ameloblastin) and lateral expansion of the hydroxyapatite crystal of the tooth (Bartlett 2013). Moreover, KLK4 is involved in degradation of amelogenin, remodeling of the organic matrix, and disruption of the intercellular junctions in tooth development (Kalinska et al 2015).

KLKs within the reproductive system

KLK3, also known as Prostate Specific Antigen (PSA) is well characterized for its ability to perform semen liquefaction and enhance sperm motility, achieved by cleaving fibronectin and seminal-gel forming proteins (Pampalakis and Sotiropoulou 2007). KLK-3 and -2 are best-characterized kallikrein biomarkers used in prostate cancer diagnosis.

KLKs within the respiratory and renal systems

The detailed function of KLKs in respiratory system is still to be explored. A few reports suggest considerable expression of KLK12 in lungs which may be related to an angiogenic function (Shaw and Diamandis 2007, Guillon-Munos et al 2011). KLK1 activity exerts multiple effects at the intersection of renal and cardiovascular systems by modulating the activity of epithelial sodium channels, inhibiting cortical collecting duct H^+, K^+-ATPase activity and regulation of renin-angiotensin-aldosterone system (RAAS) to controls blood pressure and fluid balance. Thus, dysregulation in KLK1 activity may result in cardiovascular and renal morbidity (Sharma and Narayanan 2014, Lieb et al 2015).

KLKs within neural system

The kallikrein predominantly expressed in brain (primarily in oligodendrocytes, pyramidal cells, astrocytes, and glial cells) is KLK6. It is known to be involved in demyelination in the central nervous system (CNS) through degradation of myelin basic protein. It also plays a role in proteolytic cleavage of components of blood-brain barrier system such as laminin, fibronectin and collagens. Dysregulation of KLK6 in CNS is associated with neurodegenerative disorders like Alzheimer's disease, Parkinson's disease, and multiple sclerosis (Ashby et al 2010).

In addition to these major physiological roles, KLKs also participate in cell signaling, turnover of viruses in viral infections. Few KLKs like KLK15 are yet to be explored for their distribution and function. Table 4 summarizes the specificity, expression pattern and diseases associated with known human KLKs.

Table 5: Summary of information available on human KLKs:

Protease	Specificity (Kalinska et al 2015)	Expression pattern (Diamandis et al 2000)	Association with disease (Prassas et al 2015)	Dysregulation in cancer (Kryza et al 2015) (Arrows indicate the up/ down regulation of the protein)
KLK1	Mix	Kidney, pancreas and salivary gland	Cardiac and arterial abnormalities, Myocardial ischaemia	Colorectal cancer (↓)
KLK2	Tryptic	Prostate, breast		
KLK3	Chymotryptic	Prostate, breast		Prostate cancer (↑) Pancreatic cancer (↓)
KLK4	Tryptic	Prostate, breast, testis, uterus, thyroid	Amelogenesis imperfect, Oral squamous cell carcinoma	Breast cancer (↑)
KLK5	Tryptic	Breast, brain, testis and skin	Netherton syndrome and atopic dermatitis, Acne rosacea	Breast cancer (↓) Ovarian cancer (↑)
KLK6	Tryptic	Brain, breast, ovary, kidney, uterus	Multiple sclerosis, Lewy body diseases, CNS	Colorectal cancer (↑) Gastric cancer

			inflammation	(↑)
KLK7	Chymotryptic	Skin, brain, kidney, breast, salivary glands and thymus	Skin inflammation and atopic dermatitis	Ovarian cancer (↑) esophageal cancer (↓)
KLK8	Tryptic	Brain, skin	Schizophrenia, mood and anxiety disorders , Psoriasis	Colorectal cancer (↑) Breast cancer (↓) Ovarian cancer (↑)
KLK9	Chymotryptic	Skin, thymus, trachea, cerebellum, spinal cord		
KLK10	Tryptic	Breast, ovary, testis, prostate, small intestine, lung and pancreas		Colorectal cancer (↑) Gastric cancer (↑) Breast cancer (↓)
KLK11	Mix	Brain, skin		Gastric cancer (↓)
KLK12	Tryptic		Systemic sclerosis (defective angiogenesis)	Colorectal cancer (↑)
KLK13	Tryptic	Prostate, breast, testis and salivary gland		
KLK14	Mix	Prostate and skeletal muscle		
KLK15	Tryptic			Colorectal cancer (↓) Prostate cancer

				(↑) Pancreatic cancer (↓)

1.4.3 Kallikreins in cancer and therapeutics

Many human KLKs are aberrantly expressed in cancer growths. KLK3/PSA (prostate specific antigen) was the first one amongst the group to be established as a biomarker in prostate cancer progression. Table 4 summarizes the dysregulation of KLKs studied from microarray datasets in the Oncomine database (Rhodes et al 2004). Recently, a number of *in vitro* and *in vivo* studies demonstrated the functional involvement of KLKs in cancer-related processes like regulation of cancer cell growth, migration, invasion, chemo-resistance, and importantly, in mediating interactions between cancer cells and other cell populations found in the tumour microenvironment to facilitate cancer progression (Kryza et al 2015). This highlights their potential in designing new anti-cancer approaches. Various kallikrein based therapeutic approaches include application of peptide inhibitors, small molecule inhibitors, antibody-based inhibitors and vaccines, KLK-activated prodrugs and restoration of KLK expression by chemotherapy (Kryza et al 2015, Prassas et al 2015). Understanding of principles that govern stability and conformational dynamics of KLKs under stress conditions may improve the drug design process and formulation studies.

In the present studies, we consider porcine pancreatic kallikrein (KLKp) as a model preotein for functional and conformational dynamics under denaturing conditions.

1.4.4 Porcine pancreatic kallikrein:

Porcine pancreatic kallikrein (KLKp) is the first enzyme in the kallikrein family to be purified from autolyzed porcine pancreas. Biochemical characterization of purified KLKp was reported by Zuber and Sache (1973). KLKp is a trypsin-like protease with molecular weight of 31-34 kDa depending on its glycosylation status. It shows

optimum activity at pH 8.5 at 37℃. The report shows interesting feature of KLKp that it retains considerable amount of activity even at 100˚C (Zuber and Sache 1973).

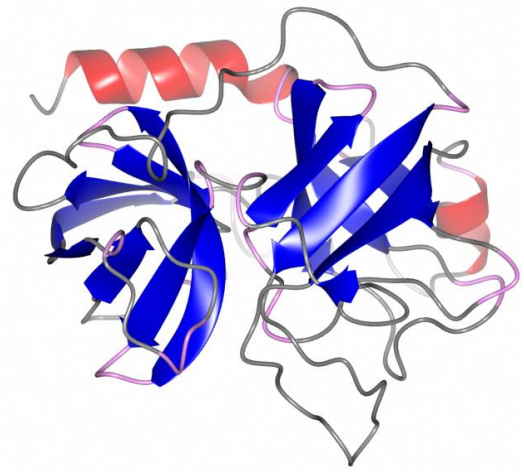

KLKp structure (PDB ID: 2PKA)

Detailed structural studies of KLKp by Bode et al (1983) have revealed remarkable similarity to trypsin except for deviations in external loops. In spite of the structural information available, KLKp is unexplored for the folding/ unfolding mechanism. With the aim of investigating novel structural and/or functional elements, KLKp was undertaken as a model system to perform unfolding transitions under denaturing conditions using biochemical, spectroscopic and molecular dynamics approach.

The studies will substantiate the existing knowledge about protease stability, functional and conformational dynamics which in turn may be applied to protein engineering and improve applicability of the proteins.

References:

- Ashby, E. L., Kehoe, P. G., & Love, S. (2010). Kallikrein-related peptidase 6 in Alzheimer's disease and vascular dementia. *Brain research, 1363*, 1-10.
- Bartlett, J. D. (2013). Dental enamel development: proteinases and their enamel matrix substrates. *ISRN dentistry*, Article ID 684607, 1-24.
- Bode, W., Chen, Z., Bartels, K., Kutzbach, C., Schmidt-Kastner, G., & Bartunik, H. (1983). Refined 2 Å X-ray crystal structure of porcine pancreatic kallikrein A, a specific trypsin-like serine proteinase: Crystallization, structure determination, crystallographic refinement, structure and its comparison with bovine trypsin. *Journal of molecular biology*, *164*(2), 237-282.
- Borgi, I., & Gargouri, A. (2014). Investigations on a hyper-proteolytic mutant of *Beauveria bassiana*: broad substrate specificity and high biotechnological potential of a serine protease. *FEMS microbiology letters*, *351*(1), 23-31.
- Campos, R. A., Arruda, W., Boldo, J. T., Silva, M. V., Barros, N. M., Azevedo, J. L., Schrank, A. & Vainstein, M. H. (2005) *Boophilus microplus* infection by *Beauveria amorpha* and *Beauveria bassiana*: SEM analysis and regulation of subtilisin-like proteases and chitinases. *Curr Microbiol 50*, 257–261.
- Canchi, D. R., & García, A. E. (2013). Cosolvent effects on protein stability. *Annual review of physical chemistry*, *64*, 273-293.
- Carvalho, F. A., Martins, I. C., & Santos, N. C. (2013). Atomic force microscopy and force spectroscopy on the assessment of protein folding and functionality. *Archives of biochemistry and biophysics*, *531*(1), 116-127.
- Chattopadhyay, A., & Haldar, S. (2013). Dynamic insight into protein structure utilizing red edge excitation shift. *Accounts of chemical research*, *47*(1), 12-19. Chaudhuri, T. K., & Paul, S. (2006). Protein-misfolding diseases and chaperone-based therapeutic approaches. *FEBS Journal*, *273*(7), 1331-1349.
- Cohen, F. E., & Kelly, J. W. (2003). Therapeutic approaches to protein-misfolding diseases. *Nature, 426*(6968), 905-909.

- Craik, C., Page, M., & Madison, E. (2011). Proteases as therapeutics. *Biochem. J, 435*, 1-16.
- Crampton, N., & Brockwell, D. J. (2010). Unravelling the design principles for single protein mechanical strength. *Current opinion in structural biology*, *20*(4), 508-517.
- Daggett, V., & Fersht, A. R. (2003). Is there a unifying mechanism for protein folding? *Trends in biochemical sciences*, *28(1)*, 18-25.
- Denny, R. A., Gavrin, L. K., & Saiah, E. (2013). Recent developments in targeting protein misfolding diseases. *Bioorganic & medicinal chemistry letters*, *23(7)*, 1935-1944.
- Diamandis, E. P., Yousef, G. M., Luo, L. Y., Magklara, A., & Obiezu, C. V. (2000). The new human kallikrein gene family: implications in carcinogenesis. *Trends in Endocrinology & Metabolism*, *11*(2), 54-60.
- Dror, R. O., Jensen, M. Ø., Borhani, D. W., & Shaw, D. E. (2010). Exploring atomic resolution physiology on a femtosecond to millisecond timescale using molecular dynamics simulations. *The Journal of general physiology*, *135*(6), 555-562.
- Eaton, W. A., Muñoz, V., Hagen, S. J., Jas, G. S., Lapidus, L. J., Henry, E. R., & Hofrichter, J. (2000). Fast kinetics and mechanisms in protein folding 1. *Annual review of biophysics and biomolecular structure*, *29*(1), 327-359.
- Eijsink, V. G., Bjørk, A., Gåseidnes, S., Sirevåg, R., Synstad, B., van den Burg, B., & Vriend, G. (2004). Rational engineering of enzyme stability. *Journal of biotechnology*, *113*(1), 105-120.
- Emami, N., & Diamandis, E. P. (2007). New insights into the functional mechanisms and clinical applications of the kallikrein-related peptidase family. *Molecular oncology*, *1*(3), 269-287.
- Fersht, A. R. (2008). From the first protein structures to our current knowledge of protein folding: delights and scepticisms. *Nature Reviews Molecular Cell Biology*, *9*(8), 650-654.

- Gecse, K. B., Khanna, R., van den Brink, G. R., Ponsioen, C. Y., Löwenberg, M., Jairath, V., Travis S. P. L., Sandborn W. J., Feagan B. J. & D'Haens, G. R. (2013). Biosimilars in IBD: hope or expectation? *Gut*, *62*(6), 803-807.
- Goettig, P., Magdolen, V., & Brandstetter, H. (2010). Natural and synthetic inhibitors of kallikrein-related peptidases (KLKs). *Biochimie*, *92*(11), 1546-1567
- Guillon-Munos, A., Oikonomopoulou, K., Michel, N., Smith, C. R., Petit-Courty, A., Canepa, S., & Courty, Y. (2011). Kallikrein-related peptidase 12 hydrolyzes matricellular proteins of the CCN family and modifies interactions of CCN1 and CCN5 with growth factors. *Journal of Biological Chemistry*, *286*(29), 25505-25518.
- Haustein, E., & Schwille, P. (2007). Fluorescence correlation spectroscopy: novel variations of an established technique. *Annu. Rev. Biophys. Biomol. Struct.*, *36*, 151-169.
- Hooper, N. (2002). Proteases: a primer. *Essays Biochem*, *38*, 1-8.
- Huang, X. W., Zhao, N. H. & Zhang, K. Q. (2004). Extracellular enzymes serving as virulence factors in nematophagous fungi involved in infection of the host. *Res Microbiol 115*, 811–816.
- Ishii, K., & Tahara, T. (2013). Two-dimensional fluorescence lifetime correlation spectroscopy. 1. Principle. *The Journal of Physical Chemistry B*, *117*(39), 11414-11422.
- Johnson, C. M. (2013). Differential scanning calorimetry as a tool for protein folding and stability. *Archives of biochemistry and biophysics*, *531*(1), 100-109.
- Kalinska, M., Meyer-Hoffert, U., Kantyka, T., & Potempa, J. (2015). Kallikreins–The melting pot of activity and function. *Biochimie* 1-13.
- Kelly, S. M., Jess, T. J., & Price, N. C. (2005). How to study proteins by circular dichroism. *Biochimica et Biophysica Acta (BBA)-Proteins and Proteomics*, *1751*(2), 119-139.

- Kryza, T., Silva, M. L., Loessner, D., Heuzé-Vourc'h, N., & Clements, J. A. (2015). The kallikrein-related peptidase family: Dysregulation and functions during cancer progression. *Biochimie* , 1-17.
- Laxman, R. S., Shankar, S.,More, S. V., Khandelwal, H. B., Narasimhan, C. B. K., Palanivel, S. & Balaram, P. (2013). Euro. Patent. EP 2531596. US. Patent. US 20130095523
- Leandro, P., & Gomes, C. M. (2008). Protein misfolding in conformational disorders: rescue of folding defects and chemical chaperoning. *Mini reviews in medicinal chemistry*, *8*(9), 901-911.
- Li, Q., Yi, L., Marek, P., & Iverson, B. L. (2013). Commercial proteases: Present and future. *FEBS letters*, *587*(8), 1155-1163.
- Lieb, W., Chen, M. H., Teumer, A., de Boer, R. A., Lin, H., Fox, E. R., & Vasan, R. S. (2015). Genome-Wide Meta-Analyses of Plasma Renin Activity and Concentration Reveal Association With the Kininogen 1 and Prekallikrein Genes. *Circulation: Cardiovascular Genetics*, *8*(1), 131-140.
- Lindquist, S. L., & Kelly, J. W. (2011). Chemical and biological approaches for adapting proteostasis to ameliorate protein misfolding and aggregation diseases–progress and prognosis. Cold Spring Harbor perspectives in biology, 3(12), a004507.
- Lundwall, Å., & Brattsand, M. (2008). Kallikrein-related peptidases. *Cellular and Molecular Life Sciences*, *65*(13), 2019-2038.
- M Gomes, C. (2012). Protein misfolding in disease and small molecule therapies. Current topics in medicinal chemistry, 12(22), 2460-2469.
- Manning, M., & Colón, W. (2004). Structural basis of protein kinetic stability: resistance to sodium dodecyl sulfate suggests a central role for rigidity and a bias toward β-sheet structure. *Biochemistry*, *43*(35), 11248-11254.
- Miranker, A., Robinson, C. V., Radford, S. E., & Dobson, C. M. (1996). Investigation of protein folding by mass spectrometry. *The FASEB journal*, *10*(1), 93-101.
- Mótyán, J. A., Tóth, F., & Tőzsér, J. (2013). Research applications of proteolytic enzymes in molecular biology. *Biomolecules*, *3*(4), 923-942.

- Neira, J. L. (2013). NMR as a tool to identify and characterize protein folding intermediates. *Archives of biochemistry and biophysics*, *531*(1), 90-99.
- Nirmal, N. P., Shankar, S. & Laxman, R.S. (2011) Fungal Proteases: An Overview. Int. *J. Biotech & Biosci. 1* (1), 1-40.
- Niyonzima, F. N., & More, S. S. (2015). Coproduction of detergent compatible bacterial enzymes and stain removal evaluation. *Journal of basic microbiology*, *55*, 1149–1158.
- Otzen, D. E., Itzhaki, L. S., Jackson, S. E., & Fersht, A. R. (1994). Structure of the transition state for the folding/unfolding of the barley chymotrypsin inhibitor 2 and its implications for mechanisms of protein folding. Proceedings of the National Academy of Sciences, 91(22), 10422-10425.
- Page, M. J., & Di Cera, E. (2008). Serine peptidases: classification, structure and function. *Cellular and Molecular Life Sciences*, *65*(7-8), 1220-1236.
- Pampalakis, G., & Sotiropoulou, G. (2007). Tissue kallikrein proteolytic cascade pathways in normal physiology and cancer. Biochimica et Biophysica Acta (BBA)-Reviews on Cancer, 1776(1), 22-31.
- Perlmutter, D. H. (2002). Chemical chaperones: a pharmacological strategy for disorders of protein folding and trafficking. *Pediatric research*, *52*(6), 832-836.
- Polgar, L. (2005). The catalytic triad of serine peptidases. *Cellular and Molecular Life Sciences CMLS*, *62*(19-20), 2161-2172.
- Pollack, L., Tate, M. W., Darnton, N. C., Knight, J. B., Gruner, S. M., Eaton, W. A., & Austin, R. H. (1999). Compactness of the denatured state of a fast-folding protein measured by submillisecond small-angle x-ray scattering. *Proceedings of the National Academy of Sciences*, *96*(18), 10115-10117.
- Prassas, I., Eissa, A., Poda, G., & Diamandis, E. P. (2015). Unleashing the therapeutic potential of human kallikrein-related serine proteases. *Nature Reviews Drug Discovery*, *14*(3), 183-202.
- Radford, S. E. (2000). Protein folding: progress made and promises ahead. *Trends in biochemical sciences*, *25*(12), 611-618.

- Rao, M. B., Tanksale, A. M., Ghatge, M. S., & Deshpande, V. V. (1998). Molecular and biotechnological aspects of microbial proteases. *Microbiology and molecular biology reviews*, *62*(3), 597-635.
- Rawlings, N. D., Barrett, A. J., & Bateman, A. (2012). MEROPS: the database of proteolytic enzymes, their substrates and inhibitors. *Nucleic acids research*, *40*(D1), D343-D350.
- Rhodes, D. R., Yu, J., Shanker, K., Deshpande, N., Varambally, R., Ghosh, D., & Chinnaiyan, A. M. (2004). ONCOMINE: a cancer microarray database and integrated data-mining platform. *Neoplasia*, *6*(1), 1-6.
- Righetti, P. G., & Verzola, B. (2001). Folding/ unfolding/ refolding of proteins: present methodologies in comparison with capillary zone electrophoresis. *Electrophoresis*, *22*(12), 2359-2374.
- Rizzuti, B., & Daggett, V. (2013). Using simulations to provide the framework for experimental protein folding studies. *Archives of biochemistry and biophysics*, *531*(1), 128-135.
- Rockwell, N. C., & Thorner, J. W. (2004). The kindest cuts of all: crystal structures of Kex2 and furin reveal secrets of precursor processing. *Trends in biochemical sciences*, *29*(2), 80-87.
- Ruan, B., London, V., Fisher, K. E., Gallagher, D. T., & Bryan, P. N. (2008). Engineering Substrate Preference in Subtilisin: Structural and Kinetic Analysis of a Specificity Mutant. *Biochemistry*, *47*(25), 6628-6636.
- Sancho, J. (2013). The stability of 2-state, 3-state and more-state proteins from simple spectroscopic techniques... plus the structure of the equilibrium intermediates at the same time. *Archives of biochemistry and biophysics*, *531*(1), 4-13.
- Scharnagl, C., Reif, M., & Friedrich, J. (2005). Stability of proteins: temperature, pressure and the role of the solvent. *Biochimica et Biophysica Acta (BBA)-Proteins and Proteomics*, *1749*(2), 187-213.
- Schuler, B., & Hofmann, H. (2013). Single-molecule spectroscopy of protein folding dynamics—expanding scope and timescales. *Current opinion in structural biology*, *23*(1), 36-47.

- Senisterra, G. A., & Finerty Jr, P. J. (2009). High throughput methods of assessing protein stability and aggregation. *Molecular BioSystems*, *5*(3), 217-223.
- Shankar, S., Rao, M., Laxman, R.S. (2011). Purification and characterization of an alkaline protease by a new strain of *Beauveria sp. Process Biochemistry*, *46*, 579–585.
- Sharma, J. N., & Narayanan, P. (2014). The Kallikrein–Kinin Pathways in Hypertension and Diabetes. In *Recent Developments in the Regulation of Kinins* (pp. 15-36). Springer International Publishing.
- Shaw, J. L., & Diamandis, E. P. (2007). Distribution of 15 human kallikreins in tissues and biological fluids. *Clinical chemistry*, *53*(8), 1423-1432.
- Southan, C. (2001). A genomic perspective on human proteases. *FEBS letters*, *498*(2), 214-218.
- Souza, P. M. D., Bittencourt, M. L. D. A., Caprara, C. C., Freitas, M. D., Almeida, R. P. C. D., Silveira, D., & Magalhães, P. O. (2015). A biotechnology perspective of fungal proteases. *Brazilian Journal of Microbiology*, *46*(2), 337-346.
- Srilakshmi, J., Madhavi, J., Lavanya, S., & Ammani, K. (2015) Commercial Potential of Fungal Protease: Past, Present and Future Prospects. *Journal of Pharmaceutical, Chemical and Biological Sciences*, 2(4): 218-234.
- Sumantha, A., Larroche, C., & Pandey, A. (2006). Microbiology and industrial biotechnology of food-grade proteases: a perspective. *Food Technology and Biotechnology*, *44*(2), 211.
- Troullier, A., Reinstädler, D., Dupont, Y., Naumann, D., & Forge, V. (2000). Transient non-native secondary structures during the refolding of α-lactalbumin detected by infrared spectroscopy. *Nature Structural & Molecular Biology*, *7*(1), 78-86.
- Valastyan, J. S., & Lindquist, S. (2014). Mechanisms of protein-folding diseases at a glance. *Disease models & mechanisms*, *7*(1), 9-14.

- Varshney, A., Rabbani, G., Badr, G., & Khan, R. H. (2014). Cosolvents Induced Unfolding and Aggregation of Keyhole Limpet Hemocyanin. *Cell biochemistry and biophysics*, *69*(1), 103-113.
- Yang, Y., jun Wen, Y., Cai, Y. N., Vallée, I., Boireau, P., Liu, M. Y., & Cheng, S. P. (2015). Serine Proteases of Parasitic Helminths. *The Korean journal of parasitology*, *53*(1), 1.
- Yike, I. (2011). Fungal proteases and their pathophysiological effects. *Mycopathologia*, *171*(5), 299-323.
- Yousef, G. M., & Diamandis, E. P. (2002). Human tissue kallikreins: a new enzymatic cascade pathway? *Biological chemistry*, *383*(7-8), 1045-1057.
- Zare, M., Talaei-Hassanloui, R., & Fotouhifar, K. B. (2014). Relatedness of proteolytic potency and virulence in entomopathogenic fungus *Beauveria bassiana* isolates. *Journal of Crop Protection*, *3*(4), 425-434.
- Zuber, M., & Sache, E. (1974). Isolation and characterization of porcine pancreatic kallikrein. *Biochemistry*, *13*(15), 3098-3110.

Chapter 2

Biophysical characterization of Serine Protease from *Beauveria sp.* MTCC 5184

Summary

Biophysical characterization of the subtilisin-like serine protease from *Beauveria* sp. MTCC 5184 (Bprot) was performed using steady state and time resolved fluorescence, circular dichroism, FT-IR spectroscopy and x-ray crystallography. Also, the enzyme was examined for its kinetic stability. The microenvironment of a single tryptophan residue in Bprot was studied using steady state and time resolved fluorescence. The emission maximum of intrinsic fluorescence was observed at 339 nm indicating Trp to be buried in the hydrophobic core. Solute quenching studies were performed with neutral (acrylamide) and ionic (I^- and Cs^+) quenchers to probe the exposure and accessibility of Trp residue of the protein. Maximum quenching was observed with acrylamide. In native state, quenching was observed with I^- and not with Cs^+ indicating presence of positively charged environment surrounding Trp residue. However, in denatured protein, quenching was observed with $Cs^{+,}$ indicating charge reorientation after denaturation. Time resolved fluorescence measurements established presence of two conformers of Trp. Bprot was proposed to have α/β hydrolase fold based on the far UV CD spectrum and known structural elements reported for subtilases. Preliminary crystallization and X-ray diffraction data for Brot was reported. Structural resistance of Bprot towards SDS and proteolytic environment suggested that it could be kinetically stable protein.

2.1 Introduction

Subtilisin-like serine proteases are the second most abundant clan of proteases after (chymo)-trypsin like proteases known. These two clans are distinguished by a highly similar arrangement of catalytic His, Asp, and Ser residues in radically different β/β (chymotrypsin) and α/β (subtilisin) protein scaffolds. Members of the subtilase superfamily present in most bacteria, archaea, and lower eukaryotes are extracellular endoproteases. They are required either for defense or for growth on proteinaceous substrates in these organisms (Siezen and Leunissen 1997).

Proteases in fungi are also known to play important metabolic roles. Proteases from entomopathogenic fungi like *Beauveria bassiana*, *Beauveria brongniartii*, and *Beauveria felina* have been established as important virulence factors in their entomopathogenic activity. Biochemical characterization shows that these are alkaline

trypsin-like serine proteases (Svedese et al 2013). Recent genomic studies in *B. bassiana* have revealed that subtilisin-like serine proteases are a part of this entomopathogenic cascade (Xiao et al 2012). These proteases are unexplored for their detailed functional and structural characterization.

The present study involves analysis of structural elements of a subtilisin-like serine protease from *Beauveria* sp. MTCC 5184 (Bprot). The enzyme has been biochemically characterized and studied for its commercial applications by Shankar et al (2011). Biophysical characterization of Bprot is done by fluorescence, CD and FTIR spectroscopy. Preliminary X-ray crystallization studies for Bprot are also reported here. Reports suggest that surface residues dramatically influence folding and dictate the folding pathways, mechanisms, and the choice between kinetic and thermodynamically stable folds in subtilases (Subbian et al 2004). Thus, the enzyme is also screened for possibility of being kinetically stable based on its resistance towards SDS and proteolytic environment.

2.2 Materials and Methods

2.2.1 Materials

Sodium dodecyl sulfate (SDS), 8-Anilinonaphthalene-1-sulfonic acid **(**ANS) were obtained from Sigma Aldrich Ltd., USA. Trypsin, chymotrypsin, and proteinase K were obtained from SRL, India. All other reagents including buffer compounds and media components used were of analytical grade. Solutions for spectroscopic measurements were prepared in MilliQ water.

2.2.3 Production and purification of Bprot

The organism *Beauveria* sp. MTCC 5184 was isolated from rabbit dung. The protocol used for the production and purification of Bprot was as described earlier (Shankar et al. 2011).

Production media (0.3 % glucose, 1 % yeast extract, and 2 % mustard seed cake as inducer) inoculated with culture of *Beauveria sp*. MTCC 5184 at 28℃ at 200 rpm for 96 hours

↓

Centrifuge at 10000 rpm for 20 min. Collect the supernatant

↓

40-70% Ammonium sulfate precipitation

↓

Centrifuge at 10000 rpm for 20 min. Collect the pellet.

↓

Dialyze the resuspended pellet to remove ammonium sulfate

↓

DEAE-cellulose column chromatography (unbound fraction)

↓

Removal of spectroscopic impurities on CM-sephadex column at pH 5.0 in Citrate phosphate buffer, 10 mM (Elution in buffer containing 250 mM NaCl).

The purified enzyme was stored at pH 7.0 where it exhibits maximum stability at 4℃.

2.2.4 Protein Estimation

Protein was estimated according to Lowry et al (1951) with bovine serum albumin (BSA) as the standard.

2.2.5 Matrix assisted laser desorption ionization –Time of flight (MALDI-TOF): The molecular mass of purified protease was also determined by MALDI–TOF mass spectrometry using a Voyager DE-STR (Applied Biosystems) equipped with a 337 nm nitrogen laser. 5 µl of the purified Bprot (1mg/ml) was mixed with 30 µl of sinapinic acid and spotted on MALDI target plate and dried in oven at 50°C and analyzed.

2.2.6 Enzyme assay

The assay was carried out by the method of Kunitz (1947), as described by Laskowski (1955). It was modified as follows: protease activity was determined by incubating 1 µg of the enzyme in 300 µl of 1 % casein (substrate) at pH 9 (300 µl, 50 mM carbonate buffer) at 50 °C for 20 min. The reaction was stopped by adding 900 µl of 5 % TCA and the reaction mixture was allowed to stand for 30 min. Any precipitate formed was then removed by centrifugation and absorbance of the supernatant removed gently was read at 280 nm. One unit of protease activity is defined as the amount of enzyme that releases 1 µmol of tyrosine per minute in the assay conditions.

2.2.7 Modification of Serine Residues with phenylmethylsulfonyl fluoride (PMSF)

The reaction mixture containing enzyme in 50 mM potassium phosphate buffer pH 7.0 and 5, 10, 15, and 30 µM of PMSF was incubated at 25 ^{0}C for 30 mins. Aliquots were removed at different time intervals and the residual activities were determined under standard assay conditions. Enzyme sample incubated in the absence of PMSF served as control. Number of serine residues in the active site of the enzyme was calculated by double logarithmic plot.

2.2.8 Modification of Trp residue with N-bromosuccinimide (NBS)

Enzyme solution in 20mM Citrate phosphate buffer pH 5.0 (1ml, 2.17µM) was titrated with freshly prepared N-bromosuccinimide (NBS) (1mM) with different aliquots (5 µl each) till the protein to NBS ratio reached 1:10. Modification of protein with NBS was accompanied by a decrease in the absorbance of modified protein at 280nm. The NBS modification was also carried out under denaturing (6M GdnHCl treated) conditions and the number of Trp residues modified were determined spectrophotometrically, assuming the molar absorption coefficient of 5,500 $M^{-1}cm^{-1}$ for the modified Trp at 280nm (Spande and Witkop 1967).

2.2.9 Steady‑state fluorescence study

Intrinsic fluorescence of Bprot (30µg/ml in 20mM potassium phosphate buffer pH 7.0) was measured using a Perkin-Elmer luminescence spectrometer LS50B connected to a Julabo F20 water bath. The protein solution was excited at 295 nm and the emission was recorded in the range of wavelength 300–400 nm at 28 °C. The slit widths for the excitation and emission were set at 7.0 nm, and the spectra were recorded at 100 nm/min. To eliminate the background emission, the signal produced by buffer solution or buffer containing the appropriate quantity of denaturants was subtracted.

2.2.10 Time-resolved fluorescence study

Fluorescence lifetime measurements were carried out on Edinburgh Instruments' FLS-920 single-photon counting spectrofluorimeter. The protein concentration used for Bprot was 1 mg/ml. A picosecond pulsed-light emitting diode of wavelength 296.8

nm, pulse width 747.8 ps and bandwidth 10.4 nm was used as the excitation source and a synchronization photomultiplier was used to detect the fluorescence. The diluted Ludox solution was used for measuring instrument response function (IRF). The sample was excited at 295 nm and emission was recorded at 339 nm. Slit widths of 15 nm each were used on the excitation and emission monochromators. The resultant decay curves were analyzed by a reconvolution fitting program supplied by Edinburgh Instruments.

2.2.11 FT‑IR spectrum

Fourier transform infrared (FT-IR) spectra were taken on a Bruker Optics ALPHA-E spectrometer in the 1,000– 2,000 cm^{-1} region. Protein concentration used for the scan was 1.5 mg/ml. The spectrum was recorded as an average of five spectra.

2.2.12 ANS‑binding assay

The hydrophobic dye binding to Bprot was studied by adding 8-Anilinonaphthalene-1-sulfonic acid (ANS) to a final concentration of 50µM to Bprot solution incubated under respective condition. Excitation wavelength used was 375 nm and total fluorescence emission was monitored between 400 and 550 nm. Reference spectrum of ANS in respective buffer was subtracted from the spectrum of the sample.

2.2.12 Circular dichroism (CD) spectroscopy

CD measurements of the purified Bprot was recorded using a Jasco J-815-150S (Jasco, Tokyo, Japan) spectropolarimeter connected to a Peltier CDFL cell circulating water bath at 28 °C. Far-UV spectra was recorded in a rectangular quartz cell of 1-mm path length in the range of 200–250 nm at a scan speed of 100 nm/min with a response time of 1 s and a slit width of 1 nm. Purified Bprot at a concentration of 0.065 mg/ml was used for all the samples. Each spectrum was recorded as an average of five scanned spectra. Conformational transition studies of Bprot were carried out by incubating Bprot at concentration of 0.065 mg/ml under mentioned conditions for respective time periods. Results are expressed as mean residue ellipticity (MRE) in deg cm^2/dmol defined as

$MRE = M\theta_\lambda/10dcr$

where M is the molecular weight of the protein, θ_i is CD in millidegree, d is the path length in cm, c is the protein concentration in mg/ml, and r is the average number of amino acid residues in the protein. The relative content of various secondary structure elements was calculated by using CDPro software (http://lamar.colostate.edu/~sreeram/ CDPro/main.html). Low NRMSD values were observed for analysis with CONTINLL.

2.2.13 Solute quenching studies by steady‑state fluorescence

Fluorescence measurements were performed for native and denatured protein with different quenchers like acrylamide (5 M) (neutral quencher), iodide (5 M), and cesium (5 M) (charged quenchers), on a Perkin-Elmer LS 50B spectrofluorimeter at 28 °C. Bprot samples were excited at 295 nm and emission spectra were recorded in range of 300–400 nm. Slit widths of 7.0 nm each were set for excitation and emission monochromators. Small aliquots of quencher stocks were added to protein samples and fluorescence spectra were recorded after each addition. Iodide stock solution contained 0.2 M sodium thiosulfate to prevent formation of tri-iodide (I^{-3}). For quenching studies with denatured protein, the protein was incubated with 6 M guanidium hydrochloride (GdnHCl) overnight at room temperature. Fluorescence intensities were corrected for volume changes before further analysis of quenching data. The steady-state fluorescence quenching data obtained with different quenchers were analyzed by Stern–Volmer (Eq. 1) and modified Stern–Volmer (Eq. 2) equations in order to obtain quantitative quenching parameters

$$F_o/F_c = 1 + K_{sv}[Q] \quad (1)$$

$$F_o/\Delta F = f_a^{-1} + 1/[K_a f_a(Q)] \quad (2)$$

where F_o and F_c are the relative fluorescence intensities in the absence and presence of the quencher, respectively, (Q) is the quencher concentration, K_{sv} is Stern–Volmer quenching constant, $\Delta F = F_o - F_c$ is the change in fluorescence intensity at any point in the quenching titration, K_a is the quenching constant, and f_a is the fraction of the total fluorophores accessible to the quencher. Equation (2) shows that the slope of a plot of $F_o/\Delta F$ versus $1/Q$ (modified Stern– Volmer plot) gives the value of $(K_a f_a)^{-1}$ and its Y-intercept gives the value of f_a^{-1}.

2.2.14 SDS resistance of Bprot:

SDS resistance of Bprot structure was monitored on 12% SDS PAGE. Protein samples were incubated with SDS at room temperature (unboiled sample) or boiled for 10 min prior to analysis by SDS-PAGE. The effect of increasing concentration on Bprot activity was monitored by incubating the enzyme with respective concentration of SDS and checking activity of appropriate aliquots by the assay method mentioned above. Intrinsic fluorescence spectra were also recorded after incubating Bprot (30µg/ml) in respective concentration of SDS for 20 minutes at room temperature.

2.2.15 Studies in proteolytic environment

Trypsin, chymotrypsin, and proteinase K were used for proteolytic digestion of Bprot at 28 °C in 20 mM Tris–HCl buffer at pH 8.0. Bprot and each protease were incubated at 10:1 and 100:1 w/w ratio for 24 h. Aliquots were removed at regular time intervals and checked for activity. There was no interference in the assay readings from the activities of the proteolytic mixture because at 50 °C (pH 9.0) where the Bprot activity was assayed, the other proteases were inactive, as confirmed by assaying suitable controls for the other proteolytic enzymes.

2.2.16 Crystallization and data collection for Bprot:

Bprot was purified to homogeneity and buffer was exchanged with 20mM HEPES buffer pH 7.0. Protein was concentrated to 7 mg/mL using Amicon Ultra-50 centrifugation filter device (10 kDa cutoff, Millipore, USA). Crystallization trials were conducted at temperature 20℃ with 1:1 ratio of protein to precipitant, exploiting commercially available screens from Hampton Research (USA) and Molecular Dimensions (UK). Self-prepared additives were also screened to improve the crystal quality. Crystals were mounted on cryoloop (Hampton research, USA) and frozen in liquid nitrogen using 30% glycerol for cryoprotection. Data were collected at 100 K on synchrotron beamline (SSRL, 12-2) using wavelength 0.9795 A° up to a resolution 8 A°.

2.3 Results and discussion:

The protease from *Beauveria* sp. MTCC 5184 (Bprot) under study is a monomeric 29-kDa subtilisin-type serine protease with maximum stability at pH 7.0

and shows optimum proteolytic activity at pH 9.0 at 50 °C (Shankar et al. 2011). It was further characterized for its structural features using fluorescence, CD and FTIR spectroscopy, as well as with X-ray crystallization.

2.3.1 Purification and kinetic modification of Bprot:

The standardized purification protocol yielded single band protein devoid of any proteinaceous impurity. Some spectroscopic impurities left in the DEAE cellulose unbound fractions were removed by ion exchange chromatography on CM-sephadex column, improving the intrinsic fluorescence spectrum of the protein (Fig.1a). Molecular weight of the protein was confirmed by MALDI-TOF to be 28.2 kDa (Fig.1b).

Bprot belongs to class of Serine proteases. This was confirmed by chemical modification of the enzyme with PMSF which is an irreversible inhibitor of serine proteases in concentration dependent and time dependent manner. A double logarithmic plot (Fig.1c) confirmed presence of a single serine residue at the active site.

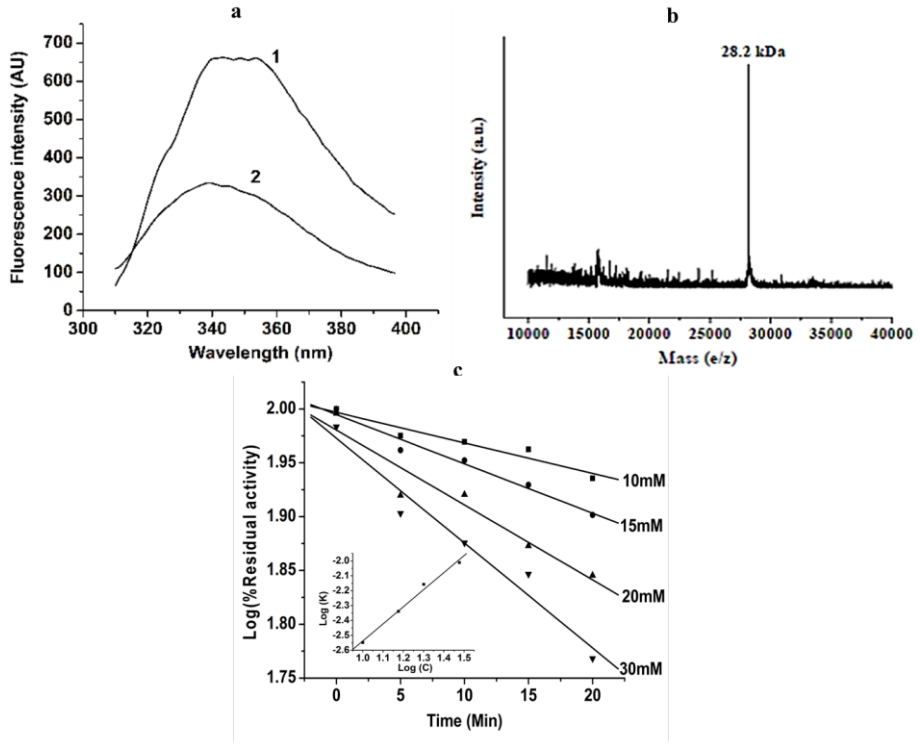

Figure 1: Purification and chemical modification of Bprot: (a) Intrinsic fluorescence spectra of Bprot (30 µg/ml) before (1) and after removal (2) of chromatogenic impurities (b)

Confirmation of molecular weight of Bprot (1mg/ml) by MALDI-TOF (c) Time dependence of activity observed at different concentrations of PMSF (Inset: A double logarithmic plot showing single serine residue at the active site).

2.3.2 Steady-state and time-resolved fluorescence

NBS titration studies indicated presence of a single Trp residue in Bprot. The intrinsic fluorescence spectrum of the Trp in Bprot showed 339 nm as λ_{max} (excitation wavelength 295 nm) indicating hydrophobic environment of the Trp residue (Fig. 2a). The decomposition analysis of intrinsic fluorescence spectrum with PFAST software (Shen et al. 2008) gave two conformers of Trp belonging to class A (55 %) i.e., buried in the hydrophobic environment and class II (45 %), which is hydrogen bonded to structured water molecules.

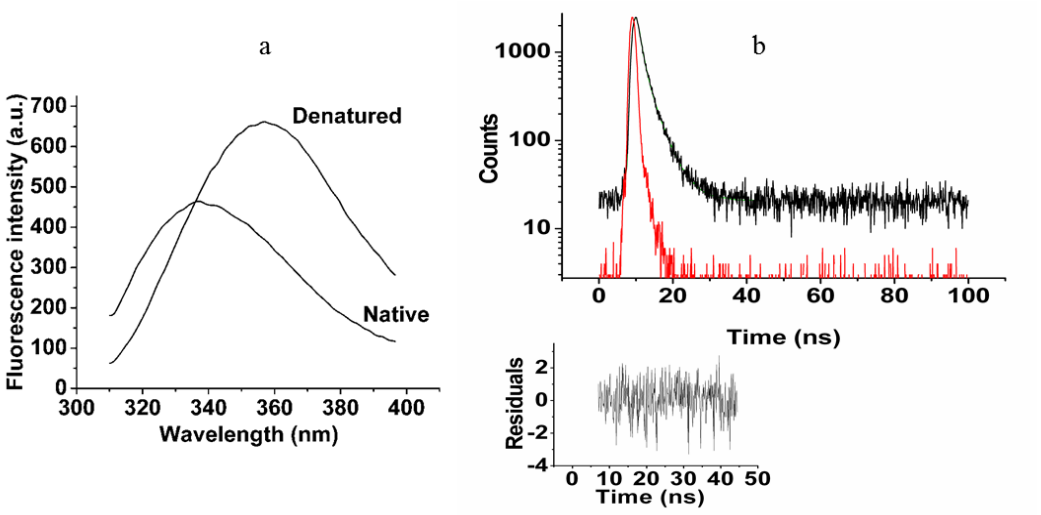

Figure 2: Fluorescence spectra of Bprot: (a) Intrinsic fluorescence spectra of native (λ_{max} 339 nm) and denatured (λ_{max} 358 nm) Bprot (30 µg/ml at pH 7, 28 °C). (b) Time-resolved fluorescence spectrum for Bprot (1 mg/ml at pH 7.0) the lower panel shows residuals.

The dynamics of the steady-state fluorescence of Bprot was analyzed by time-resolved fluorescence. The decay curves obtained from the lifetime measurement of intrinsic fluorescence of Bprot could be fitted well into a bi-exponential curve ($\chi 2 <$ 1.04) (Fig. 2b). From these fits, two decay times $\tau 1$ (1.0172 ns) with 55.54 % contribution and $\tau 2$ (3.5094 ns) with 44.46 % contribution for the Trp fluorescence of the native enzyme were obtained, indicating the presence of more than one conformer

emitting the energy. Conformers, one exposed to the surface with shorter decay time and the other buried in the hydrophobic core with longer decay time, contribute equally to the fluorescence. Thus, the presence of two conformers of the single tryptophan was established by both the above techniques.

2.3.3 FTIR and circular dichroism spectroscopy

FTIR spectrum of Bprot showed transmittance minima at 1,654 cm^{-1} corresponding to α-helices with prominent shoulder at 1,628 and 1,678 cm^{-1} for β-sheets and turns, respectively, in the secondary structure (Fig. 3a), indicating contribution of helices, sheets, and turns in forming active Bprot (Dong et al. 1990). The FTIR spectrum of Bprot matches with that of subtilisin Carlsberg (Xu et al. 1997).

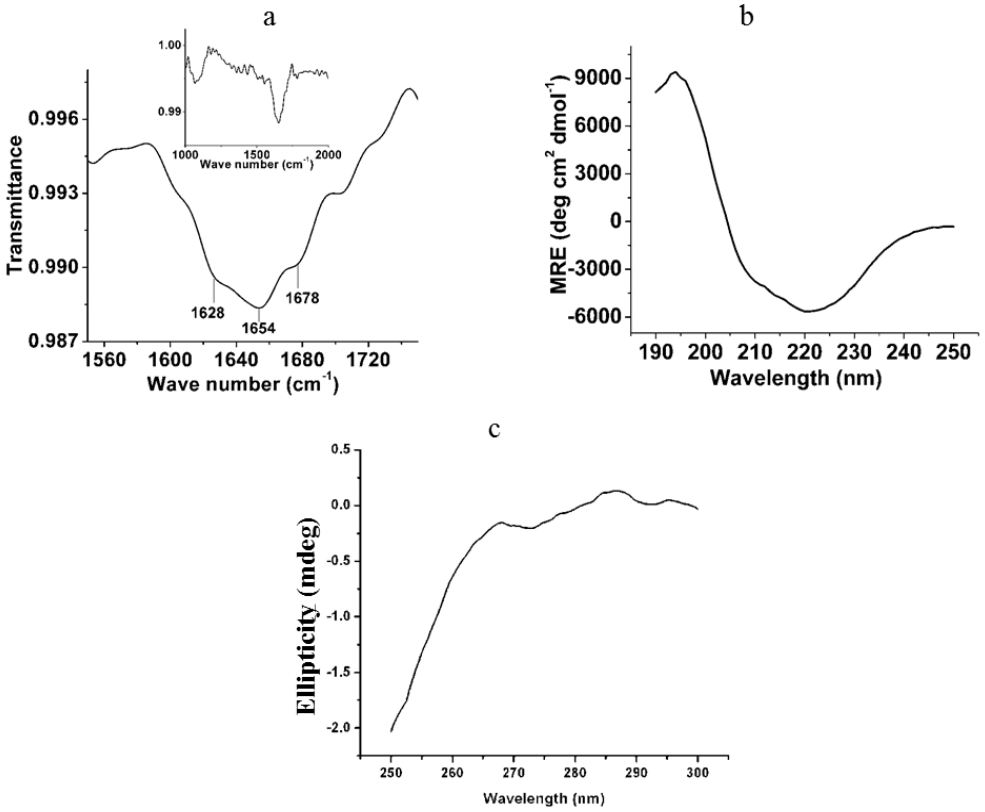

Figure 3: Secondary structure characterization of Bprot: (a) FTIR spectrum of Bprot in amide I band region (1.5 mg/ml at pH 7.0). *Inset* shows spectrum over a range of 1,000–2,000 cm^{-1}. (b) Far-UV CD spectrum (65μg/ml at pH 7.0) (c) Near UV CD spectrum of native Bprot (1.2mg/ml at pH7.0)

Far-UV CD spectrum of native Bprot showed negative ellipticity minima at 223 nm and a shoulder at 208 nm (Fig. 3b). The spectrum was analyzed with CONTINLL program of CDPro software. The secondary structure contents were estimated to be 14.4 % α-Helix, 32.9 % β-Sheet, 22.3 % Turns, 30.5 % Unordered (NRMSD = 0.029). The near UV CD spectrum of native Bprot indicated compact tertiary structure of native Bprot (Fig.3c).

Although estimated secondary structure elements are not available for comparison, the far-UV CD spectra of amidase from *Arthrobacter nitroguajacolicus* and 3 β-glucosidase from *Flavobacterium meningosepticum* show striking similarity with that of Bprot (Li et al. 2001; Kolkenbrock et al. 2006). The resemblance of CD spectrum to enzymes belonging to α/β hydrolase fold and presence of conserved active site of proteinases led to the possibility of Bprot belonging to the group of α/β hydrolase fold enzymes. The fold is characterized by conserved structure in parallel β sheets flanked on both sides by α-helices and arrangement of catalytic residues in spite of differences in sequence as shown in fig. 4 (Nardini and Dijkstra 1999). The conserved β-sheet core surrounded by α-helices in subtilases (Siezen and Leunissen 1997) supports the presence of α/β hydrolase fold in Bprot.

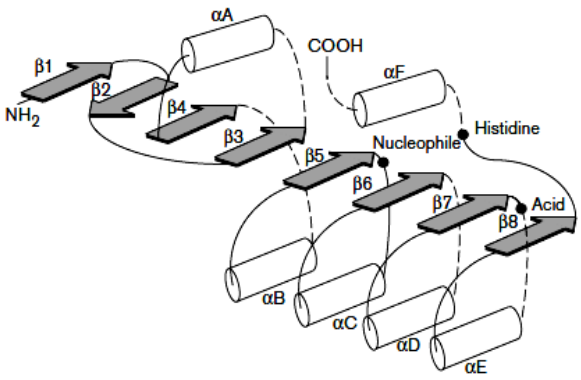

Figure 4: Secondary structure diagram of the 'canonical' α/β hydrolase fold: α helices and β strands are represented by white cylinders and gray arrows, respectively. The location of the catalytic triad is indicated by black dots. Dashed lines indicate the location of possible insertions. (Figure adapted from Nardini and Dijkstra 1999)

2.3.4 Solute quenching studies

Topological information about Bprot structure was collected by solute quenching of intrinsic tryptophan fluorescence of Bprot. The neutral quencher

acrylamide was found to be the most efficient for native Bprot, which quenched the fluorescence intensity with Stern–Volmer constant K_{sv} as 4.6 M^{-1}. KI and CsCl showed K_{sv} values as 2.25 and 0.58 M^{-1}, respectively (Fig. 5a and Table 1), indicating more of a positive charge density around the surface Trp conformer. The modified Stern–Volmer plot (Fig. 5b) showed 73 % accessibility of Trp fluorescence to acrylamide while 59% and 6.5 % accessibility to KI and CsCl, respectively. The partial access to Trp in native Bprot for acrylamide confirms the presence of buried conformer of tryptophan as indicated by decomposition analysis and time-resolved fluorescence studies. Bprot denatured with 6 M GdnHCl exhibited increased accessibility for acrylamide, KI (two times) as well as CsCl (five times), indicating change in the conformation due to unfolding of the protein (Table 1).

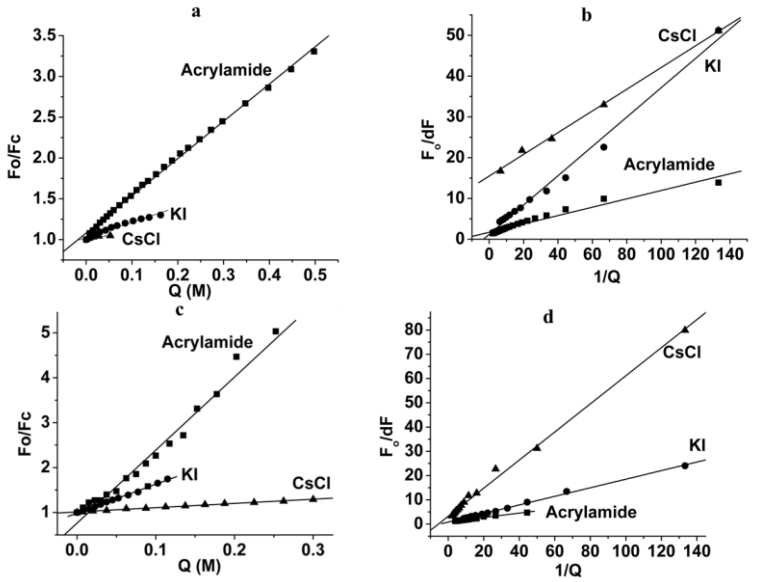

Figure 5: Solute quenching studies of Bprot: (a) and (c) Stern-Volmer plot for native and denatured Bprot, respectively (b) and (d) Modified Stern-Volmer plot for native and denatured Bprot, respectively.

Table 1: Solute quenching parameters for Bprot

Quencher		**K_{sv} (M^{-1})**	**F_a (%)**
Acrylamide	Native	4.6	73.7
	Denatured	16.3	100
KI	Native	2.25	59.1
	Denatured	6.53	100

CsCl	Native	0.58	6.5
	Denatured	0.85	31

2.3.5 SDS resistance of Bprot

SDS resistance is one of the criteria for investigating kinetic stability of protein (Manning and Colón 2004). A few proteases like *Nocardiopsis* protease and millin have been reported to be kinetically stable (Rohamare et al 2013, Yadav et al 2009). To investigate this property of Bprot, its SDS resistance was analyzed by SDS-gel electrophoresis in presence of various concentrations of SDS under boiled and unboiled conditions. Under unboiled condition, Bprot showed differential electrophoretic mobility even in presence of 1% SDS as compared to the boiled sample (Fig.6a). This suggests that Bprot structure is partially resistant to SDS.

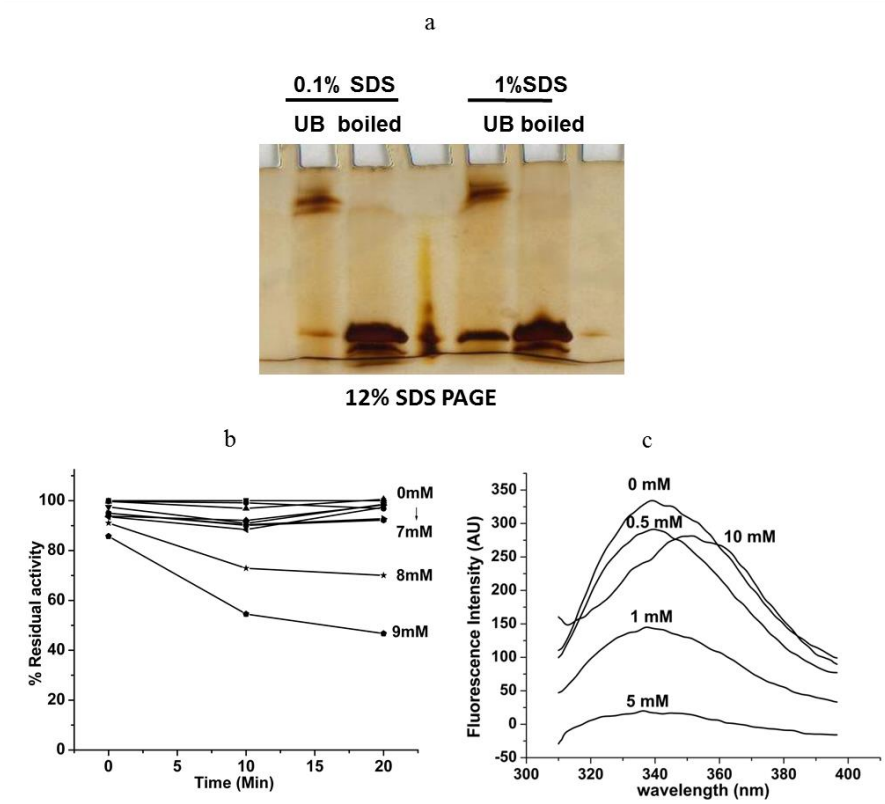

Figure 6: SDS resistance of Bprot: (a) 12% SDS-PAGE showed differential electrophoretic mobility of SDS-treated Bprot under boiled and unboiled conditions (b) Activity of Bprot in respective concentration of SDS (c) Intrinsic fluorescence spectra for Bprot incubated with respective concentration of SDS for 20 minutes.

The effect of various concentrations of SDS on Bprot activity was studied at different time intervals. The enzyme loses its activity in presence of 0.25% (8mM) SDS after 20 minutes (Fig.6b). The intrinsic fluorescence spectrum of Bprot (Fig.6c) indicated alteration in Trp environment of Bprot observed by decrease in fluorescence intensity with increasing concentration of SDS. The λ_{max} of the spectrum showed red shift to 355nm indicating exposure of Trp to the polar environment. This correlates with the loss of activity observed above 8mM SDS.

2.3.6 Effect of proteolytic enzymes

Bprot activity was increased by about 50 % in the presence of trypsin and chymotrypsin and remained constant even after 48 h. Proteinase K, which is a mixture of proteolytic enzymes, had no effect on Bprot up to 12 h. On reducing the proteinase K ratio to 100:1, Bprot retained 70 % activity even after 48 h (Fig. 7) indicating the moderate proteolytic resistance. Some proteins adopt a compact structure under harsh conditions like acidity and proteolytic environment to protect them from denaturation. This could be due to less number of cleavage sites or the sites not accessible to trypsin and chymotrypsin.

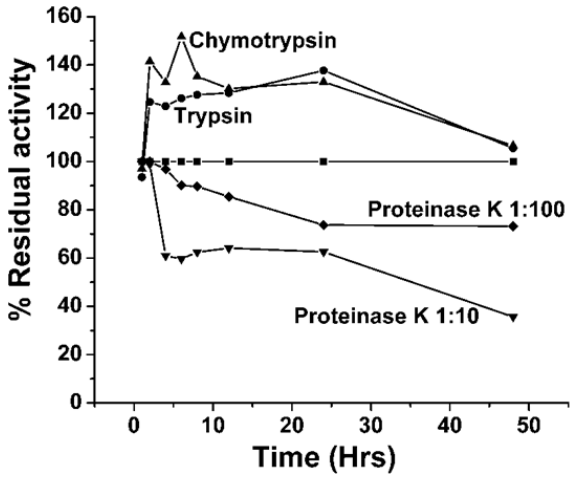

Figure 7: Activity profile of Bprot in presence of proteolytic enzymes at respective time intervals: control (*square*), Bprot + trypsin (10:1) (*circle*), Bprot + chymotrypsin (10:1) (*triangle*), Bprot + proteinase K (10:1), and Bprot + proteinase K (100:1).

Nocardiopsis protease and milin are reported to be resistant to degradation by proteolytic enzymes like trypsin and chymotrypsin for 24 h. Bprot not only exhibits stability but also shows enhancement in the activity in presence of trypsin and

chymotrypsin at 25 °C. The behavior is comparable to *Nocardiopsis* protease (Rohamare et al. 2013). Milin is more resistant to digestion by proteolytic enzymes even at 37 °C due to its glycosylated residues (Yadav and Jagannadham 2009).

2.3.7 Protein crystallization and data collection

After rigorous screening, Bprot crystallized as cubic crystals at a protein concentration 7mg/ml in the following conditions:

1. 0.1 M Sodium acetate pH 4.6, 8% (w/v) PEG 4000 (Screen: JCSG Hampton Research)
2. 50 mM Sodium ADA pH 6.6, 15- 45% (w/v) PEG 400, 50mM Mg acetate (Screen: Tray II)

The representative images of crystals obtained are given in Figure 8.

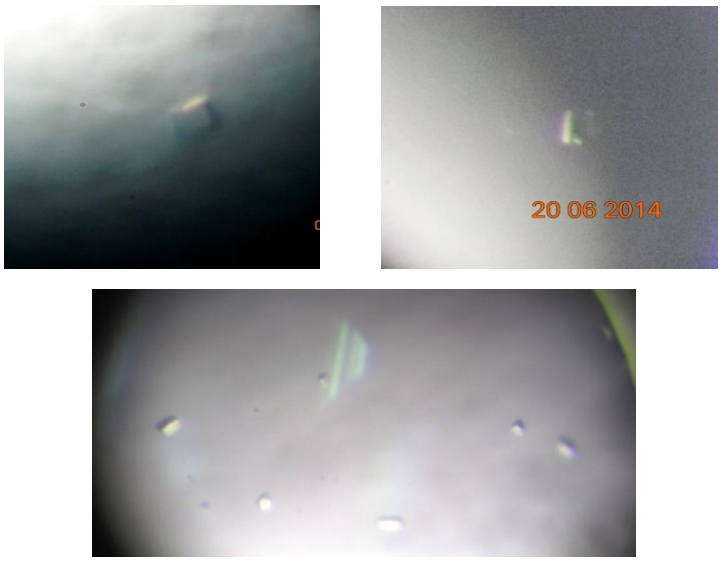

Figure 8: Representative images of Bprot crystals

The crystals diffracted to 8 A°, data were integrated in the XDS package. Bprot crystallized in space group $H3_2$ with one molecule in the asymmetric unit. The estimated Matthew's coefficient was 2.53 $A°^3$ Da^{-1} with a solvent content of 51.41%. A summary of data collection parameters is presented in Table 2.

Trials for improvement in the crystal quality by additive screens, varying pH of the condition or addition of isopropanol did not improve stability of the crystal. Thus, further data could not be collected for Bprot crystals.

Table 2: Data collection for Bprot crystal:

Resolution	8 A°
Temperature	100K
X-ray source	SSRL (BL12-2)
Wavelength	0.9795 A°
unit cell dimensions	a=b=126.0632,c= 96.1329 α=β=90.0 γ= 120.0
space group	H 3_2 (number 155)
Unit cell volume	1321280.8 A^3
Asymmetric unit volume	73404.5 A^3
Matthews coefficient:	2.53
Solvent content	51.41%

Thus, the quality of purified Bprot was improved as a first step towards the conformational transitions studies and then the structural characterization was attempted by x-ray crystallization studies. Spectroscopic characterization led us to propose hydrolase fold in the enzyme. The resistance towards SDS and proteolytic environment pointed to possibility of Bprot being a kinetically stable protein. The unfolding transitions of Bprot under denaturing conditions are described in detail in next chapter.

References

- Dong, A., Huang, P., & Caughey, W. S. (1990). Protein secondary structures in water from second-derivative amide I infrared spectra. *Biochemistry*, *29*(13), 3303-3308.
- Kolkenbrock, S., Parschat, K., Beermann, B., Hinz, H. J., Fetzner, S. (2006). *N*-Acetylanthranilate amidase from *Arthrobacter nitroguajacolicus* Rü61a, an α/β-hydrolase-fold protein active towards arylacylamides and esters, and properties of its cysteine-deficient variant. *J Bacteriol 188*, 8430–8440.
- Kunitz, M. (1947). Crystalline soybean trypsin inhibitor II. General properties. *The Journal of general physiology*, *30*(4), 291-310.
- Laskowski, M. (1955). Trypsinogen and trypsin. *Methods Enzymol 2*, 26–36.
- Li, Y. K., Chir, J., Chen, F. Y. (2001). Catalytic mechanism of a family 3β-glucosidase and mutagenesis study on residue Asp-247. *Biochem J 355*, 835–840.
- Lowry, O. H., Rosebrough, N. J., Farr, A. L., & Randall, R. J. (1951). Protein measurement with the Folin phenol reagent. *J biol Chem*, *193*(1), 265-275.
- Manning, M., & Colón, W. (2004). Structural basis of protein kinetic stability: resistance to sodium dodecyl sulfate suggests a central role for rigidity and a bias toward β-sheet structure. *Biochemistry*, *43*(35), 11248-11254.
- Nardini, M., & Dijkstra, B. W. (1999). α/β hydrolase fold enzymes: the family keeps growing. *Current opinion in structural biology*, *9*(6), 732-737.
- Rohamare, S. B., Dixit, V., Nareddy, P. K., Sivaramakrishna, D., Swamy, M. J., & Gaikwad, S. M. (2013). Polyproline fold—in imparting kinetic stability to an alkaline serine endopeptidase. *Biochimica et Biophysica Acta (BBA)-Proteins and Proteomics*, *1834*(3), 708-716.
- Shankar, S., Rao, M., & Laxman, R. S. (2011). Purification and characterization of an alkaline protease by a new strain of *Beauveria sp*. *Process biochemistry*, *46*(2), 579-585.
- Shen, C., Menon, R., Das, D., Bansal, N., Nahar, N., Guduru, N., & Reshetnyak, Y. K. (2008). The protein fluorescence and structural toolkit: Database and programs for the analysis of protein fluorescence and structural data. *Proteins: Structure, Function, and Bioinformatics*, *71*(4), 1744-1754.

- Siezen, R. J., & Leunissen, J. A. (1997). Subtilases: the superfamily of subtilisin-like serine proteases. *Protein Science*, *6*(3), 501-523.
- Spande, T. T., & Witkop, B. (1967). Determination of the tryptophan content of proteins with N-bromosuccinimide. *Methods enzymol*, *11*,498-506.
- Subbian, E., Yabuta, Y., & Shinde, U. (2004). Positive selection dictates the choice between kinetic and thermodynamic protein folding and stability in subtilases. *Biochemistry*, *43*(45), 14348-14360.
- Svedese, V. M., Tiago, P. V., Bezerra, J. D. P., Paiva, L. M., Lima, E. Á. L. A., & Porto, A. L. F. (2013). Pathogenicity of *Beauveria bassiana* and production of cuticle-degrading enzymes in the presence of *Diatraea saccharalis* cuticle. *African Journal of Biotechnology*, *12*(46), 6491-6497.
- Xiao, G., Ying, S. H., Zheng, P., Wang, Z. L., Zhang, S., Xie, X. Q., & Feng, M. G. (2012). Genomic perspectives on the evolution of fungal entomopathogenicity in *Beauveria bassiana*. *Scientific reports*, *2*.
- Xu, K., Griebenow, K., & Klibanov, A. M. (1997). Correlation between catalytic activity and secondary structure of subtilisin dissolved in organic solvents. *Biotechnology and bioengineering*, *56*(5), 485-491.
- Yadav, S. C., & Jagannadham, M. V. (2009). Complete conformational stability of kinetically stable dimeric serine protease milin against pH, temperature, urea, and proteolysis. *European Biophysics Journal*, *38*(7), 981-991.

Chapter 3

Functional and Conformational transitions of Serine Protease from *Beauveria sp.* MTCC 5184

Summary

Beauveria protease (Bprot) was studied for its functional and conformational stability under denaturing conditions using spectroscopic approach. Retention of total activity of the protease in the vicinity of (1) 3 M GdnHCl for 12 h, (2) 50 % methanol and dimethyl sulfoxide each for 24 h indicated its unusual stability. Also, the structure of the protein was stable at pH 2.0 upto 4 hours. The secondary structure of Bprot was stable in 3 M GdnHCl as seen in far-UV CD spectra. The active fraction of Bprot obtained from size-exclusion chromatography in the presence of GdnHCl (1.0–3.0 M) eluted at reduced retention time. The peak area of inactive or denatured protein with the same retention time as that of native protein increased with increasing concentration of denaturant (1.0–4.0 M GdnHCl). However, the kinetics of GdnHCl-induced unfolding as studied from intrinsic fluorescence revealed k_{unf} of native protein to be 5.407×10^{-5} s^{-1} and a half-life of 3.56 hours. The enzyme is thermodynamically stable in spite of being resistant to the denaturant, which could be due to the effect of GdnHCl imparting rigidity to the active fraction and simultaneously unfolding the partially unfolded protein that exists in equilibrium with the folded active protein. Functional stability of Bprot in 50% methanol correlated well with the maintenance of secondary structure after 24 hours. Thermal denaturation of Bprot indicated the T_m to be 56 ℃ by both fluorescence and CD studies. Acid denatured Bprot exhibited interesting structural transitions in presence of organic solvents. In presence of fluoroalcohols, Bprot was less stable in HFIP as compared to TFE. HFIP served as better helix inducer for acid denatured Bprot.

3.1 Introduction

In the previous chapter, biophysical characterization of Bprot was reported to establish the α/β hydrolase fold in it. The protein was also suspected to be a kinetically stable one due to its resistance towards SDS and proteolytic environment.

The serine protease subtilisin is an important industrial enzyme as well as a model for understanding the proteolysis mechanism. This has highlighted subtilisin as a model system for protein engineering studies since the 1980s. Most subtilisin engineering has involved catalytic amino acids, substrate binding regions and stabilizing mutations (Bryan 2000). Even though enhancing stability has been the most important area in engineering of subtilases, the principles that govern subtilase

stability still remain to be explored. Bacterial subtilisins like subtilisin BPN', Subtilisin Carlsberg, Subtilisin E have been well characterized for their three-dimensional structure and stability under denaturing conditions (Subbian et al 2004; Brownt and Schleich 1975; Neidhart and Petsko 1988; Srimathi et al 2006). From these reports it is evident that the subtilases are resistant to 3-4M GdnHCl and covalent modifications can improve the stability further. Protein unfolding induced by chemical denaturants, pH or temperature are common approaches to study proteins *in vitro*. Functional stability of subtilases in organic solvents has been an important area of research owing to their importance in peptide synthesis applications. Correlation between the secondary structure and function of the enzymes in presence of organic solvents using spectroscopic approaches like CD and FTIR has been reported (Solanki et al 2012).

Industry and academia have devoted considerable effort into developing effective strategies to enhance the lifetime of enzymes in the presence of organic solvents. The strategies can be grouped into three main categories: (i) isolation of novel enzymes active under extreme conditions, (ii) modification of enzyme structures to increase their resistance toward nonconventional media, and (iii) modification of the solvent environment to decrease its denaturing effect on enzymes. (Stepankova et al 2013). Among various alcohols, fluoroalcohols like 2,2,2-trifluoroethanol (TFE) and 1,1,1,3,3,3-hexafluoroisopropanol (HFIP) are often preferred in protein folding studies because of its high potential in stabilizing the α helical structure. The secondary structures stabilized by TFE are assumed to reflect conformations that prevail during early stages of protein folding (Gupta et al 2003). The effectiveness of fluoroalcohols to induce secondary structure is related to the fluorine atoms, which are important for enhancing the effects of the alcohol. Though various fluoroalcohol induced molten globules have been reported (Gupta et al 2003; Kanjilal et al 2003), the effect is not generalized. This demands for understanding of conformational dynamics of the protein in presence of organic solvents.

The present study involves detailed analysis of functional and conformational transitions of Bprot under a range of denaturing conditions using biophysical techniques like fluorescence and CD spectroscopy and attempts to understand the unusual stability of the protein. The denaturing conditions here include guanidine hydrochloride, organic solvents, pH-induced denaturation and thermal denaturation.

Additional studies about the conformational behavior of this subtilase may improve the understanding of the folding pathway of this class of proteins.

3.2 Materials and methods

3.2.1 Materials

Guanidine hydrochloride (GdnHCl), ANS was obtained from Sigma Aldrich Ltd., USA. All other reagents including buffer compounds and organic solvents used were of analytical grade. Solutions for spectroscopic measurements were prepared in MilliQ water.

3.2.2 Production and purification of Bprot

The purification of Bprot was performed as mentioned in section 2.2.3. Purified Bprot was stored at pH 7.0 at 4℃.

3.2.3 Circular dichroism (CD) and fluorescence measurements:

The fluorescence and CD studies were performed as described in section 2.2.9 and 2.2.12, respectively.

3.2.4 Treatment of the enzyme with GdnHCl

To study the effect of GdnHCl on the function of the enzyme, samples of Bprot (1 mg/ml) were incubated with various concentrations of GdnHCl (1.0–6.0 M), in 20 mM phosphate buffer pH 7.0 for 12 h at 28 °C. Suitable aliquots were removed at regular time intervals and assayed for enzyme activity. The readings were corrected for blank samples containing respective concentration of GdnHCl without the enzyme.

3.2.5 Unfolding kinetics

The kinetics of GdnHCl-induced unfolding of Bprot were monitored by using Perkin-Elmer luminescence spectrometer LS50B. Protein solution (30 μg/ml) was manually mixed with GdnHCl solution to obtain protein samples with final denaturant concentrations ranging from 2 to 5 M. Excitation and emission wavelengths for the time scans were 295 and 339 nm, respectively. Kinetic traces were analyzed by fitting to a first-order exponential function.

3.2.6 Size‑exclusion chromatography

The denaturation of Bprot with GdnHCl was also monitored using a WATERS HPLC unit and a WATERS gel filtration Protein Pak™ 300SW (7.5 × 300 mm column). Phosphate buffer (25 mM) (with 0.15 M NaCl), pH 7.0 containing respective concentrations of GdnHCl served as the mobile phase. Then, 100 µl of protein (600µg/ml) incubated in 0–4 M GdnHCl for 4 h was injected into the column. The flow rate was maintained at 0.5 ml/min and the elution profile was monitored at 280 nm.

3.2.7 pH‑induced denaturation

The purified Bprot was incubated against buffers of different pH for 4 h before activity assay and recording the spectra. The different buffers used were glycine–HCl (pH 1.0– 3.0), citrate–phosphate buffer (pH 4.0–6.0), potassium phosphate buffer (pH 7.0), Tris–HCl (pH 8.0–9.0), and glycine–NaOH (pH 10.0–12.0) at concentration of 20mM each.

3.2.8 Thermal denaturation

Activity of Bprot was monitored during thermal denaturation by incubating the enzyme at respective temperature for 10 minutes and then performing the assay as previously mentioned. Peltier unit was used to control the temperature during far UV CD measurements with the ramp rate of 5˚C/min and incubation time set at 10 minutes after attaining the temperature. Spectra were recorded as mentioned earlier.

3.2.9 Treatment of the enzyme with solvents

For the assay-based studies, Bprot (1 mg/ml) was incubated in 50 % (v/v) of methanol, ethanol, propanol, acetonitrile (ACN), and dimethyl sulfoxide (DMSO) at pH 7 for 48 h at 28 °C. The enzyme solvent systems were incubated in static condition and the solvents were miscible in the buffer. The incubation mixtures were kept in tightly closed vials and change in the volume was monitored throughout the period, and no changes were detected in the volumes of the samples. Aliquots were removed at regular time intervals and assayed for the enzyme activity.

Effect of fluorinated alcohols like 2,2,2-trifluoroethanol (TFE) and 1,1,1,3,3,3-hexafluoroisopropanol (HFIP) (5% and 10% *v/v*) on Bprot activity was checked by incubating Bprot in the solvents for 4 hours. Aliquots were assayed for caseinolytic

activity at respective time intervals as described previously. Bprot (at pH 7.0 and pH 1.0) was incubated with TFE and HFIP (5-50% *v/v*) for 4 hours before recording far UV CD spectra.

3.3 Results and discussion

3.3.1 Bprot stability towards GdnHCl

Interestingly, the protein was not only stable but also showed 1.4 times enhanced activity in subdenaturing concentrations of GdnHCl (3 M), which remained constant for 12 h (Fig. 1a). The enzyme retained 80 % activity in the vicinity of 4 M GdnHCl after 2 h, and lost activity immediately in 5 and 6 M GdnHCl. Since, the mixture of GdnHCl and enzyme (after incubation) gets diluted after removing and then mixing the aliquot in the assay mixture, the activity detected thereafter could be due to the stability of the enzyme in presence of GdnHCl or due to reversible inactivation of the protein. The resistance of a protein towards chaotropic agent is conferred on them by kinetic stability (Sanchez-Ruiz 2010). The above results led us to investigate this property of Bprot.

Fluorescence and circular dichroism studies

Bprot (with enhanced activity) in the presence of 1, 2, and 3 M GdnHCl, showed a red shift in λ_{max} by 3, 11, and 14 nm, respectively (Fig. 1b), indicating increased polarity or hydrophilic environment of tryptophan. At concentrations above 4 M GdnHCl, a red shift by 17 nm in λ_{max} was observed (356 nm). This implied gradual unfolding of the protein and could not be correlated with the functional stability, observed as mentioned above.

The far-UV CD spectra of activated Bprot (up to 3 M GdnHCl) showed slight ordering of the structure (as indicated by decrease in the ellipticity), although data could not be collected below 210 nm. Substantial loss of the structure was observed at ≥4.0 M GdnHCl (Fig. 1c). Retention of the activity of Bprot could be correlated with the retention of secondary structure up to 3.0 M GdnHCl.

Unfolding kinetics

Fluorescence decay analysis has been used as the parameter to calculate the half-life and unfolding rate of several proteins like papain, chymopapain, superoxide

dismutase, etc. by Manning and Colo´n (2004). The stability of Bprot in 3 M GdnHCl for 12 h was indicative of higher unfolding barrier of Bprot as compared to other globular proteins. The rate constants (*k*) for GdnHCl-induced unfolding of Bprot were calculated by first-order exponential decay analysis. Plotting the unfolding rate constants of the protein against GdnHCl concentration and extrapolating to 0 M yielded a native unfolding rate of 5.407×10^{-5} s^{-1} (Fig. 1d) and half-life of native Bprot was calculated to be 3.56 h. This indicated that the enzyme is thermodynamically stable rather than a kinetically stable protein. The cause of functional stability still remained a question.

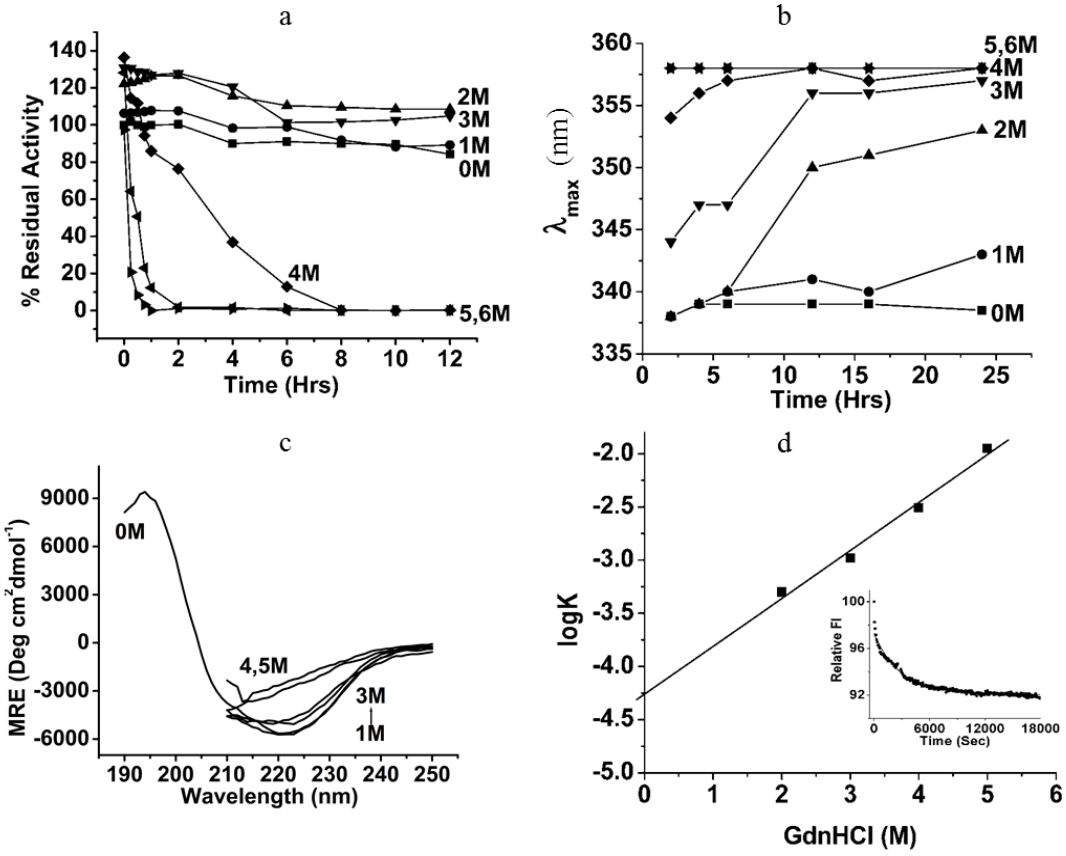

Figure 1: Effect of GdnHCl on Bprot: (a) activity profile of Bprot incubated in different concentrations of GdnHCl at pH 7, 28 °C, for different time intervals. (b) Shift in λ_{max} of intrinsic fluorescence spectra when incubated in GdnHCl; 0 M (*square*), 1 M (*circle*), 2 M (*triangle*), 3 M (*inverted triangle*), 4 M (*diamond*), 5 M (*left-sided triangle*), 6 M (*right-sided triangle*). (c) Far-UV CD spectra of Bprot (65 μg/ml) incubated in different concentrations of GdnHCl for 4 h. Molarity of GdnHCl used is indicated in each case. (d) Unfolding kinetics of Bprot examined in presence of 2–5 M GdnHCl: *Inset* shows representative single exponential fit of decay curve for Bprot in 3 M Gdn-HCl to determine rate constant. The log of the rate

constants was plotted against GdnHCl concentration and fitted to a linear function. Extrapolation of the plot to 0 M GdnHCl yielded native unfolding rate of 5.4×10^{-5} s^{-1}.

Subtilisin BPN and other subtilases have also been shown to be resistant to unfolding under harsh denaturing conditions. Subtilisin BPN is resistant to 4 M Gdn-HCl (for 1 h) (Bryan et al 1992). Subtilisin enzymes are reported to exhibit the slowest amide-proton exchange rates indicating the "tight" secondary and tertiary structure as compared to less stable enzymes (Ogino et al 2007). The exceptional conformational stability of subtilisins may be a consequence of structural rigidity, thereby denying access of denaturants to the hydrogen-bonded protein interior (Brownt and Schleich 1975). Thus, it may be proposed that conformational stability of Bprot to denaturation by Gdn- HCl may be due to the inability of GdnHCl in penetrating the compact structure of Bprot, thereby protecting the hydrogen-bonded protein interior. However, the unfolding half-life of native Bprot was found to be 3.56 h, which is much less as compared to established kinetically stable proteins like papain and chymopapain (Manning and Colón 2004). Also, Bprot is more susceptible to GdnHCl-induced unfolding as compared to milin (Yadav and Jagannadham 2009), α-lytic protease (Cunningham et al 1999) and *Nocardiopsis* protease (Rohamare et al 2013), which are resistant to even 6 M GdnHCl.

Size‑exclusion chromatography

Size-exclusion chromatography has been a valuable method for detecting potential folding intermediates that are stabilized by low concentrations of the denaturant. Typically, such intermediates exhibit Stokes' radii that are larger than that of the fully folded protein (Bryan et al 1992). In the present study, Bprot showed the existence of two conformations under equilibrium in the presence of subdenaturing concentrations of GdnHCl. The native protein exhibited a retention time of 23.2 min (P1) (Fig. 2a). In the presence of 1–3 M GdnHCl, two peaks were observed, one with a lower retention time of 20.5 min (P1') and the heterogenous peak at 22–24 min (P2). The species with a lower retention time (P1') in presence of 3 M GdnHCl showed three times higher specific activity as compared to the native protein (23.2 min) (P1). The heterogenous peak in SEC profile with retention time of 22–23 min (P2) turned out to be of inactive and denatured Bprot.

GdnHCl is reported to change the hydrodynamic properties of proteins as studied by SEC profile in case of ribonuclease, hen egg white lysozyme, and staphylococcal β lactamase (Uversky 1993). Reduced entropy in the presence of denaturant could be the reason for enhanced activity (Bhuyan 2002).

Intrinsic fluorescence spectra of P1' is blue-shifted by 3 nm (336 nm) as compared to that of the native Bprot (Fig. 2b), suggesting a hydrophobic environment of trp. λ_{max} of P2 as 352–356 nm indicated denatured Bprot.

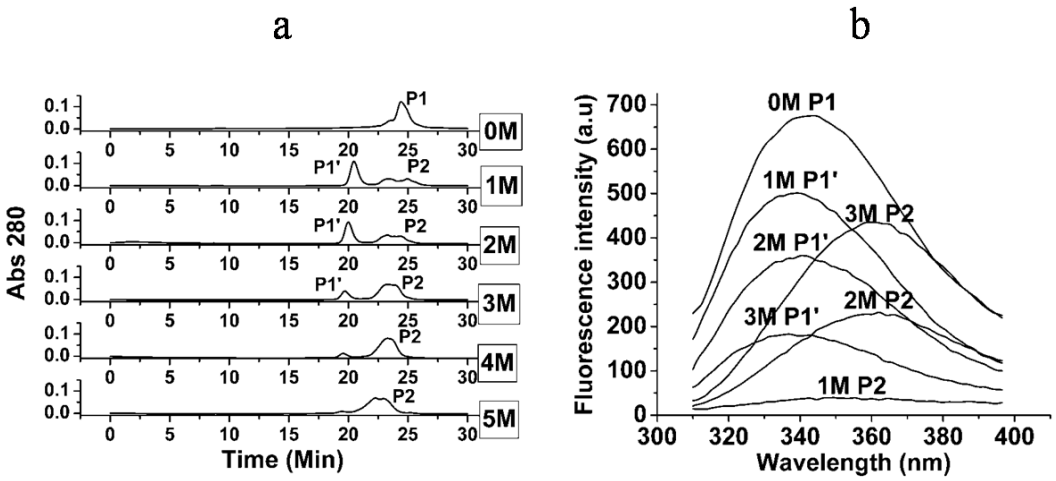

Figure 2: Size-exclusion chromatography of Bprot in the presence of GdnHCl. (a) SEC profile showing differential retention time for Bprot (0.6 mg/ml) incubated in different concentrations of GdnHCl as indicated in each case for 4 h. (b) Intrinsic fluorescence spectra corresponding to active (*P1'*) and inactive forms (*P2*) of Bprot.

A small population of partially unfolded Bprot could exist under native conditions which by the trigger of even low concentration of denaturant (1 M) gets detached or unbound from the active enzyme, which in turn expresses enhanced activity. In the presence of 2 and 3 M Gdn-HCl, the population further increases, still allowing the native fraction to express more activity. The red shift of 3, 11, and 14 nm λ_{max} of intrinsic fluorescence under these conditions must be that of a mixture of active and denatured fractions (Fig. 1b). With further increase in denaturant concentration, 4 and 5 M, only the denatured population exists.

3.3.2 Thermal denaturation of Bprot

Thermal denaturation of Bprot was observed to be an irreversible two-step process. The enzyme lost proteolytic activity on incubation at 55 °C within 30 min (Fig. 3a). Intrinsic fluorescence spectrum showed a fast red shift in λ_{max} to 346 nm at 55 °C, 353 nm at 60 °C and 356 nm at 65 °C, indicating unfolding of the protein. Sigmoid fit (R^2 = 0.99) of the thermal denaturation curve indicated T_m of the protein to be 56.5 °C.

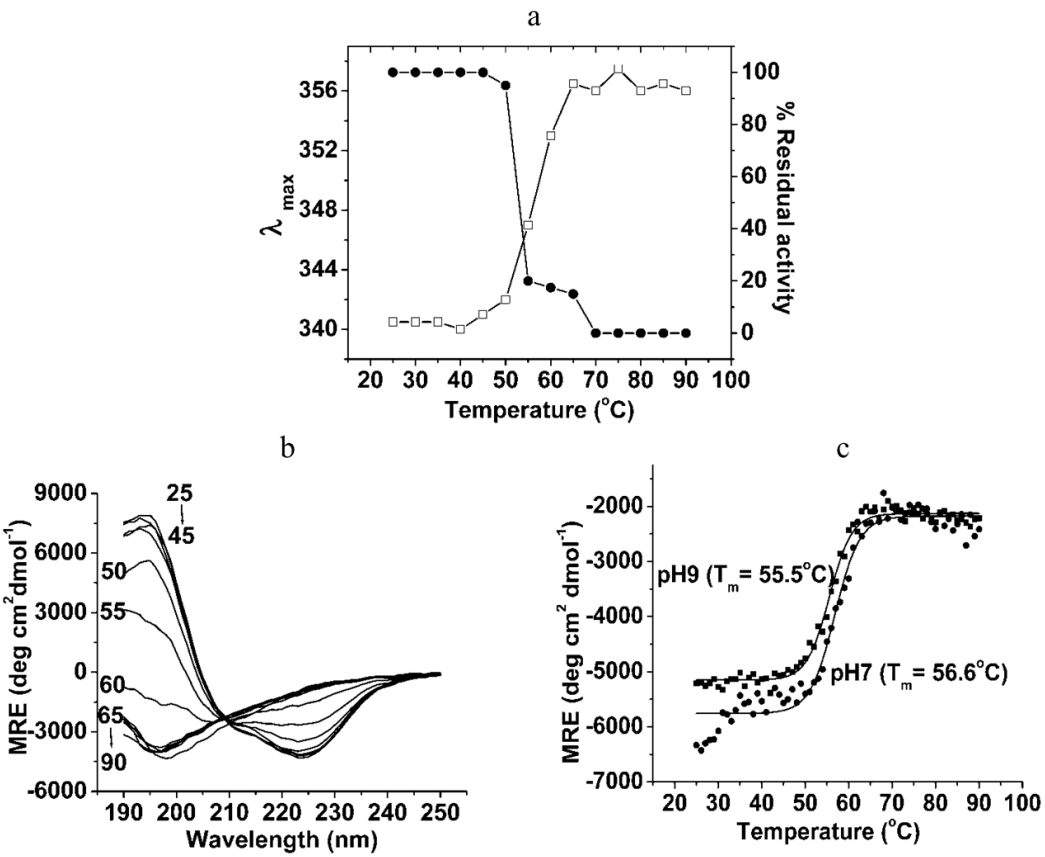

Figure 3: Thermal denaturation of Bprot: (a) activity profile (*circle*) and change in λ_{max} (*square*) of intrinsic fluorescence spectrum during thermal denaturation. (b) Far-UV CD spectra of Bprot (65 µg/ml) incubated at respective temperature for 5 min. The numbers on the spectra indicate temperatures in ℃. (c) Sigmoidal fit of the change in ellipticity at 223 nm at pH 7.0 and pH 9.0 during thermal denaturation (Bprot 65 µg/ml).

Monitoring of the secondary structure during thermal denaturation by far-UV CD spectroscopy (Fig. 3b) showed a partial decrease in the ellipticity when heated to 55 °C, which correlated well with the loss of activity. Major change leading to a complete loss of the structure was observed at and above 60 °C. Sigmoidal fit analysis

of the change in ellipticity at 223 nm estimated the same *T*m value of 56 °C (R^2 = 0.98) (Fig. 3c) close to that obtained from the fluorescence studies. Analysis of far-UV CD spectra in CONTINLL shows that α-helical content of Bprot decreased to 4.5 % above 60 °C. However, the spectra above 65 °C visibly show the transformation of the structure into a random coil, which is not detected by the software (Table 1).

The isodichroic point at 208 nm in CD spectra indicates the equilibrium between conformational transitions to attain a random coil structure finally above 60 °C. The melting temperature does not change considerably at pH 9, which is the optimum pH for activity of the enzyme (Fig. 3c). Thermostability of other proteases like milin upto 60℃ (Yadav and Jagannadham 2009) and *Nocardiopsis* protease upto 65℃ (Rohamare et al 2013) is comparable to that of Bprot.

Table 1: Secondary structure analysis of Bprot by the CDPro program (CONTINLL software)

Sample	α helix	B sheet	Turns	Unordered	NRMSD
Native Bprot					
Bprot at pH 7	15.6	32.8	21.1	30.5	0.023
pH induced denaturation					
1	3.9	42.3	20.8	33.0	0.016
2	18.1	31.6	20.2	29.2	0.010
3	17.9	33.4	20.6	28.0	0.017
4	16.3	33.6	21.4	28.9	0.023
5	18.9	30.8	20.8	29.4	0.025
6	17.6	30.9	22.0	28.5	0.095
7	16.5	32.2	21.5	30.7	0.018
8	18.9	31.2	21.2	28.8	0.032
9	15.7	33.6	21.5	29.3	0.03
10	17.4	32.3	21.2	29.0	0.04
11	3.1	38.8	21.1	37.0	0.091
12	2.9	38.7	21.0	37.3	0.135
Thermal unfolding					
25℃	15.6	32.8	21.1	30.5	0.023

50℃	14.3	33.7	21.8	30.2	0.036
55℃	5.2	40.5	21.9	32.3	0.059
60℃	4.5	40.0	22.0	33.5	0.085
65℃	4.3	39.0	22.3	34.4	0.052
90℃	4.4	39.0	22.4	34.2	0.050
Organic solvents					
Methanol	15.7	33.6	21.7	29.0	0.025
Ethanol	6.3	41.6	22.9	29.3	0.055
n-propanol	7.4	41.0	22.3	29.4	0.076
Acetonitrile	8.3	29.1	24.0	37.6	0.029
Effect of organic solvents on acid denatured Bprot					
pH 1	4.8	40.4	21.3	33.5	0.041
pH1+Methanol	6.7	39.9	22.2	31.1	0.071
pH1+Ethanol	15.5	41.1	22.7	30.6	0.076
pH1+Propanol	10.4	36.5	21.9	31.1	0.124

3.3.3 pH‑induced denaturation of Bprot

Bprot activity is fairly stable in the pH range of 5.0–10.0 up to 4 h (Fig. 4a, c). A drastic loss in activity was observed at highly acidic and alkaline pH. Intrinsic fluorescence profiles were more or less similar in the wide range of pH 3.0–11.0. At pH 1.0, intrinsic fluorescence spectrum shows a red shift by 3 nm, indicating slightly increased polarity of Trp (Fig. 4e). Noticeable ANS binding at pH 1.0 indicated exposure of hydrophobic amino acids to the surface of the protein, thus indicating a change in conformation (Fig.4f).

Secondary structure, as indicated by far-UV CD spectra, was stable in the pH range of 2.0–10.0 for 4 h (Fig. 4b, d). Enzyme incubated at extreme acidic pH (pH 1.0) attains a random coil structure (Fig. 4b). The only condition under which structural and functional stability of Bprot are not correlated is pH 2.0. Slight alteration at pH 9.0 and 10.0 (reduced ellipticity at 195 nm) was observed, and under these conditions, Bprot exhibits optimum activity. Extreme alkaline pH 11.0 and 12.0 denature the protein completely forming unordered structure (Fig. 4d). However,

these visible changes are not translated in the values calculated by the software (Table 1).

In spite of the observed loss in activity, the secondary structure of Bprot showed more resistance to acid-induced denaturation. The structure remained intact at pH 2 even after 4 hours. Thus, the activity loss might be due to change in ionization of amino acids near the active site. A similar pattern of decrease in α-helical content and increase in β-sheet and unordered structure content suggest similar modes of unfolding in thermal and acid-induced denaturation.

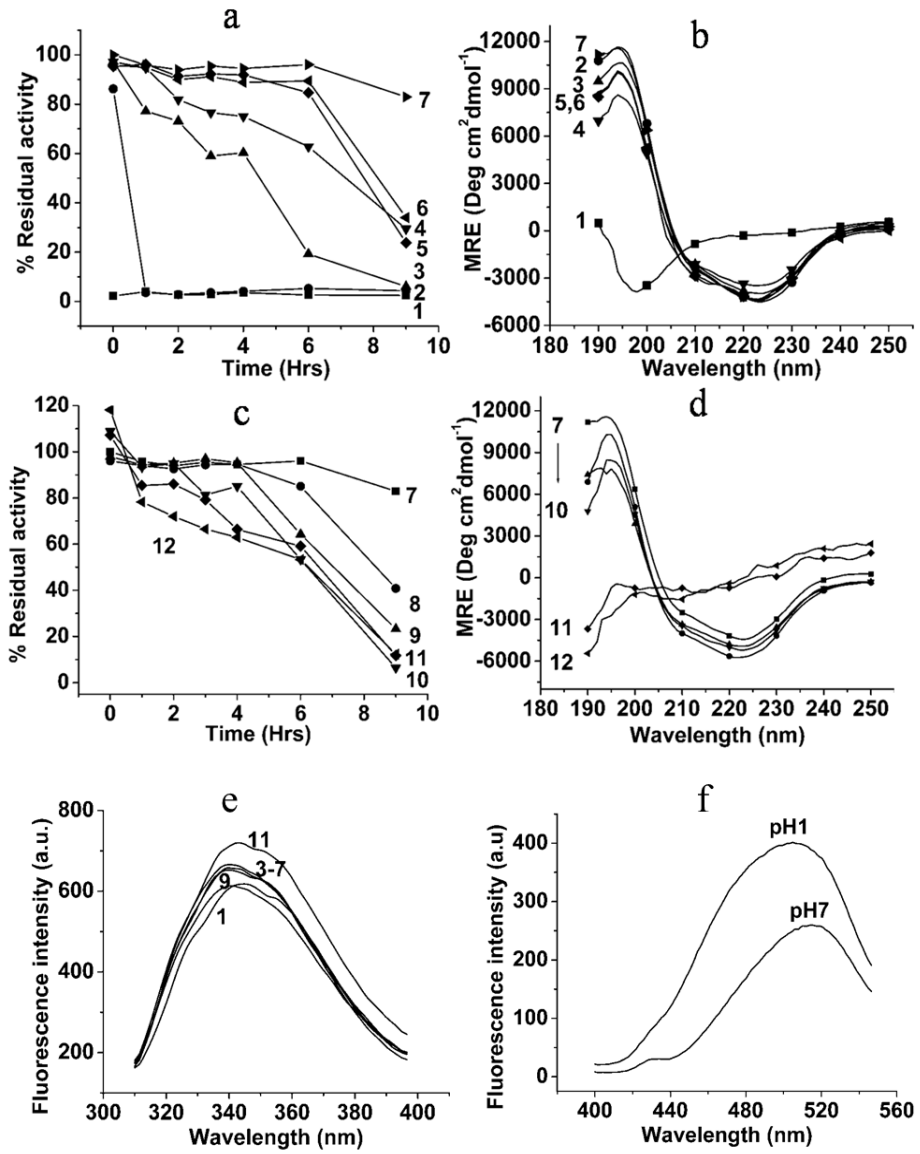

Figure 4: pH-induced denaturation of Bprot: (a) activity profile at respective time intervals for pH 1.0-7.0 and (b) far-UV CD spectra of Bprot incubated for 4 h in acidic pH

range; pH 1 (*square*), pH 2 (*circle*), pH 3 (*triangle*), pH 4 (*inverted triangle*), pH 5 (*diamond*), pH 6 (*left-sided triangle*) and pH 7 (*right-sided triangle*). (c) Activity profile at respective time intervals for pH 7.0-12.0 and (d) far-UV CD spectra of Bprot incubated for 4 h in alkaline pH range; pH 7 (*square*), pH 8 (*circle*), pH 9 (*triangle*), pH 10 (*inverted triangle*), pH 11 (*diamond*), pH 12 (*left-sided triangle*) (e) Intrinsic fluorescence spectra of Bprot incubated at respective pH for 4 hours. Numbers on the spectra indicate the pH. (f) ANS binding to Bprot incubated at pH 1.0 for 4 hours.

3.3.4 Stability of Bprot in organic solvents

Bprot showed tolerance towards high concentrations of organic solvents. The proteolytic activity of the enzyme was enhanced two times in the presence of 50 % methanol and 50 % DMSO and remained constant up to 24 h (Fig. 5a). The stability of Bprot in solvents decreased with an increase in the carbon chain length of the solvent (ethanol and propanol) as well as in acetonitrile. This effect was reflected in secondary structure of the protein as indicated by far-UV CD spectra (Fig. 5b). Methanol at 50 % had no effect on the secondary structure even after 6 h, whereas ethanol and propanol reduced α-helical content of Bprot to 7 % and enhanced β-sheet structure to 40 % (Table 1). The shoulder at 208 nm disappeared and a minima at 219 nm was observed. Thus, alteration rather than loss of structure in the vicinity of non-polar groups caused the inactivation of the enzyme. Bprot completely lost its structure in the presence of 50 % acetonitrile with considerable increase in unordered structure within 6 hours.

Doukyu and Ogino (2010) have thoroughly reviewed organic solvent-tolerant enzymes, which mainly include enzymes like lipase, proteases, and amidases. Proteases like subtilisin, PST01, and papain have been reported to be extremely solvent-tolerant. Methanol at 25 % stabilizes activity and secondary structure of PST01 and subtilisin even after 24 h. Higher stability and enhanced activity of the enzyme can be attributed to altered favorable hydrophobic interactions and hydrogen bonding in aqueous–organic mixtures (Ogino et al 2007).

3.3.5 Characterization of acid‑denatured Bprot

Acid-denatured (pH 1.0) Bprot transforms into the random coil conformation that was characterized further for its response to heat and organic solvents. The structure was resistant to thermal denaturation even at 90 °C. Interestingly, acid-denatured Bprot

got refolded in the presence of simple aliphatic alcohols under consideration (Fig. 5c). Methanol served as the least effective refolding agent whereas ethanol and propanol refold the random coil more effectively into a stable secondary structure of Bprot with high β-sheet content. However, the refolded structure is different from that of the native one (Table 1); also, there is absolutely no recovery of the activity. The refolding effect may be due to weakening of nonlocal hydrophobic interactions and enhancement in hydrogen bond of proteins as proposed by Dill et al (1995).

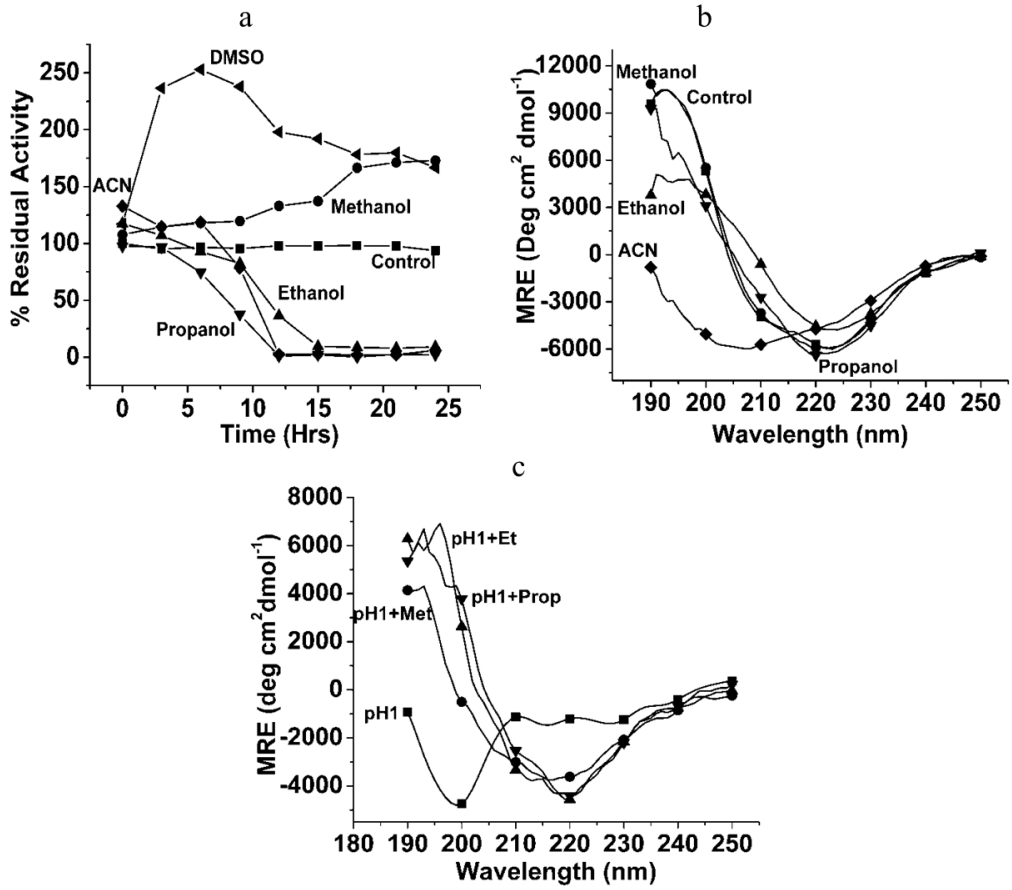

Figure 5: Effect of organic solvents on Bprot: (a) activity profile of Bprot incubated in 50 % organic solvents at respective time intervals and (b) far-UV CD spectra after 6 h; control (*square*), methanol (*circle*), ethanol (*triangle*), propanol (*inverted triangle*), acetonitrile (*diamond*), DMSO (*left-sided triangle*)* (far-UV CD spectrum not available due to instrument limitations). (c) Far-UV CD spectra of acid denatured Bprot at pH 1 treated with 50 % organic solvent for 4 hours; Bprot at pH 1 (*square*), methanol (*circle*), ethanol (*triangle*), and propanol (*inverted triangle*) in acid-denatured Bprot.

3.3.6 Effect of fluorinated alcohols:

Bprot is functionally stable in 5% TFE for 4 hours. HFIP (5% *v/v*) deactivates the enzyme gradually over 4 hours (Fig.6a and b). Retention of activity in presence of 5% TFE was reflected in compaction of secondary structure. Far UV CD spectra did not show significant change upto 20% TFE concentration, whereas, the structure was totally lost in presence of 50% TFE at pH 7.0 (Fig. 6c). On the other hand, HFIP induced loss of helical structure of Bprot at 5% concentration (Table 2) which was indicated by reduced ellipticity of far UV CD spectrum at 208 nm and shift of minima to 228 nm. With increase in HFIP concentration, gradual unfolding of Bprot was observed in decreasing ellipticity, ultimately resulting in non-native ordered Bprot structure at 50% HFIP concentration (Fig. 6d).

Induction of ordered structure in acid denatured Bprot at pH 1.0 was observed with increasing concentrations of both TFE (Fig. 6e) and HFIP (Fig. 6f). Far UV CD spectra of acid denatured Bprot in 5% TFE and 20-50% HFIP showed non-native refolded structure similar to that of native Bprot with minima at 223 nm. 50% HFIP has higher helix induction capacity than 50% TFE as shown from CDpro analysis of the far UV CD spectra. The refolding event may be due to alteration in surface of the protein in contact with the solvent. With the increased alcohol concentration, a number of previously water-exposed residues may become buried within the protein, while buried residues may become exposed to the solvent, experiencing a more and more hydrophobic microenvironment. This solvent-induced rearrangement results in a complex redistribution of water and alcohol molecules between the protein hydration shell and bulk phase ultimately stabilizing the ordered structure in unfolded protein (Kanjilal et al 2003). Such equilibrium intermediate structures have been reported for stem bromelein, acylphosphatase and β-lactoglobulin (Gupta et al 2003; Chiti et al 1999 and Kanjilal et al 2003)

Table 2: Analysis of secondary structure of Bprot in presence of fluoroalcohols:

Sample	α-helix (%)	β- sheet (%)	Turns (%)	Unordered (%)	NRMSD
Control pH 7.0	14.4	32.9	22.3	32.5	0.029
TFE (10% *v/v*)	10.4	25.5	23.2	41.2	0.036

HFIP (10%*v/v*)	4.4	48.8	26.8	20.1	0.071
Control pH 1.0	3.8	42.3	20.8	33.0	0.056
TFE (50% *v/v*)	11.7	31.5	22.5	34.3	0.045
HFIP (50% *v/v*)	16.1	32.1	19.8	32.1	0.029

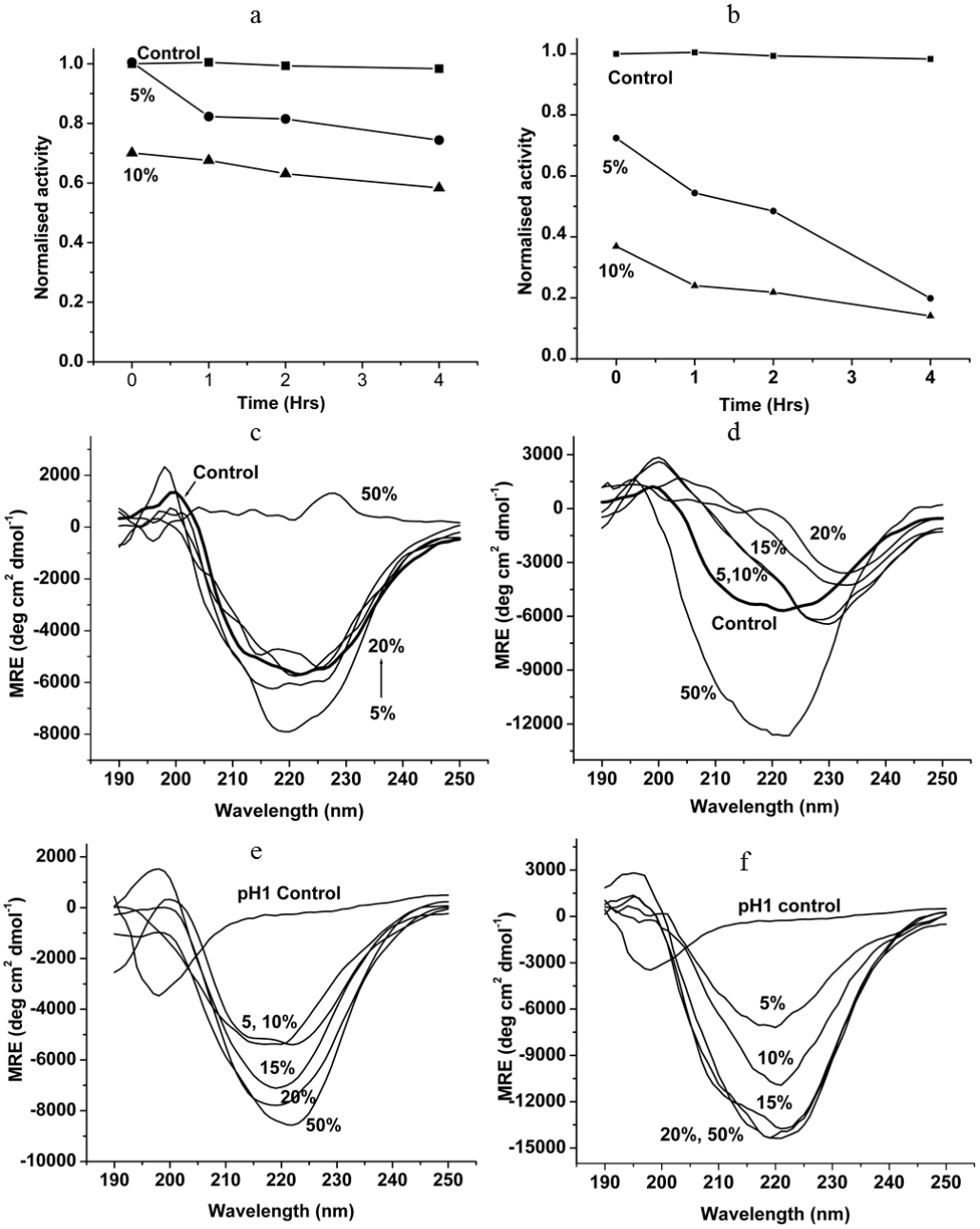

Figure 6: Effect of fluoroalcohols on Bprot: Activity profile of Bprot incubated in TFE (a) and HFIP (b) at respective time intervals. Far UV CD spectra of Bprot incubated in TFE (c) and HFIP (d) at pH 7.0 for 4 hours. (Control indicated as bold line). Far UV CD spectra of

Bprot in presence of TFE (e) and HFIP (f) at pH 1.0 for 4 hours. Concentration of fluoroalcohols used is mentioned on each spectrum.

In summary, the stability of Bprot towards GdnHCl, methanol, and other proteases can be attributed to the rigidity of the structure, i.e., the protein being difficult to unfold. The above-mentioned denaturants are chemically or biologically different and have different mechanisms for denaturation of a protein. Here, they exert a similar effect on Bprot, i.e., enhancing the activity and stabilizing it. Firstly, the stabilization of Bprot could be a consequence of structural rigidity, thereby prohibiting access of GdnHCl to the hydrogen-bonded protein interior. Second, altered favorable hydrophobic interactions and hydrogen bonding may impart the resistance towards organic solvents. Third, adoption of a compact structure under harsh conditions like acidity and proteolytic environments protects Bprot from denaturation. All the above factors lead to the conclusion that Bprot is more than stable, i.e., rigid. The presence of these entities could facilitate faster release of the product during proteolysis, leading to binding of new substrate molecules to the active site. Loss in activity under particular denaturing conditions correspond well with the loss in α-helical content, indicating it to be crucial in determining the active conformation and retention of β-turns (Table 1), suggesting their possible role in maintaining the stability as reported in case of α-lytic protease (Truhlar and Agard 2005). The properties of Bprot responsible for its high stability may prove to be useful lead in existing knowledge of protein engineering. A schematic representation of functional and conformational transitions of Bprot is given in fig. 7:

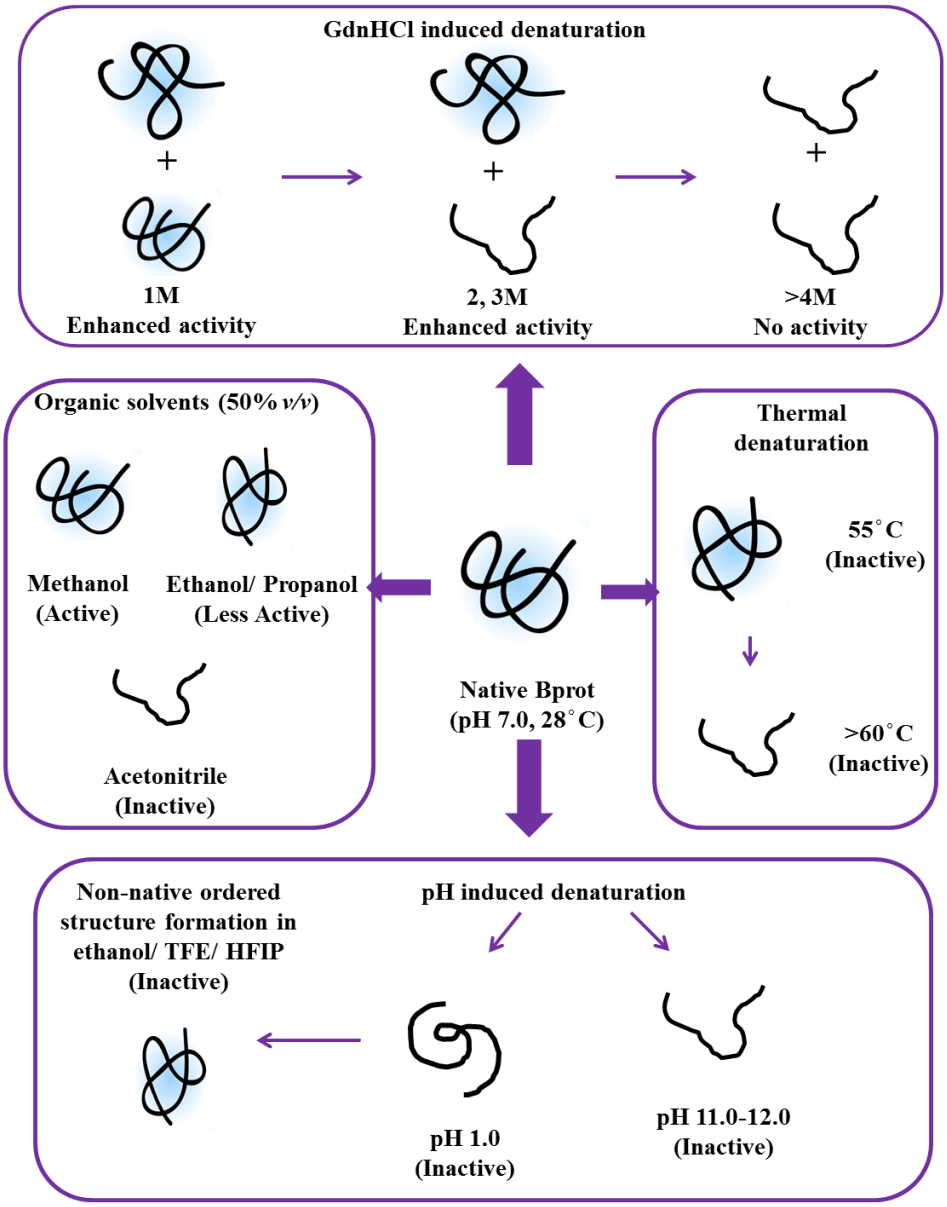

Figure 7: Schematic representation of unfolding transitions of Bprot

References

- Bhuyan, A. K. (2002). Protein stabilization by urea and guanidine hydrochloride. *Biochemistry*, *41*(45), 13386-13394.
- Brown, M. F., & Schleich, T. (1975). Circular dichroism and gel filtration behavior of subtilisin enzymes in concentrated solutions of guanidine hydrochloride. *Biochemistry*, *14*(14), 3069-3074.

- Bryan, P. N. (2000). Protein engineering of subtilisin. *Biochimica et Biophysica Acta (BBA)-Protein Structure and Molecular Enzymology*, *1543*(2), 203-222.
- Bryan, P., Alexander, P., Strausberg, S., Schwarz, F., Lan, W., Gilliland, G., & Gallagher, D. T. (1992). Energetics of folding subtilisin BPN'. *Biochemistry*, *31*(21), 4937-4945.
- Chiti, F., Webster, P., Hamada, D., Fiaschi, T., Ramponi, G., & Dobson, C. M. (1999). Acceleration of the folding of acylphosphatase by stabilization of local secondary structure. *Nature Structural & Molecular Biology*, *6*(4), 380-387.
- Cunningham, E. L., Jaswal, S. S., Sohl, J. L., & Agard, D. A. (1999). Kinetic stability as a mechanism for protease longevity. *Proceedings of the National Academy of Sciences*, *96*(20), 11008-11014.
- Dill, K. A., Bromberg, S., Yue, K., Fiebig, K. M., Yee, D. P., Thomas, P. D., & Chan, H. S. (1995). Principles of protein folding--a perspective from simple exact models. *Protein science: a publication of the Protein Society*, *4*(4), 561.
- Doukyu, N., & Ogino, H. (2010). Organic solvent-tolerant enzymes. *Biochemical Engineering Journal*, *48*(3), 270-282.
- Gupta, P., Khan, R. H., & Saleemuddin, M. (2003). Trifluoroethanol-induced "molten globule" state in stem bromelain. *Archives of biochemistry and biophysics*, *413*(2), 199-206.
- Kanjilal, S., Taulier, N., Le Huerou, J. Y., Gindre, M., Urbach, W., & Waks, M. (2003). Ultrasonic studies of alcohol-induced transconformation in β-lactoglobulin: the intermediate state. *Biophysical journal*, *85*(6), 3928-3934.
- Manning, M., & Colón, W. (2004). Structural basis of protein kinetic stability: resistance to sodium dodecyl sulfate suggests a central role for rigidity and a bias toward β-sheet structure. *Biochemistry*, *43*(35), 11248-11254.
- Neidhart, D. J., & Petsko, G. A. (1988). The refined crystal structure of subtilisin Carlsberg at 2.5 Å resolution. *Protein engineering*, *2*(4), 271-276.
- Ogino, H., Gemba, Y., Yutori, Y., Doukyu, N., Ishimi, K., & Ishikawa, H. (2007). Stabilities and conformational transitions of various proteases in the presence of an organic solvent. *Biotechnology progress*, *23*(1), 155-161.
- Rohamare, S. B., Dixit, V., Nareddy, P. K., Sivaramakrishna, D., Swamy, M. J., & Gaikwad, S. M. (2013). Polyproline fold—in imparting kinetic stability

to an alkaline serine endopeptidase. *Biochimica et Biophysica Acta (BBA)-Proteins and Proteomics*, *1834*(3), 708-716.

- Sanchez-Ruiz, J. M. (2010). Protein kinetic stability. *Biophysical chemistry*, *148*(1), 1-15.
- Solanki, K., Gupta, M. N., & Halling, P. J. (2012). Examining structure–activity correlations of some high activity enzyme preparations for low water media. *Bioresource technology*, *115*, 147-151.
- Srimathi, S., Jayaraman, G., & Narayanan, P. R. (2006). Improved thermodynamic stability of subtilisin Carlsberg by covalent modification. *Enzyme and microbial technology*, *39*(2), 301-307.
- Stepankova, V., Bidmanova, S., Koudelakova, T., Prokop, Z., Chaloupkova, R., & Damborsky, J. (2013). Strategies for stabilization of enzymes in organic solvents. *Acs Catalysis*, *3*(12), 2823-2836.
- Subbian, E., Yabuta, Y., & Shinde, U. (2004). Positive selection dictates the choice between kinetic and thermodynamic protein folding and stability in subtilases. *Biochemistry*, *43*(45), 14348-14360.
- Truhlar, S. M., & Agard, D. A. (2005). The folding landscape of an α-lytic protease variant reveals the role of a conserved β-hairpin in the development of kinetic stability. *Proteins: Structure, Function, and Bioinformatics*, *61*(1), 105-114.
- Uversky, V. N. (1993). Use of fast protein size-exclusion liquid chromatography to study the unfolding of proteins which denature through the molten globule. *Biochemistry*, *32*(48), 13288-13298.
- Yadav, S. C., & Jagannadham, M. V. (2009). Complete conformational stability of kinetically stable dimeric serine protease milin against pH, temperature, urea, and proteolysis. *European Biophysics Journal*, *38*(7), 981-991.

Chapter 4

Functional and conformational transitions of Kallikrein

Summary

Porcine pancreatic kallikrein (KLKp) was taken up as a model for functional and conformational dynamics studies under denaturing conditions like presence of GdnHCl, thermal denaturation and pH induced denaturation by spectroscopic approach (fluorescence and CD spectroscopy). Fluorescence and solute quenching studies revealed the positively charged and partial hydrophilic environment of Trp residues. β-sheet dominant secondary structure of KLKp was studied by far UV CD studies that correlated well with existing crystal structure information available. Although kallikrein was structurally stable up to 90°C as indicated by secondary structure monitoring, it was functionally stable only up to 45°C, implicating thermolabile active site geometry. In GdnHCl [1.0 M], 75% of the activity of KLKp was retained after incubation for 4h, indicating its denaturant tolerance. A molten globule like structure of KLKp formed at pH 1.0 was more thermostable and exhibited interesting structural transitions in organic solvents.

4.1 Introduction

In the last few years, combination of theoretical and experimental approaches has substantiated structural knowledge about proteins with physiological importance at molecular level (Udgaonkar and Marqusee 2013). The Structural and conformational transitions of proteins depending on solvent conditions are a significant way to elucidate their stability, folding pathways, and intermolecular aggregation behavior. Chemical denaturation using chaotropic agents, pH induced denaturation and thermal denaturation constitute major share in these studies. Stable structural intermediates during the unfolding processes have been reported and characterized for various proteins that include a range of proteases like trypsin (Bittar et al 2003), stem bromelein, papain, streblin, cryptolepain at low pH (Haq et al 2002; Amri and Mamboya 2012; Kumar et al 2014; Prasanna Kumari et al 2013).

Kallikreins are a group of serine proteases in mammals encompassing various plasma kallikreins and tissue kallikreins. Tissue kallikreins (EC 3.4.21.35) and the kallikrein-related peptidases are (chymo) trypsin-like serine proteases, belonging to family S1A of clan PA(S) according to the MEROPS classification (Barrett et al 2003). Physiological role of various kallikreins in cardiovascular, renal and central nervous system diseases, as well as their application as cancer biomarkers (Costa-

Neto et al 2008; Paliouras et al 2007) is well established. Porcine pancreatic kallikrein (KLKp) is the first enzyme in the family to be purified and biochemically characterized (Zuber and Sache 1974). Structural studies of KLKp by Bode et al (1983) have revealed remarkable similarity to trypsin except for deviations in external loops.

In spite of the structural information available, KLKp is unexplored for the folding/ unfolding mechanism. With the aim of geting deeper understanding of structural and/or functional elements, KLKp was selected as a model system to perform these studies. Present studies involve biophysical characterization of KLKp with respect to its secondary structure and tryptophan environment using steady state, time resolved fluorescence and CD studies. KLKp was studied for its stability towards GdnHCl and thermal denaturation. Existence of molten-globule like structure for KLKp was established and it was characterized.

4.2 Materials and methods:

4.2.1 Materials:

Porcine pancreatic kallikrein (KLKp) was procured from Sigma-Aldrich (USA). Guanidine hydrochloride (GdnHCl), ANS were obtained from Sigma Aldrich Ltd., USA. All other reagents including buffer compounds and organic solvents used were of analytical grade. Solutions for spectroscopic measurements were prepared in MilliQ water.

4.2.3 Protein preparation:

KLKp was dissolved and stored in 20mM tris-HCl buffer pH 8.5 at 4℃ as it was reported to be most stable under these conditions.

4.2.4 Enzyme assay

The caseinolytic activity was measured by the method of Kunitz (1947), as described by Laskowski (1955) with some modification. The protocol was: Protease activity was determined by incubating 2.5 µg of the enzyme in 300 µl of 1% casein (substrate) at pH 8.5 (300 µl, 20mM tris-HCl buffer) at 37 °C for 30 min to make the total volume 600 µl. The reaction was stopped by adding 900 µl of 5% TCA and the reaction mixture was allowed to stand for 30 min. Any precipitate formed was then removed

by centrifugation and absorbance of the supernatant was read at 280 nm. One unit of protease activity is defined as the amount of enzyme which releases 1 μmol of tyrosine per minute in the assay conditions.

4.2.5 Circular dichroism (CD) and fluorescence measurements:

The fluorescence and CD studies were performed as per protocol mentioned in section 2.2.9 and 2.2.12, respectively.

4.2.6 Solute quenching studies:

Solute quenching studies for native and denatured KLKp (40μg/ml) were performed with Neutral quencher (acrylamide) and charged quenchers (I^- and Cs^+) at pH 8.5 as described in section 2.2.13.

4.2.7 ANS binding studies:

ANS binding studies for KLKp incubated at pH1.0 were performed as described previously in chapter 3.

4.2.8 Treatment of the enzyme with GdnHCl

To study the effect of GdnHCl on the function of the enzyme, samples of KLKp (0.5 mg/ml) were incubated with various concentrations of GdnHCl (1.0–6.0 M), in 20 mM tris-HCl buffer pH 8.5 for 4 h at 28 °C. Suitable aliquots were removed at regular time intervals and assayed for enzyme activity. The readings were corrected for blank samples containing respective concentration of GdnHCl without the enzyme.

4.2.9 Thermal denaturation

Activity of KLKp during thermal denaturation was monitored by incubating the enzyme at respective temperature for 10 minutes and then performing the assay as previously mentioned. Peltier unit was used to control the temperature during far UV CD measurements with the ramp rate of 5˚C/min and incubation time set at 10 minutes after attaining the temperature. Spectra were recorded as mentioned earlier.

4.2.10 pH-induced denaturation

KLKp was incubated in buffers of different pH for 4 hours before activity assay and recording the spectra. The buffers used were glycine–HCl (pH 1.0– 3.0), citrate–

phosphate buffer (pH 4.0–6.0), potassium phosphate buffer (pH 7.0), Tris–HCl (pH 8.0–9.0) and glycine–NaOH (pH 10.0–12.0); all at 20mM concentration.

4.2.11 Characterization of molten globule:

KLKp (0.62mg/ml) was incubated in 20mM glycine-HCl buffer of pH 1.0 for 4 hours and the sample was used for thermal denaturation studies using far UV CD spectroscopy. To study the effect of organic solvents, acid denatured KLKp was further treated with the respective solvents to final concentration of 75% (*v/v*) for 24 hours. The organic solvents used were methanol, ethanol, isopropanol and acetonitrile.

4.3 Results and Discussion:

4.3.1 Biophysical Characterization of KLKp:

As per the available structural information of porcine pancreatic kallikrein (PDB ID: 2PKA), the protein has 7 tryptophan residues (Fig. 1).

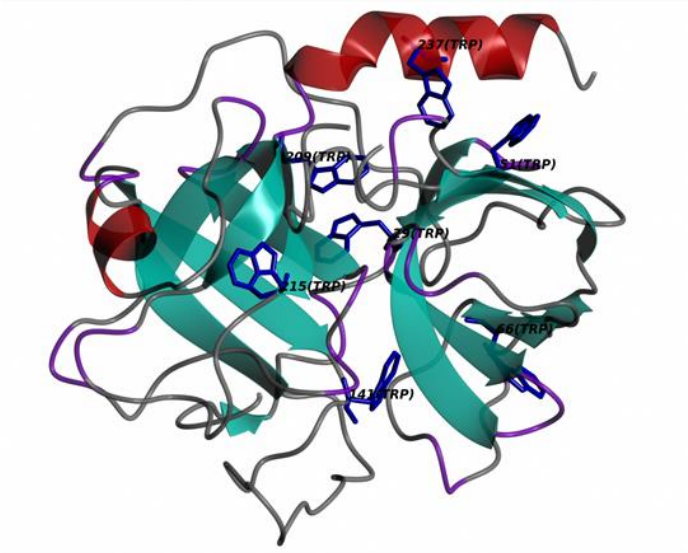

Figure 1: Crystal structure of porcine pancreatic kallikrein (KLKp; PDB ID: 2PKA) highlighting the partial hydrophilic environment of the 7 Trp residues (Shown in blue). (visualization in CCP4mg).

In the present studies, intrinsic fluorescence spectrum of KLKp showed λ_{max} of 343 nm indicating moderate hydrophilic environment of the tryptophan residues (Fig. 2a). Decomposition analysis of the spectrum using PFAST software (Shen et al 2008) showed that all the trp residues belong to either class I or II suggesting possible interaction of indole rings (although in non-polar environment) with structured water molecules. The results are supported by the time resolved fluorescence spectrum

analysis of KLKp. Bi-exponential fitting of the decay curve obtained from the lifetime measurement of intrinsic fluorescence of KLKp (Fig. 2b) revealed two decay times τ_1 (1.271 ns) with 38 % contribution and τ_2 (4.34 ns) with 62 % contribution (χ^2 =1.015). This shows two populations of trp residues, one with shorter lifetime with less contribution present in the polar environment i.e. on the surface and the other one with longer lifetime with much higher contribution to fluorescence present in the non-polar environment. This correlated well with the steady state fluorescence data.

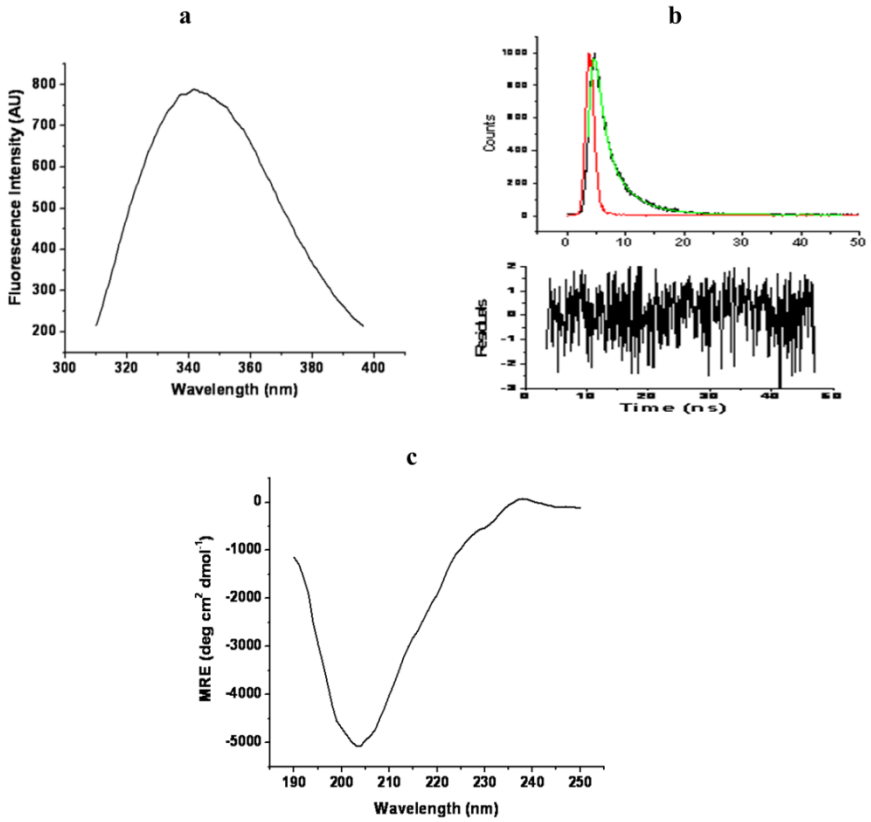

Figure 2: Biophysical characterization of KLKp: (A) Intrinsic fluorescence spectrum of KLKp (40 µg/ml) (B) Time resolved fluorescence spectrum of KLKp (1mg/ml) (C) Far UV CD spectrum of KLKp (130 µg/ml) at pH 8.5, 28℃.

Native KLKp showed far UV CD spectrum with minima at 204 nm and negative ellipticity at 190 nm (Fig. 2c), suggesting majority of β-sheet structure and significant content of unordered structure due to which, shift from the ideal β-sheet position (minima at 210-220 nm) towards 204 nm was observed. Analysis of this spectrum with CDPro deduced the secondary structure composition values as 4.8% α-helix, 38.1% β-sheets, 22.8% turns and 34.3% unordered structure (NRMSD 0.056) which correlates with that of DSSP analysis of crystal structure available (Table 1).

Table 1: Secondary structure composition of native KLKp:

Method	Helix (%)	Sheets (%)	Turns (%)	Unordered (%)
Continll (CDpro)	5.5	39.8	21.7	33.0
DSSP (Crystal structure)	10.35	34.9	26.3	28.45

4.3.2 Solute quenching studies:

Tryptophan environment in KLKp was studied by solute quenching studies (Fig.3). The neutral quencher acrylamide was found to be the most efficient for native KLKp, which quenched the fluorescence intensity with Stern–Volmer constant K_{sv} as 5.12 M^{-1}. KI quenched the Trp fluorescence with K_{sv} value as 1.26 M^{-1} (Table 2), indicating positive charge density around the surface Trp conformer. CsCl did not show significant quenching efficiency confirming the positively charged environment with negligible negative charge density.

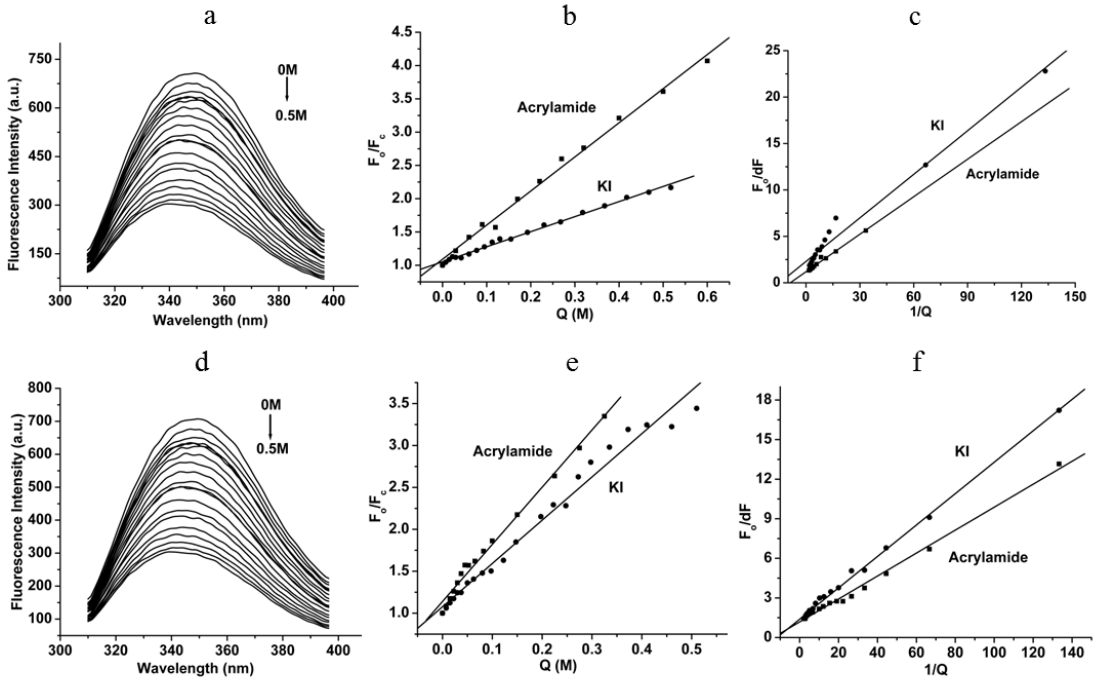

Figure 3: Solute quenching studies of Bprot: Decrease in fluorescence intensity in solute-quenching with acrylamide for native (a) and denatured (d) KLKp (40µg/ml). Stern-Volmer plot for native (b) and denatured (e) KLKp, respectively. Modified Stern-Volmer plot for native (c) and denatured (f) KLKp, respectively.

The modified Stern–Volmer plot showed 84% and 43% accessibility of Trp fluorescence to acrylamide and KI, respectively. KLKp denatured with 6 M GdnHCl exhibited increased accessibility for KI (~two times), indicating increase in positive charge density around Trp residues due to unfolding of the protein (Table 2).

Table 2: Solute quenching parameters for KLKp:

Quencher		K_{sv} (M^{-1})	F_a (%)
Acrylamide	Native	5.12	84.4
	Denatured	6.82	86.0
KI	Native	1.26	43.6
	Denatured	5.16	72.1

4.3.3 Thermal transitions of KLKp

The proteolytic activity of KLKp reduced to 10% at 55˚C in 30 minutes. However, the residual 10% activity was retained upto 90˚C (Fig.4a). The loss in activity was reflected in intrinsic fluorescence spectra, where λ_{max} showed red shift by 7nm above 60˚C (Fig.4b). Sigmoidal fit of the curve indicated the T_m of KLKp as 61.5˚C. Far UV CD spectra did not show significant change in secondary structure even at 90˚C, except reduction in the ellipticity at 190 nm indicating reduction in the ordered structure (Fig.4c). The rigidity of secondary structure of KLKp might be responsible for protecting the active site leading to retention of residual activity upto 90˚C.

Similar trend of unusual thermostability of KLKp has also been reported for human KLK1, where it retained 25% activity upto 100˚C (Gao et al 2006). Retention of 20% activity even at 80 ˚C was also observed in bovine, dog and rat pancreatic kallikreins (Hojima et al 1977). Camel pancreatic kallikrein was partially active till 70˚C, while total deactivation was observed at 80˚C (Fyiad et al 2007). The structural basis of the considerable thermotolerance of pancreatic kallikreins is unexplored. The analysis of the KLKp structure [PDB ID: 2PKA] in iRDP server revealed presence of 5 disulfide bridges in KLKp which are all buried in the hydrophobic core making it inaccessible for thermal denaturation. This may help in retaining the secondary structure intact as seen in the far UV CD spectra at higher temperatures.

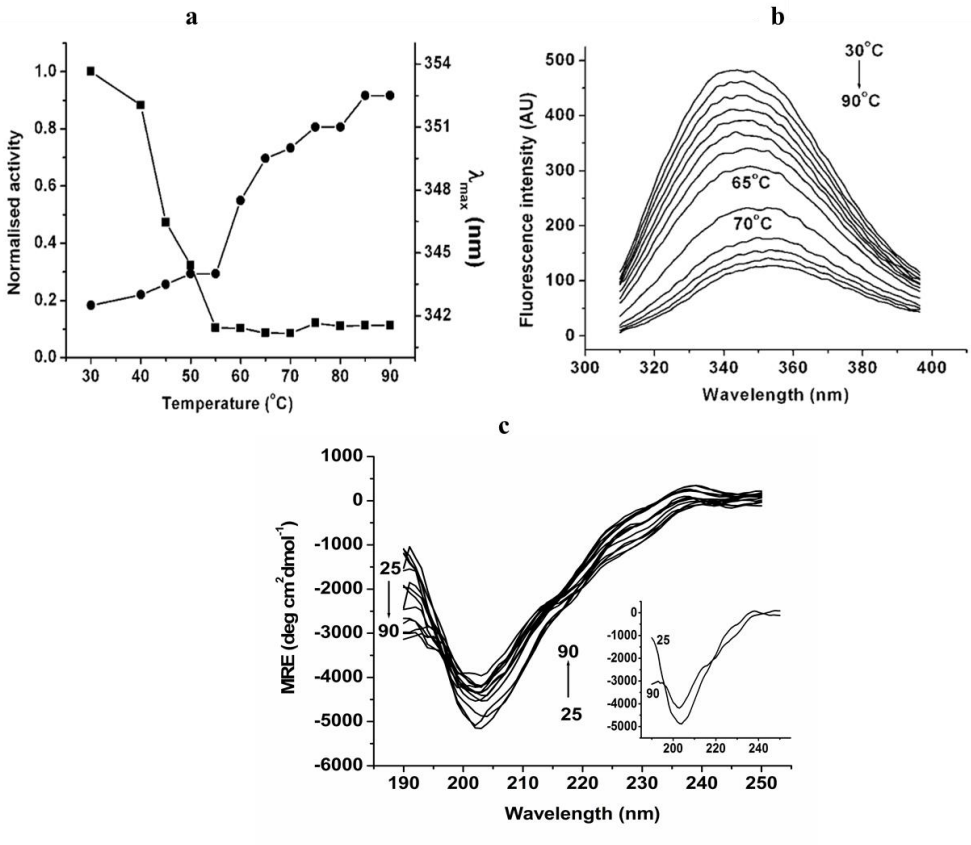

Figure 4: Thermal denaturation of KLKp: (a) activity profile (square) and change in λ_{max} (circle) of intrinsic fluorescence spectra during thermal denaturation. (b) Intrinsic fluorescence spectra of KLKp (40 μg/ml) and (c) Far-UV CD spectra of KLKp (130 μg/ml) incubated at respective temperature for 10 min as described in materials and methods.

4.3.4 GdnHCl induced denaturation

KLKp expressed 90% and 60% proteolytic activity even after incubation of 4 hours in presence of 1.0 M and 2.0 M GdnHCl, respectively (Fig.5a). Secondary structure, as monitored by CD spectra, was stable in 1M GdnHCl for 4 hours (Fig.5b). Equilibration of KLKp in GdnHCl for 24 hours caused red shift in λ_{max} of intrinsic fluorescence of the protein indicating that unfolding of KLKp is a multistep process (Fig.5c) Under renaturing conditions, λ_{max} values of refolded samples overlapped with those in unfolding process at respective GdnHCl concentrations (Fig.5d) indicating the reversibility of the process.

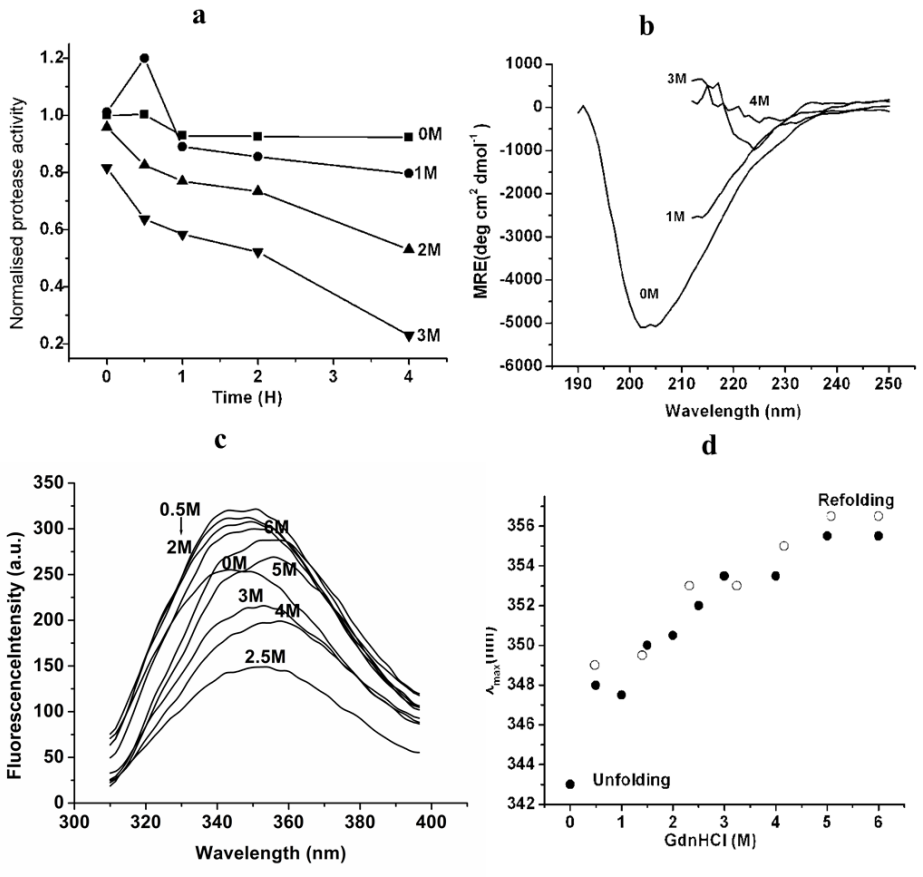

Figure 5: GdnHCl induced unfolding of KLKp: (a) Activity profile of KLKp incubated in GdnHCl for respective time interval (b) Far UV CD spectra of KLKp (130 μg/ml) and (c) Intrinsic fluorescence spectra of KLKp (40 μg/ml) incubated in GdnHCl (d) Shift in λ_{max} of intrinsic fluorescence spectra when incubated in GdnHCl during unfolding (Filled circle) and refolding (open circles).

4.3.5 pH induced conformational changes

KLKp is functionally stable in the pH range of 5.0-9.0; although at pH 3.0, the activity reduced to 60% after incubation for 72 hours. Immediate loss in activity was observed at pH 1.0 (Fig. 6a) of the protein. The loss in activity was reflected in intrinsic fluorescence spectra where λ_{max} showed red shift by 3 nm at pH 1.0, 3.0 and 11.0 (Fig. 6b). The fluorescence intensity showed considerable decrease suggesting quenching due to protonation of Trp at low pH. As seen in far UV CD spectra, the secondary structure showed noticeable although not significant change in pH range 1.0-11.0 (Fig. 6c). Slight increase in negative ellipticity at pH 11.0 indicated compaction of structure.

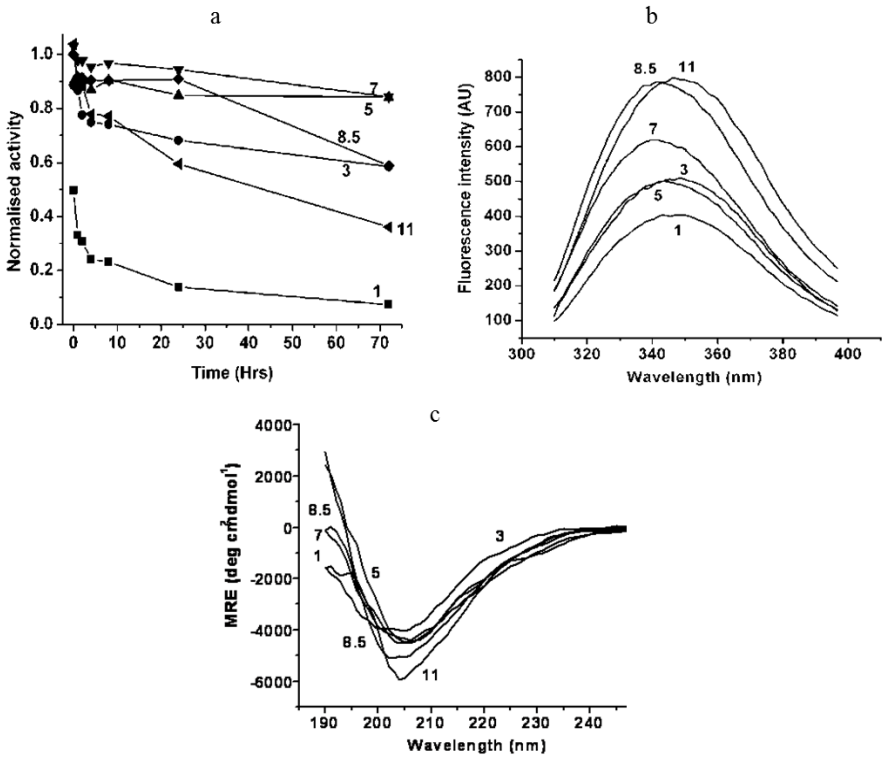

Figure 6: pH-induced conformational changes in KLKp: (a) Activity profile of KLKp incubated at respective pH (b) Intrinsic fluorescence spectra of KLKp (40µg/ml) and (c) far UV CD spectra of KLKp (130µg/ml) of KLKp incubated at respective pH for 4 hours.

4.3.6 Characterization of Molten globule-like structure at pH 1.0:

KLKp retained its secondary structure at pH 1.0 as seen in far UV CD spectra (Fig. 7a). The near UV CD spectra showed drastic loss in tertiary structure at pH 1.0 in decreased ellipticity (Fig. 7b). Significant ANS binding observed only at pH 1.0 indicated exposure of hydrophobic residues on the surface of the protein preceding alteration of tertiary structure (Fig. 7c). Similar secondary structure, loss in tertiary structure and exposure of hydrophobic residues on the surface of the protein at pH 1.0 confirmed existence of a molten globule-like structure of KLKp at pH 1.0.

The molten globule like structure of KLKp observed at pH 1.0 did not show any further change in the secondary structure up to 85˚C (Fig. 7d). Unlike native KLKp, ellipticity of MG at 190nm remained unaltered till 85˚C indicating higher thermostability of MG-like structure. Higher stability of structural intermediate as observed for KLKp has been reported for GdnHCl-induced molten globule of α-

mannosidase from *Canavalia ensiformis* (Kumar and Gaikwad 2010). Siddiqui et al have proposed entropy-driven mechanism for higher thermostability of molten globule of α-amylase (Siddiqui et al 2010).

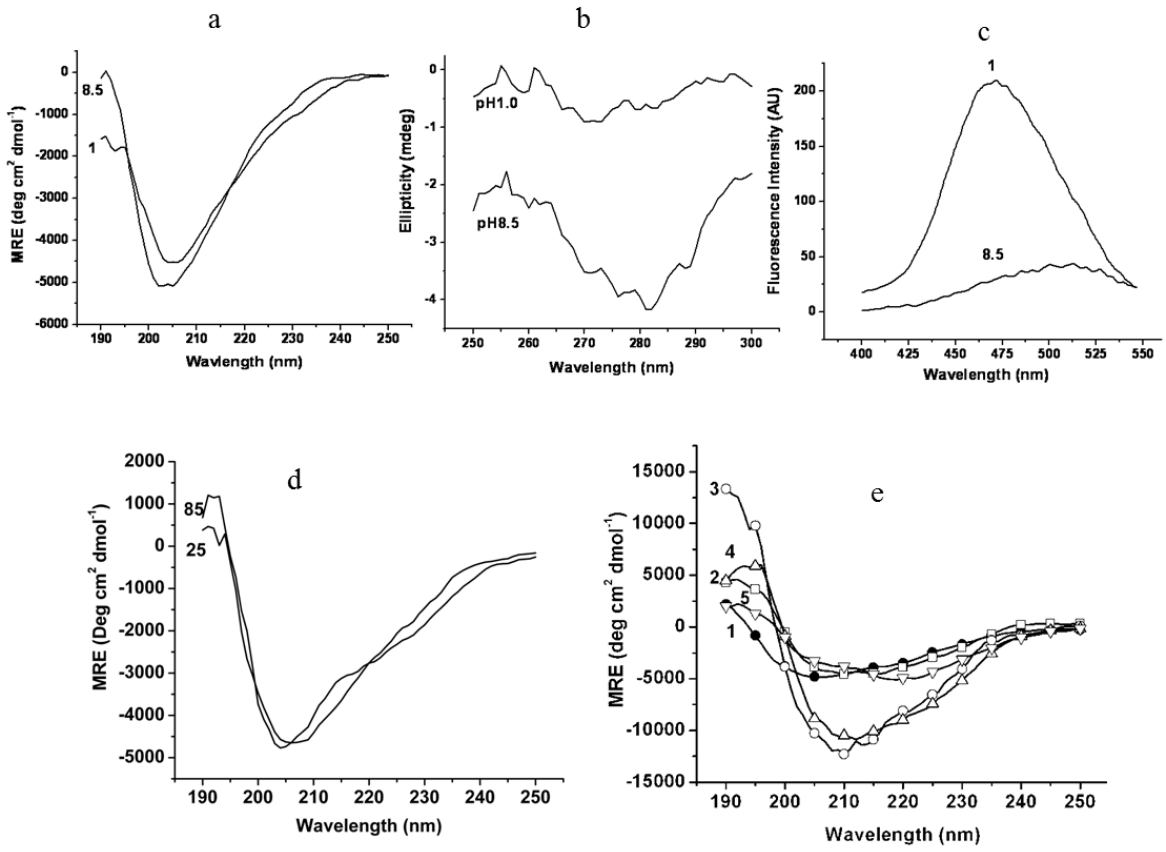

Figure 7: Formation of molten globule of KLKp at pH1.0: (a) Far UV CD spectra of KLKp (130µg/ml) incubated at respective pH 1for 4 hours (b) Altered tertiary structure of KLKp (1mg/ml) at pH1.0 as seen in near UV CD spectra after 4 hours of incubation (c) ANS binding to KLKp incubated at pH 1.0 for 4 hours (d) Far UV CD spectra for thermal denaturation of molten globule of KLKp (e) effect of organic solvents on molten globule of KLKp (130 µg/ml): 1. KLKp at pH1 control (-●-●-), 2. methanol (-□-□-), 3. ethanol (-○-○-) 4. isopropanol (-Δ-Δ-), 5. Acetonitrile (▼-▼-).

Analysis of secondary structural transitions of KLKp at pH 1.0 in 75% alcohols and acetonitrile (Fig. 7e) indicated significant α-helix induction in MG-like structure of KLKp. Methanol and acetonitrile were least effective as helix-inducers, whereas ethanol and isopropanol enhanced helix-formation in MG-like structure from 6% to 24% (Table 3). The activity of the enzyme though was not regained in presence of these solvents.

Table 3: Secondary structure analysis of molten globule of KLKp in organic solvents

Sample	Helix	sheets	Turns	Unordered	NRMSD
pH1 Control	6.9	37.4	22.2	33.4	0.034
Methanol	7.1	39.0	21.6	32.3	0.049
Ethanol	23.5	23.1	20.7	32.7	0.058
Isopropanol	24.7	23.2	22.2	30.0	0.033
Acetonitrile	9.0	34.3	22.8	34.0	0.042

Induction of structural transitions in molten globule of KLKp by organic solvents was an interesting observation in the present studies. Dill et al (1995) have proposed that alcohols stabilize α-helical conformation in unfolded proteins by weakening non-local hydrophobic interactions and enhancing local polar interactions. The hydrogen bonds thus formed result in stabilization of extended helical rods in which the hydrophobic side chains are exposed and polar amide groups are shielded from the solvents. This explains higher α-helix propensity of ethanol and isopropanol which are less polar solvents as compared to methanol and acetonitrile having very low α-helix induction capacity. Similarly, helix propensity of alcohols was recorded for structural intermediates of stem bromelain and subtilase from *Beauveria sp.* MTCC 5184 (Haq et al 2005; Dalal et al 2014).

To summarize, KLKp was studied for its biophysical properties that revealed β-sheet dominated structure and positively charged partial hydrophilic environment of Trp residues. KLKp exhibited interesting stability of structure upto 90 ℃ and it was functionally stable in 1M GdnHCl. A molten globule- like structure for KLKp at pH 1.0 was confirmed and characterized for its thermostability and conformational changes in presence of organic solvents. The unfolding transitions of KLKp are represented schematically in Fig. 8:

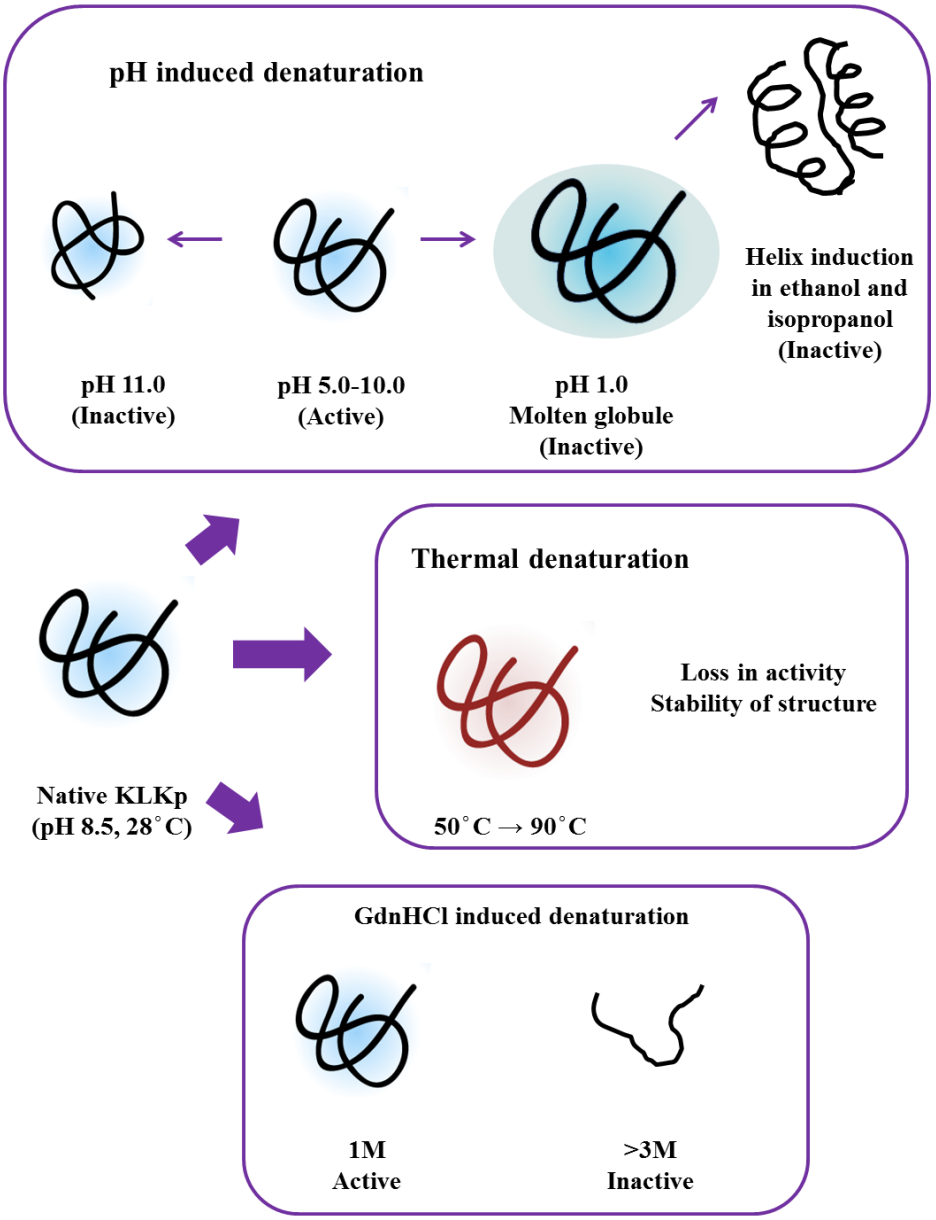

Figure 8: Schematic representation of unfolding transitions of KLKp

References:

- Amri, E., & Mamboya, F. (2012). Papain, a plant enzyme of biological importance: a review. *American Journal of Biochemistry and Biotechnology*, *8*(2), 99-104.
- Barrett, A. J., Tolle, D. P., & Rawlings, N. D. (2003). Managing peptidases in the genomic era. *Biological chemistry*, *384*(6), 873-882.
- Bittar, E. R., Caldeira, F. R., Santos, A. M. C., Günther, A. R., Rogana, E., & Santoro, M. M. (2003). Characterization of β-trypsin at acid pH by differential scanning calorimetry. *Brazilian journal of medical and biological research*, *36*(12), 1621-1627.
- Bode, W., Chen, Z., Bartels, K., Kutzbach, C., Schmidt-Kastner, G., & Bartunik, H. (1983). Refined 2 Å X-ray crystal structure of porcine pancreatic kallikrein A, a specific trypsin-like serine proteinase: Crystallization, structure determination, crystallographic refinement, structure and its comparison with bovine trypsin. *Journal of molecular biology*, *164*(2), 237-282.
- Costa-Neto, C. M., Dillenburg-Pilla, P., Heinrich, T. A., Parreiras-e-Silva, L. T., Pereira, M. G., Reis, R. I., & Souza, P. P. (2008). Participation of kallikrein–kinin system in different pathologies. *International immunopharmacology*, *8*(2), 135-142.
- Dalal, S. A., More, S. V., Shankar, S., Laxman, R. S., & Gaikwad, S. M. (2014). Subtilase from Beauveria sp.: conformational and functional investigation of unusual stability. *European Biophysics Journal*, *43*(8-9), 393-403.
- Dill, K. A., Bromberg, S., Yue, K., Fiebig, K. M., Yee, D. P., Thomas, P. D., & Chan, H. S. (1995). Principles of protein folding-a perspective from simple exact models. *Protein science: a publication of the Protein Society*, *4*(4), 561.
- Fyiad, A. A., & Khafagy, E. Z. (2007). Isolation and Some Properties of Camel Pancreatic Kallikrein. *Journal of Applied Sciences Research*, *3*(10), 1223-1228.
- Gao, B., Sun, H. C., Fang, H. X., Qian, K., Zhao, M. S., Qiu, H. L. & Wang, Z. Y. (2006). Expression and preliminary characterization of recombinant human tissue kallikrein in egg white of laying hens. *Poultry science*, *85*(7), 1239-1244.

- Haq, S. K., Rasheedi, S., & Khan, R. H. (2002). Characterization of a partially folded intermediate of stem bromelain at low pH. *European Journal of Biochemistry*, *269*(1), 47-52.
- Hojima, Y., Yamashita, M., Norimichi, O. C. H. I., MORIWAKI, C., & MORIYA, H. (1977). Isolation and some properties of dog and rat pancreatic kallikreins. *Journal of biochemistry*, *81*(3), 599-610.
- Kumar, R., Tripathi, P., de Moraes, F. R., Caruso, Í. P., & Jagannadham, M. V. (2014). Identification of Folding Intermediates of Streblin, The Most Stable Serine Protease: Biophysical Analysis. *Applied biochemistry and biotechnology*, *172*(2), 658-671.
- Kumar, A., & Gaikwad, S. M. (2010). Multistate unfolding of α-mannosidase from Canavalia ensiformis (Jack Bean): Evidence for the thermostable molten globule. *Biochemical and biophysical research communications*, *403*(3), 391-397.
- Kumari, N. P., Dubey, V. K., & Jagannadham, M. V. (2013). SDS induced refolding of pre-molten globule state of cryptolepain: Differences in chemical and temperature-induced equilibrium unfolding of the protein in SDS-induced state. *Proceedings of the National Academy of Sciences, India Section B: Biological Sciences*, *83*(1), 71-80.
- Kunitz, M. (1947). Crystalline soybean trypsin inhibitor II. General properties. *J Gen Physiol 30*, 291-310.
- Laskowski, M. (1955). Trypsinogen and trypsin. *Method Enzymol 2*, 26-36.
- Paliouras, M., Borgono, C., & Diamandis, E. P. (2007). Human tissue kallikreins: the cancer biomarker family. *Cancer letters*, *249*(1), 61-79.
- Shen, C., Menon, R., Das, D., Bansal, N., Nahar, N., Guduru, N., & Reshetnyak, Y. K. (2008). The protein fluorescence and structural toolkit: Database and programs for the analysis of protein fluorescence and structural data. *Proteins: Structure, Function, and Bioinformatics*, *71*(4), 1744-1754.
- Siddiqui, K. S., Poljak, A., De Francisci, D., Guerriero, G., Pilak, O., Burg, D. & Cavicchioli, R. (2010). A chemically modified α-amylase with a molten-globule state has entropically driven enhanced thermal stability. *Protein Engineering Design and Selection*, *23*(10), 769-780.

- Udgaonkar, J., Marqusee, S. (2013). Folding and binding. *Curr Opin Struct Biol 23*, 1–3.
- Zuber, M., & Sache, E. (1974). Isolation and characterization of porcine pancreatic kallikrein. *Biochemistry*, *13*(15), 3098-3110.

Chapter 5

Stability of Kallikrein in organic solvents

Summary

Porcine pancreatic kallikrein (KLKp) was investigated for its functional and conformational transitions in presence of organic solvents using biochemical and biophysical techniques and molecular dynamics (MD) simulations approach. The enzyme was exceptionally stable in isopropanol and ethanol showing 110% and 75% activity, respectively after 96h, showed moderate tolerance in acetonitrile (45% activity after 72 h) and much lower stability in methanol (40% activity after 24h) (all the solvents [90% *v/v*]). Far UV CD and fluorescence spectra indicated apparent reduction in compactness of KLKp structure in isopropanol system. MD simulation studies of the enzyme in isopropanol revealed 1) minimal deviation of the structure from native state 2) marginal increase in radius of gyration (Rg) and solvent accessible surface area (SASA) of the protein and the active site and 3) loss of density barrier at the active site possibly leading to increased accessibility of substrate to catalytic triad as compared to methanol and acetonitrile.

5.1 Introduction

Organic solvents are known to alter enzyme catalysis by improving solubility of substrate, enhancing reaction rates, altering specificity and hydrophobic interactions in a reaction (Serdakowski and Dordick 2008). Recent advances have devised many strategies like propanol-rinsed enzyme preparations for stabilizing enzymes like phenylalanine ammonia lyase in water-organic solvent mixtures (Stepankova et al 2013). In spite of the stabilization strategies available, prolonged exposure of proteins like subtilisin Carlsberg to solvents like acetonitrile still proves to be unfavorable to enzyme activity limiting its use (Bansal et al 2010). Understanding the effect of organic solvents on various proteins at molecular level is obligatory for the development of further strategies. The concept of solvent compatibility implies that in order for a protein to be active in organic solvents it must be able to retain its overall shape and that it must not become too rigid such that catalytic activity is compromised. Moreover, the active site region should not be obstructed by conformational changes that block or structurally alter the active site and the active site pocket should not be blocked by solvent molecules (Toba and Merz 1997). Many hydrolases e.g. amylases, cutinases, lipases and proteases have been

studied and modified for their behavior in organic solvents for their better industrial applications (Doukyu and Ogino 2010; Castillo et al 2005).

Serine proteases, especially Trypsin, chymotrypsin and subtilisins are widely used for peptide and amino acid ester syntheses in different organic solvents (Cabral et al 1997; Kise and Fujimoto 1988). Various biochemical studies have established the stability of proteases in presence of organic solvents (Doukyu and Ogino 2010). The effect of polarity of organic solvents used in these reactions has been studied in case of subtilisin (Kim et al 2000). Porcine pepsin is reported to alter tertiary structure and microenvironment leading to functional loss in presence of high concentrations (70%) of organic solvents (Simon et al 2007). Earthworm protease has been biochemically characterized for its long term stability towards polar and non-polar solvents (Nakajima et al 2000). In recent days, MD simulation approach has enabled the understanding of protein-organic solvent interaction at molecular level (Lousa et al 2013). Lousa et al (2012) theoretically reported the differential stability of pseudolysin and thermolysin in ethanol/water solutions. The study indicates tendency of ethanol molecules to interact with thermolysin, which masks the intra-protein hydrophobic interactions and results in protein unfolding. The effect of organic solvents such as acetonitrile and hexane has been studied on trypsin by Meng et al (2013). They investigated the effect of polar and nonpolar solvent on the binding affinity of the substrate. It is observed that polar solvents affect the binding strength significantly by weakening the electrostatic interactions at active site of enzyme.

Present experimental data reveals the unusual stability of KLKp towards high concentrations of polar organic solvents as examined using biochemical and spectroscopic (CD and intrinsic and extrinsic fluorescence) studies and was also monitored at molecular level by theoretical approaches. The solvents chosen were methanol, ethanol, isopropanol which are polar protic solvents and acetonitrile and DMSO which are polar aprotic solvents.

5.2 Materials and methods

5.2.1 Materials:

Porcine pancreatic kallikrein (KLKp) was procured from Sigma-Aldrich (USA). All buffer reagents and organic solvents used were of analytical grade. Solutions for spectroscopic measurements were prepared in MilliQ water.

5.2.2 Functional stability of the enzyme in presence of solvents

KLKp (0.5 mg/ml) was incubated in 75% and 90% (*v/v*) of methanol, ethanol, isopropanol, acetonitrile (ACN) and dimethyl sulphoxide (DMSO) at pH 8.5 (tris-HCl, 20 mM) for 96 hours at 28˚C. The enzyme solvent mixtures were incubated in static condition and the solvents were miscible in the buffer. The incubation mixtures were kept in tightly closed vials to avoid the volatile losses. 50 µl aliquots were removed at regular time intervals and assayed for the enzyme activity. Caseinolytic activity assay was performed as described previously.

5.2.3 Steady state fluorescence and solute quenching studies

Fluorescence measurements were performed for KLKp (40µg/ml) incubated in respective solvent systems (90% *v/v* for 72 hours) as mentioned in section 2.2.9. Solute quenching studies for the solvent-incubated KLKp were performed with neutral quencher (acrylamide) and charged quenchers (I^- and Cs^+) as described in section 2.2.13.

5.2.4 Circular dichroism (CD) measurements

Conformational transition studies of KLKp were carried out by incubating KLKp (0.13 mg/ml) in respective solvents systems (75% *v/v* for 72 hours), since, further increase in organic solvent concentration led to high background noise. The Far UV CD spectra were recorded for the incubated KLKp samples as described in section 2.2.12.

5.2.5 Simulation details:

The high resolution X-ray crystal structure of porcine pancreatic kallikrein is reported in Protein Data Bank (Bode et al 1983). This crystal structure (2PKA) was considered

as a starting structure for simulations. In the present theoretical investigation, we have studied the effect of organic-water mixture on the conformational stability of the protein. The simulations were performed by taking one test case of the experimental condition of protein stability/activity in the organic/water (75 % *v/v*) mixture. The water mixture of organic solvents such as methanol, ethanol, isopropanol and acetonitrile were used to perform simulations. The kallikrein protein (2PKA) was solvated with these organic-water mixtures and then subjected to MD simulation. Simulation was also carried out in water (without organic solvent) and termed as reference/control simulation. Therefore, five different simulations (including with water and water/organic mixture) were performed using different solvents to understand their effect on the protein conformations.

MD simulations were performed using Gromacs 4.5.5 simulation package (Van der Spoel et al 2005; Hess et al 2008). The united atom Gromos-53a6 force field was used to model the protein and a Simple Point Charged (SPC) model was used to represent the water molecules (Toukan and Rahman 1985). The parameters for the organic solvents based on GROMOS-53a6 were taken from Automated Topology Builder (http://compbio.biosci.uq.edu.au/atb) (Malde et al 2011). The isothermal–isobaric (NPT) ensemble and periodic boundary conditions were applied to perform the initial 5 ns equilibration run to allow the solvent (water and organic solvent) to penetrate the solvent accessible surface area. The protein was position restrained (for equilibration run) with the force constant of 1000 kJ/mol^{-1}which allows efficient equilibration. The temperature was kept constant at 300 K using V-rescale thermostat with a coupling constant of 0.1 ps. The isotropic pressure coupling was applied using Berendsen barostat (Berendsen et al 1984) and pressure coupling constant of 2 ps was used to keep pressure constant at 1 bar. The non-bonded interactions, Lennard-Jones potential were taken care with the cut-off of 1.4 nm and the electrostatic interactions were considered in the 0.9 nm cut off. A reaction field correction was used for electrostatic interactions using dielectric constants of 67, 68, 68 and 56 for methanol/water, ethanol/water, isopropanol/water and acetonitrile/water mixture, respectively. The particle meshewald (PME) method was used in protein water simulations to account the electrostatic interactions (Patra et al 2003). The production runs were carried out for 150 ns using same isothermal-isobaric ensemble and simulation trajectories written after every 5 ps of time. These trajectories were then used further for analysis.

Analysis of KLKp structure simulated in respective solvent systems was carried out in iRDP (http://irdp.ncl.res.in) ICAPS module. The structure visualization was carried out using CCP4mg (McNicholas et al 2011).

5.3 Results and discussion

Functional and conformational transitions of porcine pancreatic kallikrein (KLKp) in organic solvents were studied using biochemical, spectroscopic and MD simulation approach. The solvent systems chosen were methanol, ethanol, and isopropanol which are polar protic solvents and acetonitrile and DMSO which belong to group of polar aprotic solvents.

5.3.1 Functional stability of KLKp in organic solvents:

Functional stability of KLKp was monitored over 96 hours in presence of 75% (*v/v*) (Fig.1a) and 90% (*v/v*) (Fig. 1b). The protein exhibited similar trends of proteolytic activity in both concentrations of solvents. KLKp showed 110% activity even after 96 hours of incubation in presence of isopropanol (90% *v/v*) (Fig. 1b). In methanol, at same concentration, 25% loss in activity was observed within 2 hours which slowed down later with 45% of activity after 24 hours. The residual activity of the enzyme in presence of ethanol was comparable to that of control reaction up to 48 hours. Acetonitrile slowly deactivated KLKp with 65% retention of activity even after 48 hours. DMSO instantly inactivated the enzyme.

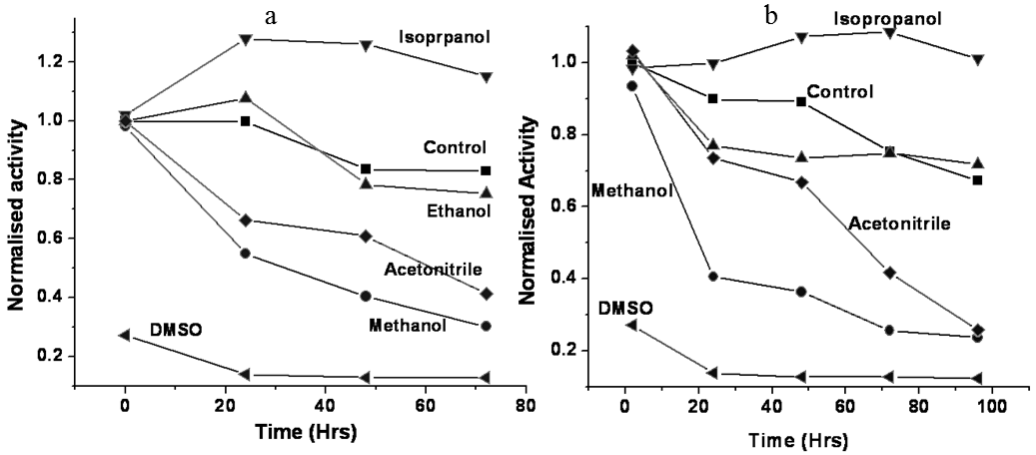

Figure 1: Activity profile of KLKp in organic solvents: KLKp (50µg/ml) incubated in 75% (*v/v*) (a) and 90% (*v/v*) (b) solvents for 96 hours: Enzyme assay was carried out after removing 50µl aliquot from the incubation mixture as described in material and methods.

The polarity of solvents used in the present study was in the order of Isopropanol <ethanol < Methanol < Acetonitrile < DMSO (Reichardt and Welton 2011). The functional stability of KLKp in these solvents was inversely proportional to their polarity. Failure of aprotic solvents (acetonitrile and DMSO) to maintain activity of KLKp could be due to different modes of solvation they assume as compared to the protic ones. The instability of KLKp in more polar solvents (methanol) could be due to the stripping of water molecules from the active site leading to unfavorable changes in the conformation.

The intrinsic activation energy of subtilisin catalyzed reactions in organic solvents is strongly dependent on the polarity of the reaction medium (Kim et al 2000). Our results were also supported by the report of trypsin from bovine and porcine pancreas, marine crab and European sea bass, where, enhancement in the activity was observed in presence of propanol (Saborowski et al 2004; Harpaz et al 1994). The effect of ethanol on trypsin activity was found to be less distinct and methanol was the least activating solvent. As compared to trypsin, chymotrypsin is less stable in presence of polar solvents but showed improved stability when supplemented with 1M Ca^{+2} (Kotormán et al 2003). In contrast to trypsin-like proteases, subtilases from *Pseudomonas aeruginosa, Bacillus thermoproteolyticus* and *Beauveria sp.* MTCC 5184 are reported to be more stable in methanol for 24 hours (Ogino et al 2007; Dalal et al 2014). Earthworm serine protease is reported to be highly stable in 25% organic solvents for prolonged duaration upto 100 days (Nakajima et al 2000). KLKp stands out as a mammalian protease with high organic solvent stability in concentration as high as 90% for 4 days.

Further structural investigations of the present protein were performed by studying secondary structure, Trp environment, and MD simulation studies.

5.3.2 Secondary structure:

Far UV CD spectra were monitored in presence of 75% solvents since further increase in solvent concentration produced high background noise (Fig.2a). Interestingly, in presence of isopropanol, KLKp showed considerable reduction in negative ellipticity as compared to native enzyme, still retaining the minima to 204 nm. This indicated apparent reduction in compactness of the conformation or formation of an altered structure, which might have stabilized the active its geometry to retain the activity of KLKp upto 96 hours. The negative ellipticity of KLKp at 190

nm remained unaltered in isopropanol while it turned to positive values in other solvent systems confirming the structural transitions. In 75% methanol, formation of α-helix like structure was induced showing increase in ellipticity and shift in minima to 207 nm in far UV CD spectrum (Table 1). Ethanol caused the shift in the minima of the ellipticity to 207 nm, while shift to 213 nm in presence of 75% acetonitrile indicated β sheet induction in the structure. However, most of these visible changes were not reflected in secondary structure composition analyzed by CDpro software (Table 1).

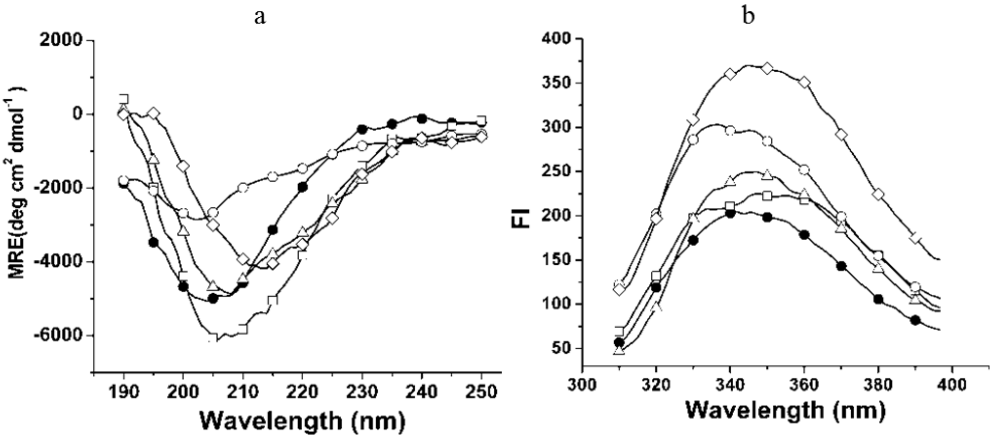

Figure 2: Structural changes of KLKp in presence of organic solvents: (a) Far UV CD spectra of KLKp (0.13mg/ml) incubated in 75% (*v/v*) solvents for 72 hours (b) Intrinsic fluorescence spectra of KLKp (40µg/ml) incubated in 90% (*v/v*) solvents. Samples were excited at 295nm- Control (●--●), Methanol (□--□), Ethanol (Δ--Δ), Isopropanol(○--○), Acetonitrile (◊--◊).

Table 1: Secondary structure analysis of solvent incubated KLKp by CDpro (CONTINLL) software:

Solvent (75% *v/v*)	α-helix (%)	β-sheet (%)	Turns (%)	Unordered (%)	NRMSD
Control	4.8	38.1	22.8	34.3	0.034
Methanol	6.9	37.7	22.5	33.0	0.049
Ethanol	4.8	40.3	22.1	32.7	0.058
Isopropanol	4.7	41.0	22.0	32.4	0.033
Acetonitrile	4.4	40.3	22.5	32.9	0.042

5.3.3 Intrinsic fluorescence and solute quenching studies

Intrinsic fluorescence spectra and solute quenching parameters of KLKp are shown in fig. 2b and table 2, respectively. The Stern-Volmer plots have been presented in Fig.3.

KLKp in isopropanol showed a blue shift of 4 nm (Fig.2b), indicating increased polarity of Trp. Although K_{sv} for acrylamide was almost similar to that of native protein, the value for KI had increased two-fold (1.057 M^{-1} to 2.57 M^{-1}) and that for CsCl had increased several (20) fold. Thus, overall charge density around surface Trp had significantly increased with net negative charge density. This could have been the ultimate result of stable conformation leading to functional stability of the protein. Ethanol did not cause change in the spectrum, while only minor increase in the negative charge density was observed.

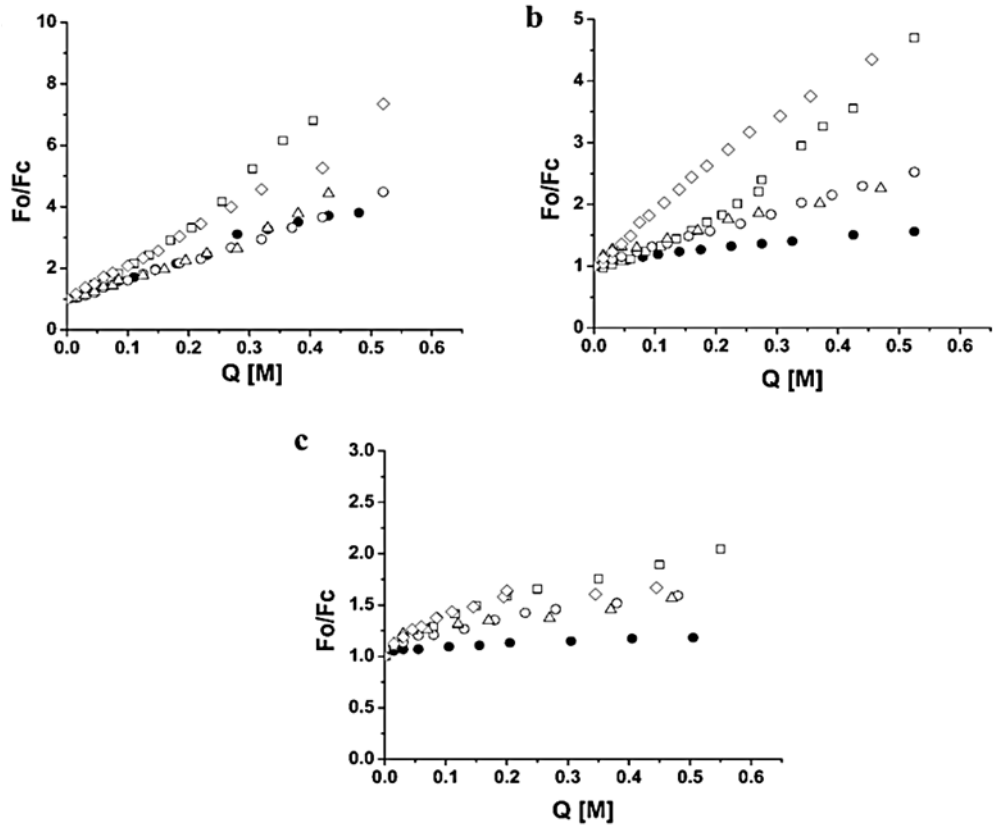

Figure 3: Solute quenching studies of solvent treated KLKp: Stern-Volmer plots for solute quenching of KLKp (40µg/ml) treated with 90% solvents for 72 hours using (a) acrylamide (b) KI (c) CsCl. The solvents used are; control (●--●), Methanol (□--□), Ethanol (○--○), Isopropanol(Δ--Δ), Acetonitrile (◊--◊).

In acetonitrile, λ_{max} of the protein was unaltered but considerable increase in fluorescence intensity indicating altered Trp microenvironment was observed. Two-fold increase in K_{sv} for acrylamide and seven-fold increase in K_{sv} for KI could be due to the significantly increased fluorescence emission. This could be due to the destabilizing effect of acetonitrile. Significant red shift in λ_{max} (354nm) was observed in presence of 90% methanol indicating apparent unfolding leading to inactivation of the protein. Higher rate of fluorescence quenching was observed with acrylamide (14.59 M^{-1}) as well as with KI (7.25 M^{-1}).

Table 2: Summary of conformational parameters of KLKp in presence of organic solvents from spectroscopic studies:

Solvent (Dielectric constant)	Activity	Fluorescence λ_{max} (nm)	Solute quenching studies Stern-Volmer constant (M^{-1})				CD Wavelength of minimum ellipticity (nm)
			Acrylamide	KI	CsCl		
					$K_{sv}1$	$K_{sv}2$	
Water (78.36)	++	343	6.25	1.06	0.27		204
Isopropanol (19.92)	+++	339	7.67	2.57	5.64	0.70	204 50% Reduced ellipticity
Ethanol (24.55)	++	343	6.5	2.98	1.36	0.74	207
Methanol (32.66)	+	354	14.6	7.3	2.88	1.3	207 Increased ellipticity
Acetonitrile (35.94)	+	343 Increased intensity	11.4	7.60	3.23	0.51	212

5.3.4 MD simulation:

MD simulations of KLKp in solvent systems were analyzed over 150 ns (Fig.4). The parameters over last 50 ns were averaged in order to get the numerical values for root-mean-squared (RMS) deviation, radius of gyration (Rg) and solvent accessible surface area (SASA) (Table 3). The RMS deviations of the protein structure equilibrated in respective solvent systems from the initial structures are plotted as a function of simulation time in Figure 4a. As compared to control simulation, RMS deviation for the protein backbone atoms was in order of, water (3.35 Å) < isopropanol (4.9 Å) < ethanol (5.5 Å) <acetonitrile (7.1 Å) < methanol (16.3 Å) (Table 2). This clearly indicated that water, isopropanol and ethanol systems favor the structural stability of KLKp. On the other hand, protein in acetonitrile and methanol shows more structural fluctuation depicted from the higher RMS values.

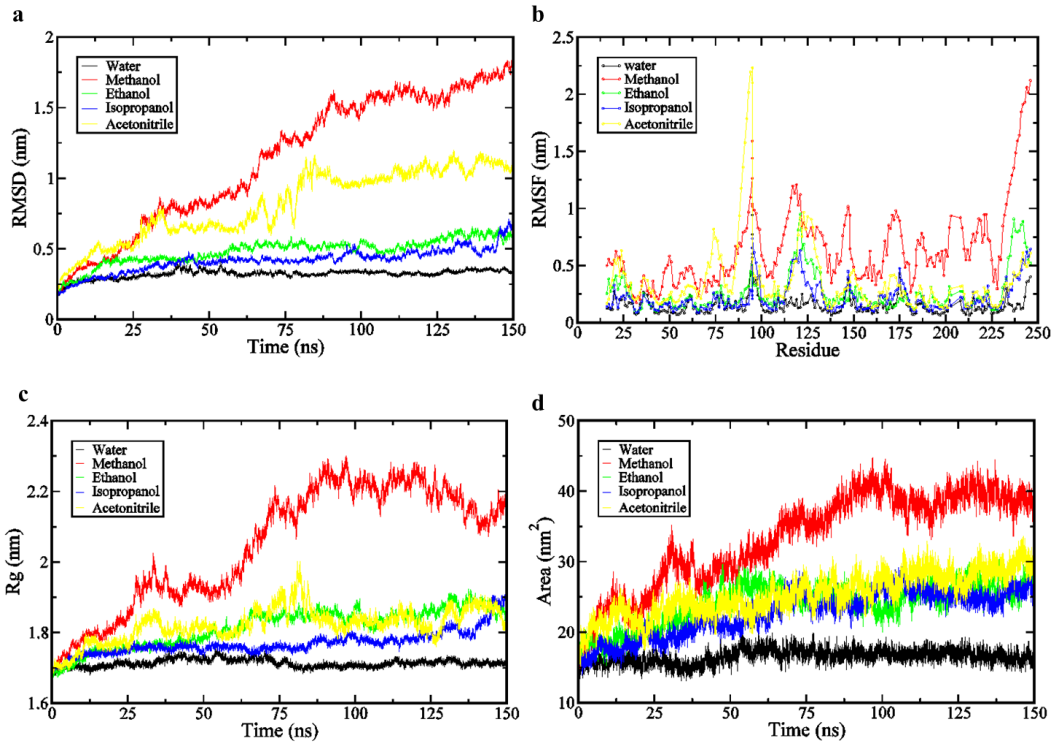

Figure 4: MD simulation analysis of KLKp structure in respective solvents systems over 150ns: (a) RMSD from the KLKp structure calculated for protein backbone atoms as a function of time (b) RMSF values for total structure of KLKp (c) Radius of gyration (Rg) (d) Solvent accessible surface area (SASA) for respective solvent systems, Control (black), methanol (red), ethanol (green), isopropanol (blue), acetonitrile (yellow).

The structural compactness of the protein was analyzed from radius of gyration (Rg) and Solvent accessible surface area (SASA) of the protein. In methanol, significant increase in the Rg and SASA values of KLKp indicated the structural disorderdness in the protein which affects the compactness of the protein (Table 3). This might be the reason for the loss of activity of the protein observed in the experiment. On the contrary, Rg and SASA values remained comparable to that in water (1.73 nm) in isopropanol, ethanol and acetonitrile.

Table 3: Summary of structural parameters of KLKp simulated in respective solvent systems:

Solvent	RMSD (nm)		Rg (nm)		SASA	
	TS	ASC	TS	AS	TS	ASC
Water	0.335 ± 0.015	0.3 ± 0.01	1.73 ± 0.007	0.91 ± 0.0075	113.5 ± 2.4	30.35 ± 0.7
Isopropanol	0.49 ± 0.06	0.39 ± 0.021	1.8 ± 0.034	1.0 ± 0.01	133.38 ± 2.88	34.5 ± 1.04
Ethanol	0.55 ± 0.047	0.35 ± 0.023	1.86 ± 0.023	0.965 ± 0.024	135.5 ± 4.8	32.41 ± 1.1
Methanol	1.63 ± 0.077	1.4 ± 0.065	2.19 ± 0.045	1.77 ± 0.069	176.5 ± 4.65	44.17 ± 1.52
Acetonitrile	0.71 ± 0.071	0.68 ± 0.1	1.83 ± 0.031	1.114 ± 0.08	130.42 ± 2.99	32.63 ± 0.9

TS: Total structure ASC: Active site conformation

5.3.5 Active site conformation:

The active site residues within the 0.5 nm radial distances from the catalytic triad (His57-Asp102-Ser195) were identified and their spatial arrangement in different solvent systems (last frame from MD simulation) were shown as surface representation in Fig.5a.

KLKp active site in control simulations showed a channel for substrate movement from Ser195 to Asp102 through His57, as seen in the fig.5a. The active site conformation remains almost the same in ethanol system, while, in case of isopropanol system, it shows a minor increase in Rg and SASA values, indicating slightly altered pocket conformation that provides its better accessibility for the substrate molecules (Table 3). This justifies the elevated proteolytic activity of KLKp

in presence of isopropanol. In case of acetonitrile system, the altered active site conformation of KLKp results in buried catalytic triad residues thus reducing the catalytic efficiency of the enzyme, while in methanol it is disoriented which correlates the loss of activity in these systems.

The analysis of KLKp structures equilibrated in respective solvent systems using iRDP server and the structural superimposition of active site residues of KLKp in water with those in respective solvent systems revealed the structural changes in catalytic triad of the enzyme (Fig.5b). In isopropanol, the catalytic triad is more stabilized owing to minor displacement of Asp102 that results in additional hydrogen bond formation between His57-Asp102. Ethanol induced a minor displacement of His57 without considerable change in the conformation of active site residues. Methanol system induced distortion of the active site conformation as seen in fig.5b leading to functional loss of the enzyme.

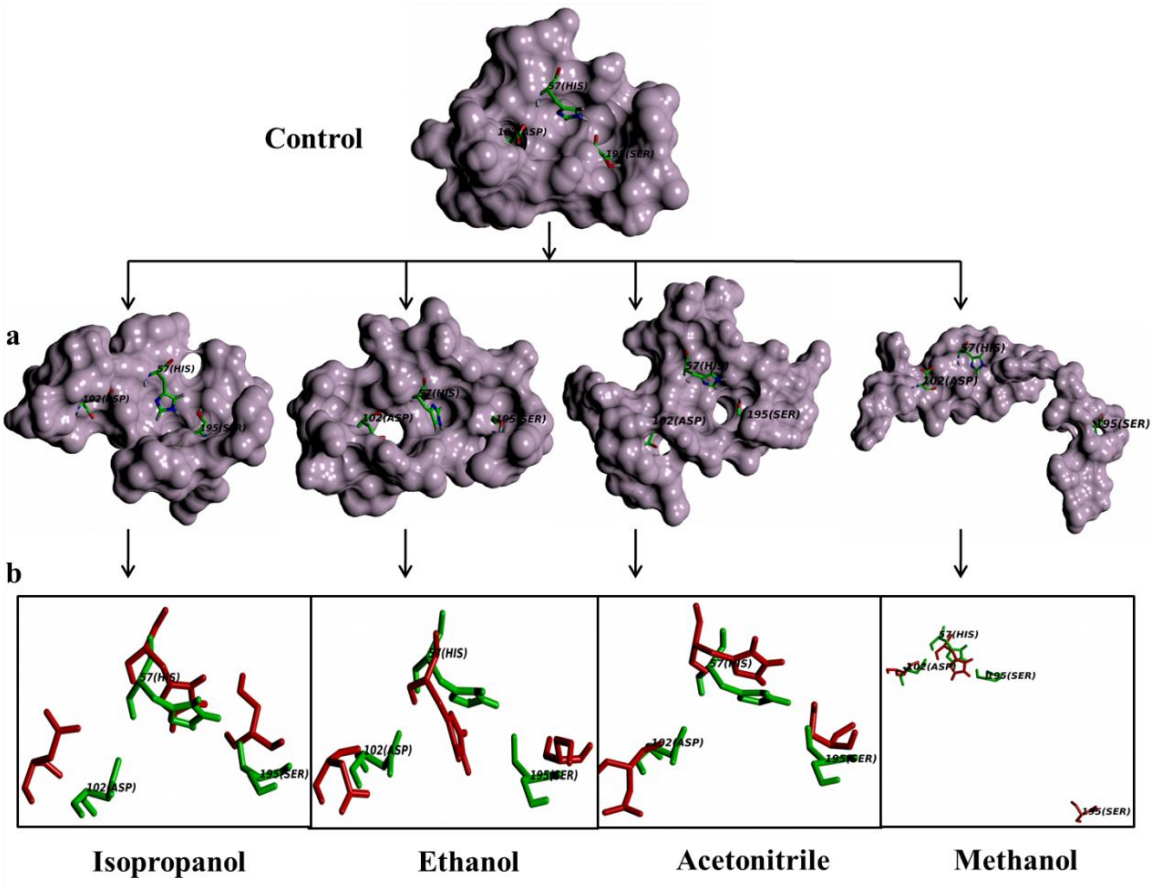

Figure 5: Analysis of active site conformation: Panel A: Surface representation of the residues in cut-off radius of 5Å from active site residues (His57-Asp102-Ser195) Panel B:

Superposition of active site residues of KLKp in respective solvents (Red) with those of KLKp in water (Green). (Visualization in CCP4mg).

Analysis of the active site conformation (ASC) supports these conformational changes as RMSD and RMSF values for ASC are in the order of water < isopropanol < ethanol < acetonitrile < methanol (Fig. 6 a and b). The increase in the radius of gyration (Rg) values in ASC of KLKp in methanol (18.3 Å) suggests loss of compact conformation integrity (Fig. 6c). Increased SASA value in isopropanol validates better accessibility of the active site for the substrate molecules as well as release of the products after catalysis (Fig. 6d, table 2).

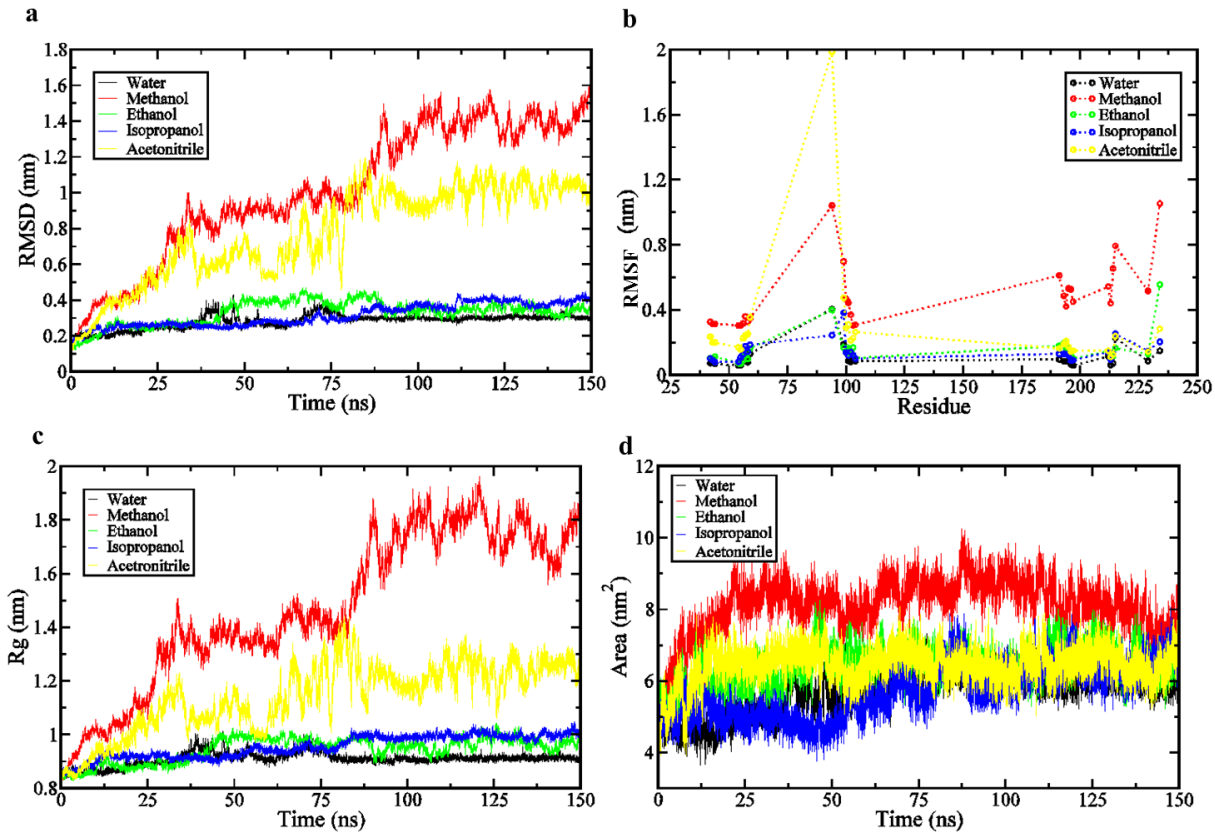

Figure 6: Structural parameters for active site conformation of KLKp simulated in respective solvent system for 150 ns: (a) RMSD of KLKp structure calculated for protein backbone atoms as a function of time (b) RMSF values for active site conformation (c) Radius of gyration (Rg) (d) Solvent accessible surface area (SASA) for respective solvent systems, Control (black), methanol (red), ethanol (green), isopropanol (blue), acetonitrile (yellow).

Functional stability of KLKp in isopropanol was strongly supported by conformational analysis viz retention of CD minima at 204 nm, similar accessibility of Trp towards neutral quencher and minimum deviation of the structure from that of control simulation. It can be mentioned that apparent reduction in the compactness of secondary structure as seen in significantly reduced negative ellipticity and intermediate increase in R_g and SASA values as compared to control were also observed. Blue shift in λ_{max} of intrinsic fluorescence spectrum in isopropanol and increased negative charge density around trp indicated some change in conformation. All these changes could contribute to the stability and enhanced activity of KLKp after incubation in isopropanol.

In ethanol, the secondary structure, Trp environment and accessibility to neutral quencher were comparable to those of control. The structural parameters of the protein observed marginally differ from control simulations validating stabilizing effect of ethanol.

Conversely, methanol and acetonitrile changed the conformation of KLKp significantly as seen in CD, fluorescence and MD simulation studies. The alteration of far UV CD spectrum and red shift in λ_{max} of intrinsic fluorescence spectrum suggested structural modification of KLKp in methanol which could be unfavorable. These conformational changes were validated by observation of highest RMSD and RMSF values of the protein in methanol. These structural modifications could lead to loss in the activity of KLKp in methanol and acetonitrile.

Analysis of simulation data in iRDP (in-silico Rational Design of Proteins) web server (http://irdp.ncl.res.in) revealed that the extent of hydrogen bonding increases considerably in isopropanol as compared to other systems, with additional hydrogen bond formation between His57-Asp102. Additionally, the ionic bond between His57 and Asp102 is maintained only in water and isopropanol system. The ion pair is disrupted in all other solvent systems. As indicated by superimposition of active site residues, ethanol and isopropanol maintain the conformational integrity of active site residues. Burial of active site residues may hinder the catalytic efficiency of KLKp in acetonitrile. In methanol, the drastic change in orientation of active site residues could disrupt the formation of oxyanion hole, which is a rate limiting step for protease activity. Similar changes in the conformation of active site residues have been documented in case of subtilisin Carlsberg where displacement of Asn155 disrupts

formation of oxyanion hole leading to loss of the enzyme in acetonitrile (Cruz et al 2009).

In spite of several reports on serine proteases being stable in organic solvents, studies describing the structural transitions and their correlation with the functional transitions are scarce. The unusual stability of KLKp under harsh conditions like high organic solvent concentration and high temperature makes it an interesting model to examine. The present studies of KLKp bring deeper understanding of the enzyme at molecular level and may help in emerging therapeutic applications of several kallikreins.

References

- Bansal, V., Delgado, Y., Fasoli, E., Ferrer, A., Griebenow, K., Secundo, F., & Barletta, G. L. (2010). Effect of prolonged exposure to organic solvents on the active site environment of subtilisin Carlsberg. *Journal of Molecular Catalysis B: Enzymatic*, *64*(1), 38-44.
- Berendsen, H. J., Postma, J. P. M., van Gunsteren, W. F., DiNola, A. R. H. J., & Haak, J. R. (1984). Molecular dynamics with coupling to an external bath. *The Journal of chemical physics*, *81*(8), 3684-3690.
- Bode, W., Chen, Z., Bartels, K., Kutzbach, C., Schmidt-Kastner, G., & Bartunik, H. (1983). Refined 2 Å X-ray crystal structure of porcine pancreatic kallikrein A, a specific trypsin-like serine proteinase: Crystallization, structure determination, crystallographic refinement, structure and its comparison with bovine trypsin. *Journal of molecular biology*, *164*(2), 237-282.
- Cabral, J. M. S., Aires-Barros, M. R., Pinheiro, H., & Prazeres, D. M. F. (1997). Biotransformation in organic media by enzymes and whole cells. *Journal of biotechnology*, *59*(1), 133-143.
- Castillo, B., Pacheco, Y., Al-Azzam, W., Griebenow, K., Devi, M., Ferrer, A., & Barletta, G. (2005). On the activity loss of hydrolases in organic solvents: I. Rapid loss of activity of a variety of enzymes and formulations in a range of organic solvents. *Journal of molecular catalysis b: enzymatic*, *35*(4), 147-153.
- Cruz, A., Ramirez, E., Santana, A., Barletta, G., & López, G. E. (2009). Molecular dynamic study of subtilisin Carlsberg in aqueous and nonaqueous solvents. *Molecular Simulation*, *35*(3), 205-212.
- Dalal, S. A., More, S. V., Shankar, S., Laxman, R. S., & Gaikwad, S. M. (2014). Subtilase from Beauveria sp.: conformational and functional investigation of unusual stability. *European Biophysics Journal*, *43*(8-9), 393-403.
- Doukyu, N., & Ogino, H. (2010). Organic solvent-tolerant enzymes. *Biochemical Engineering Journal*, *48*(3), 270-282.
- Harpaz, S., Eshel, A., & Lindner, P. (1994). Effect of 1-propanol on the activity of intestinal proteolytic enzymes of the European sea bass Dicentrarchus labrax. *Journal of agricultural and food chemistry*, *42*(1), 49-52.

- Hess, B., Kutzner, C., Van Der Spoel, D., & Lindahl, E. (2008). GROMACS 4: algorithms for highly efficient, load-balanced, and scalable molecular simulation. *Journal of chemical theory and computation*, *4*(3), 435-447.
- Kim, J., Clark, D. S., & Dordick, J. S. (2000). Intrinsic effects of solvent polarity on enzymic activation energies. *Biotechnology and bioengineering*, *67*(1), 112-116.
- Kise, H., & Fujimoto, K. (1988). Enzymatic reactions in aqueous-organic media. VIII. Medium effect and nucleophile specificity in subtilisin-catalyzed peptide synthesis in organic solvents. *Biotechnology letters*, *10*(12), 883-888.
- Kotormán, M., Laczkó, I., Szabó, A., & Simon, L. M. (2003). Effects of Ca^{2+} on catalytic activity and conformation of trypsin and α-chymotrypsin in aqueous ethanol. *Biochemical and biophysical research communications*, *304*(1), 18-21.
- Lousa, D., Baptista, A. M., & Soares, C. M. (2012). Analyzing the molecular basis of enzyme stability in ethanol/water mixtures using molecular dynamics simulations. *Journal of chemical information and modeling*, *52*(2), 465-473.
- Lousa, D., Baptista, A. M., & Soares, C. M. (2013). A molecular perspective on nonaqueous biocatalysis: contributions from simulation studies. *Physical Chemistry Chemical Physics*, *15*(33), 13723-13736.
- Malde, A. K., Zuo, L., Breeze, M., Stroet, M., Poger, D., Nair, P. C., & Mark, A. E. (2011). An automated force field topology builder (ATB) and repository: version 1.0. *Journal of chemical theory and computation*, *7*(12), 4026-4037.
- McNicholas, S., Potterton, E., Wilson, K. S., & Noble, M. E. M. (2011). Presenting your structures: the CCP4mg molecular-graphics software. *Acta Crystallographica Section D: Biological Crystallography*, *67*(4), 386-394.
- Meng, Y., Yuan, Y., Zhu, Y., Guo, Y., Li, M., Wang, Z. & Jiang, L. (2013). Effects of organic solvents and substrate binding on trypsin in acetonitrile and hexane media. *Journal of molecular modeling*, *19*(9), 3749-3766.
- Nakajima, N., Sugimoto, M., & Ishihara, K. (2000). Stable earthworm serine proteases: application of the protease function and usefulness of the earthworm autolysate. *Journal of bioscience and bioengineering*, *90*(2), 174-179.

- Ogino, H., Gemba, Y., Yutori, Y., Doukyu, N., Ishimi, K., & Ishikawa, H. (2007). Stabilities and conformational transitions of various proteases in the presence of an organic solvent. *Biotechnology progress*, *23*(1), 155-161.
- Patra, M., Karttunen, M., Hyvönen, M. T., Falck, E., Lindqvist, P., & Vattulainen, I. (2003). Molecular dynamics simulations of lipid bilayers: major artifacts due to truncating electrostatic interactions. *Biophysical journal*, *84*(6), 3636-3645.
- Reichardt, C., Welton, T. (2011). Solvents and solvent effects in organic chemistry. John Wiley & Sons.
- Saborowski, R., Sahling, G., del Toro, M. N., Walter, I., & Garcıa-Carreno, F. L. (2004). Stability and effects of organic solvents on endopeptidases from the gastric fluid of the marine crab Cancer pagurus. *Journal of Molecular Catalysis B: Enzymatic*, *30*(3), 109-118.
- Serdakowski, A. L., & Dordick, J. S. (2008). Enzyme activation for organic solvents made easy. *Trends in biotechnology*, *26*(1), 48-54.
- Simon, L. M., Kotormán, M., Szabó, A., Nemcsók, J., & Laczkó, I. (2007). The effects of organic solvent/water mixtures on the structure and catalytic activity of porcine pepsin. *Process Biochemistry*, *42*(5), 909-912.
- Stepankova, V., Bidmanova, S., Koudelakova, T., Prokop, Z., Chaloupkova, R., & Damborsky, J. (2013). Strategies for stabilization of enzymes in organic solvents. *Acs Catalysis*, *3*(12), 2823-2836.
- Toba, S., & Merz, K. M. (1997). The concept of solvent compatibility and its impact on protein stability and activity enhancement in nonaqueous solvents. *Journal of the American Chemical Society*, *119*(42), 9939-9948.
- Van Der Spoel, D., Lindahl, E., Hess, B., Groenhof, G., Mark, A. E., & Berendsen, H. J. (2005). GROMACS: fast, flexible, and free. *Journal of computational chemistry*, *26*(16), 1701-1718.

Chapter 6

Summary and Conclusion

Summary and conclusions:

The events of folding, unfolding, refolding and misfolding of proteins are vital for living systems. As a consequence of growing knowledge on physiological and commercial importance of various proteases from microbial, plant and animal origin, these enzymes have been studied for the stability and unfolding transitions under denaturing conditions. Understanding the principles responsible for stability of these proteases under stress conditions is an active area of research. The present studies characterized two serine proteases (1) Subtilase from *Beauveria sp.* MTCC 5184 (Bprot) and (2) Porcine pancreatic kallikrein (KLKp) for their functional and conformational dynamics under denaturing conditions.

Although the enzymes under study have different origins, they share common characteristics like stability in the denaturing agent, at higher temperature, in the wide range of pH, and in high concentration of organic solvents. However, the order of polarity of the organic solvents stabilizing the respective proteins is reverse, which highlights the differential structural features.

The highlights of the thesis are:

- Bprot is subtilisin–like serine protease with α/β hydrolase fold.
- Single tryptophan residue in Bprot is buried in hydrophobic core and is present in positively charged environment.
- Crystallization and preliminary characterization of Bprot was performed.
- Structural resistance of Bprot towards SDS and proteolytic environment makes it a potential kinetically stable protein.
- Bprot is stable functionally in presence of chaotropic agent indicating structural rigidity of the protein.
- Bprot exhibits functional and structural stability towards polar organic solvents like methanol and DMSO.
- Acid denatured Bprot refolded into ordered but inactive structure in presence of organic solvents, HFIP exhibiting maximum helix propensity.

- Seven tryptophan residues were located in partially polar and positively charged environment in native KLKp.
- β-sheet dominant secondary structure of KLKp correlated well with existing crystal structure.
- Structure of KLKp is thermostable though functional stability is lost above 50°C.
- Acid induced molten-globule like structure of KLKp was characterized.
- Higher stability of KLKp in high concentration of isopropanol was investigated by biochemical, biophysical and MD simulation studies.

Besides giving better understanding, the studies on properties of the proteases responsible for their high stability may prove to be useful lead in existing knowledge of protein engineering.

Table 1: Comparative account of stability of Bprot and KLKp:

Denaturing agent		**Bprot**	**KLKp**
		Stability observed under the conditions	
GdnHCl		12 hours in 3M	4 hours in 1M
pH		Activity: 5.0-10.0	Activity: 5.0-10.0
		Structure: 2.0-10.0	Structure: 1.0-10.0
Temperature		Activity: 55℃	Activity: 50℃
		Structure: 55℃	Structure: 90℃
Organic solvents	Control	++	++
	Concentration →	(50% *v/v*)	(90% *v/v*)
	Methanol	+++	+
	Ethanol	++	++
	Propanol	+	+++
	Acetonitrile	+	+
	DMSO	+++	+
	TFE	++ (5% *v/v*)	NA*
	HFIP	+ (5% *v/v*)	NA

*NA: Not Applicable

LIST OF PUBLICATIONS

1. **Sayli Dalal**, Snehal V. More, Shiv Shankar, R. Seeta Laxman, and Sushama M. Gaikwad. "Subtilase from Beauveria sp.: conformational and functional investigation of unusual stability." *European Biophysics Journal* 43, no. 8-9 (2014): 393-403.

2. **Sayli Dalal**, Anil Mhashal, Narendra Kadoo, and Sushama Gaikwad "Functional Stability and Structural Transitions of Kallikrein: Spectroscopic and Molecular dynamics studies" (Manuscript under review)

3. Sonali Rohamare, Vaishali Javdekar, **Sayli Dalal**, Pavan Kumar Nareddy, Musti J. Swamy, and Sushama M. Gaikwad. "Acid Stability of the Kinetically Stable Alkaline Serine Protease Possessing Polyproline II Fold." *The protein journal* 34, no. 1 (2015): 60-67.

4. Rashmi Tupe, Amruta Kulkarni, Krishna Adeshara, Neena Sankhe, Shamim Shaikh, **Sayli Dalal**, Siddharth Bhosale, and Sushama Gaikwad. "Zinc inhibits glycation induced structural, functional modifications in albumin and protects erythrocytes from glycated albumin toxicity." *International Journal of Biological Macromolecules* 79 (2015): 601-610.

5. **Book Chapter**: Madhurima Wakankar, **Sayli Dalal**, Sushama Gaikwad. "Protein folding, misfolding and aggregation: implications in human health care." *Biotechnology: Beyond Borders* ISBN No.978-93-5212-714-6. Page No. 212-222.

PRESENTATIONS AND POSTERS

- Oral presentation entitled "Structural stability and dynamics of Porcine Pancreatic Kallikrein under denaturing conditions" in 9th International Conference on Structure and stability of biomacromolecules, Institute of experimental physics, Kosice, Slovakia in July 2015.

- Presented a poster on '*Beauveria* Serine protease: A kinetically stable protein?' in Fluorescence correlation spectroscopy 2013, IISc Bangalore.

- Presented a poster on 'Monitoring structural and functional transitions of a serine protease from *Beauveria sp*. MTCC 5184' in International symposium for protein folding and dynamics, National Centre for Biological Sciences (NCBS), Bangalore in October 2012.

- Presented a poster on 'Conformational characterization of serine protease from *Beauveria sp* MTCC 5184'on Science Day in National Chemical Laboratory, Pune in January 2012.